Colloidal Semiconductor Nanocrystals:

A Study of the Syntheses of and Capping Structures for CdSe

Erik Herz
Virginia Polytechnic Institute and State University
Master of Science
Materials Science and Engineering

Dr. Richard O. Claus, Chairman

Dr. Kenith E. Meissner

Dr. Dwight D. Viehland

July 18, 2003
Blacksburg, Virginia

Keywords: Colloidal quantum dot, semiconductor nanoparticle, capping structure, cadmium selenide

Colloidal Semiconductor Nanocrystals:

A Study of the Syntheses of and Capping Structures for CdSe

By Erik Herz

Dr. R.O. Claus, Chairman

Abstract

Luminescent quantum dots (QDs) or rods are semiconductor nano-particles that may be used for a wide array of applications such as in electro-optical devices, spectral bar coding, tagging and light filtering. In the case under investigation, the nano-particles are cadmium-selenide (CdSe), though they can be made from cadmium-sulfide, cadmium-telluride or a number of other II-VI and III-V material combinations. The CdSe quantum dots emit visible light at a repeatable wavelength when excited by an ultraviolet source. The synthesis of colloidal quantum dot nanoparticles is usually an organo-metallic precursor, high temperature, solvent based, airless chemical procedure that begins with the raw materials CdO, a high boiling point ligand, and a Se-trioctylphosphine conjugate. This investigation explores the means to produce quantum dots by this method and to activate the surface or modify the reaction chemistry with such molecules as trioctylphosphine oxide, stearic acid, dodecylamine, phenyl sulfone, aminophenyl sulfone, 4,4'dichlorodiphenyl sulfone, 4,4'difluorodiphenyl sulfone, sulfanilamide and zinc sulfide during the production to allow for further applications of quantum dots involving new chemistries of the outer surface. Overall, the project has been an interesting and successful one, producing a piece of equipment, a lot of ideas, and many dots with varied capping structures that have been purified, characterized, and stored in such a way that they are ready for immediate use in future projects.

Acknowledgements

I would like to express my appreciation to my master's thesis advisor, Dr. Richard O. Claus for his guidance and support. I wish to thank Dr. Ken Meissner for his daily input, support, motivation, and the sharing of his expertise. Dr. Dwight Viehland has led me to a broader materials understanding with his undergraduate class on ceramics and his encouragement as a committee member. I thank Dr. William Spillman Jr. for his financial, in kind, and academic support as director of Optical Sciences and Engineering Research.

In order to produce and investigate the materials I have made, I relied on Dr. Tim Long and Dr. Karen Brewer for the use of their chemical synthesis and photoluminescence investigation equipment, respectively. Stephen McCartney deserves many thanks for his help with transmission electron microscopy.

I also wish to thank my fiancée, Ashley Puig, for her support, love and the occasional motivational kick. Thanks to Danielle Irving for her excellent and persistent editing, formatting, and synthesis work. Molly Tinius has created Figures 2, 5, and 6 and has been an immense aide with data collection. Without Pam Granger the more than 2000 samples that have been produced would be in even greater disarray. I thank her for sample organization.

Additional thanks are extended to the Barry M. Goldwater Scholarship and Excellence in Education Foundation for financially supporting my final year at Virginia Tech and the American Cancer Society and the Carillion Biomedical Institute for their support of the Optical Sciences and Engineering Research Group at Virginia Polytechnic Institute and State University.

Dedication

I dedicate this work to my father and mother. The first, who is deceased, but has influenced my life and determination tremendously by the example he provided me in my early years. He inspires me to think, dream, and stand tall on a daily basis. The second for raising me, guiding me, and continuing to be my sounding board for every important decision I make. Thank you mom for listening and for always being there through everything. Your love and care are what have made possible the many opportunities I have had, thank you.

Table of Contents

Section **Page Number**

1. Introduction and Motivation …… 1
2. Background to Quantum Dots – Physics…….. 2
3. The Colloidal Quantum Dot System……. 6
    3.1 Indium Phosphide, Gallium Phosphide, and Gallium Indium Phosphide …… 7
    3.2 Zinc Sulfide and Zinc Selenide……... 8
    3.3 Lead Selenide…….. 9
    3.4 Cadmium Sulfide…… 10
    3.5 Cadmium Telluride……. 10
    3.6 Cadmium Selenide…….. 11
        3.6.1 Cadmium Selenide Structures…… 12
4. Chemistry…….. 13
    4.1 Capping Structures…….. 14
        4.1.1 Organic Capping Structures……... 14
        4.1.2 Inorganic Capping Structures……. 15
5. Facilities and Equipment …..…… 17
6. Procedure…… 18
    6.1 Experimental Details…… 19
        6.1.1 Materials…….. 19
        6.1.2 Procedural Safety……. 19
        6.1.3 Synthesis of TOPO Capped CdSe Quantum Dots…….…….. 20
        6.1.4 Synthesis of Stearic Acid Capped CdSe Quantum Dots…….. 21
        6.1.5 Synthesis of Dodecylamine Capped CdSe Quantum Dots…….. 21
        6.1.6 Comparison of Stearic Acid and Dodecylamine Capped CdSe in Terms of Reaction Rate……. 22
        6.1.7 Synthesis of Phenyl Sulfone Capped CdSe Quantum Dots……. 23
        6.1.8 Synthesis of Aminophenyl Sulfone Capped CdSe Quantum Dots …… 23
        6.1.9 Synthesis of 4,4’ Dichlorodiphenyl Sulfone and 4,4’ Difluorodiphenyl Sulfone Capped CdSe Quantum Dots…… 24
        6.1.10 Synthesis of Sulfanilamide Capped CdSe Quantum Dots…….. 26
    6.2 Synthesis of Zinc Sulfide Capped CdSe Quantum Dots (CdSe/ZnS)… 27
    6.3 Characterization of Resulting Quantum Dots……..…… 28
        6.3.1 Fluorimetry…… 28
        6.3.2 Spectophotometry……. 32
        6.3.3 Size Selective Precipitation…….. 35
        6.3.4 Transmission Electron Microscopy…….. 36
7. Results……. 37
    7.1 Fluorimetry and Spectrophotometry Investigation of CdSe …….. 37
        7.1.1 TOPO Capped CdSe Quantum Dots……. 37
        7.1.2 Stearic Acid Capped CdSe Quantum Dots……. 39
        7.1.3 Dodecylamine Capped CdSe Quantum Dots……. 41

Section **Page Number**

7.1.4 Comparison of Stearic Acid and Dodecylamine Capped CdSe Quantum Dots…… 43
7.1.5 Phenyl Sulfone Capped CdSe Quantum Dots…… 46
7.1.6 Aminophenyl Sulfone Capped CdSe Quantum Dots……. 49
7.1.7 4,4'-Dichlorodiphenyl Sulfone and 4,4'-Difluorodiphenyl Sulfone Modified CdSe Reactions……. 50
7.1.8 Sulfanilamide Modified CdSe Quantum Dot Reactions…… 53
7.2 Zinc Sulfide Capped CdSe Quantum Dots (CdSe/ZnS)……. 54
7.3 Transmission Electron Microscopy (TEM)……. 56
7.3.1 CdSe/TOPO – Rods, Dots, Tetrapods, and Other Shapes…….. 56
7.3.2 CdSe/SA TEM Results…… 59
7.4 Predicting Quantum Dot Emission from Reaction Length…….. 59
8. Discussion of Objectives and Results …..…… 61
9. Summary ……... 64
10. Future Work……. 65
References…….. 66
Appendix A…… 69
Appendix B…… 75
Appendix C…… 76
Appendix D…… 78
Vita…….…… 81

List of Figures

Figure		Page Number
Figure 1.	Schematic of electron occupancy of allowed energy bands for given materials ……	2
Figure 2.	The progression of confinement and the effects on the density of states……	5
Figure 3.	Emission spectra of different sized CdSe nanoparticles from the same reaction ……	6
Figure 4.	CdSe quantum dots embedded in polystyrene microspheres emitting at three distinct visible wavelengths simultaneously, all under the same ultraviolet light source……	11
Figure 5.	Schematic of wurtzite structure ……	12
Figure 6.	Schematic of zinc blende structure ……..	13
Figure 7.	Spectra corresponding to the second, third and fourth vials shown previously in Figure 3; note how the spectra are clearly distinct at full-width half maximum.……	14
Figure 8.	Trioctylphosphine oxide structure……	14
Figure 9.	Peng and Alivisatos's schematic of how TOPO interacts with the surface of a CdSe quantum dot nanoparticle……	15
Figure 10.	Chemical structures of stearic acid (left) and dodecylamine (right); Note: hydrogens are not shown in the carbon chains C_{18} and C_{12}…	15
Figure 11.	Schematic of SiO_2 capping of CdSe/ZnS structure with various functional groups as proposed by Gerion et al.……	17
Figure 12.	A schematic of the structure of phenyl sulfone……	23
Figure 13.	A schematic of the structure of 4-aminophenyl sulfone……..	24
Figure 14.	The structure of 4,4'-dichlorodiphenyl sulfone……	25
Figure 15.	The structure of 4,4'-difluorodiphenyl sulfone…….	25
Figure 16.	The structure of sulfanilamide…….	26

Figure **Page Number**

Figure 17. Photoluminescence data for a stearic acid reaction, as received from the fluorimeter, showing intensities relative to the most intense sample in the set…… 29

Figure 18. The same data as Figure 17, but with normalized intensity…….. 30

Figure 19. Full-width half maxima differences: an indication of quantum dot size distribution differences…… 31

Figure 20. Demonstration of CdSe QD emission consistency over a broad range of excitation wavelengths……. 32

Figure 21. Absorption spectrum of a CdSe/TOPO sample before normalization and deletion of TOPO absorption…… 33

Figure 22. Absorption spectrum of the same CdSe/TOPO sample as Figure 21, but after normalization and deletion of TOPO absorption…… 34

Figure 23. The emission of size selective precipitated samples, performed to decrease FWHM…… 35

Figure 24. The full array of emission colors as sampled from a single 44 hour reaction of CdSe quantum dots capped with TOPO…… 38

Figure 25. Emission color and time progression of quantum dot growth during reaction…… 38

Figure 26. Absorption and emission plots for the six hour sample from Figure 25…… 39

Figure 27. Stearic acid capped quantum dots' luminescent emission spectra under ultraviolet excitation…….. 40

Figure 28. Absorption and emission of the 12-minute sample from Figure 27, representative of the entire set……. 41

Figure 29. 50% dodecylamine capped quantum dots' luminescent emission spectra under ultraviolet excitation……. 42

Figure 30. Absorption and emission spectra for the 40 minute sample of Figure 29, 50% CdSe/DA…….. 42

Figure **Page Number**

Figure 31. Plot of emission peaks of varied percentage of TOPO/SA reactions versus reaction time…… 43

Figure 32. Dodecylamine reaction plots of emission peak versus time …….. 44

Figure 33. 95% SA/5%TOPO reactions performed at different temperatures; plots of emission peak versus time ……. 45

Figure 34. 50% Phenyl sulfone/ 50% TOPO capped quantum dots' luminescent emission spectra under ultraviolet excitation……. 47

Figure 35. Emission spectra from 100% phenyl sulfone capped CdSe…… 47

Figure 36. Reaction time vs wavelength plot, showing the similarity between 50% and 100% phenyl sulfone reactions.…… 48

Figure 37. Absorption and emission spectra for the one hour sample in Figure 34, 50% CdSe/PS ……. 48

Figure 38. A 100% aminophenyl sulfone reaction produced quantum dots luminescing with the above emission spectra under ultraviolet excitation…..…… 49

Figure 39. Absorption and emission plots of a representative 100% CdSe/APS sample taken at 1440 seconds…… 50

Figure 40. The final sample from a 50% ClPS reaction indicates the presence of some CdSe…… 51

Figure 41. A representative plot of the 30-minute sample of the 50% FPS/TOPO reaction emission, indicating that inhibition of the reaction is occurring when the QDs reach a certain size……. 52

Figure 42. 100% Sulfanilamide reaction samples that indicate inhibited nucleation and growth…… 53

Figure 43. Yellow spectrum is the 556nm emitting CdSe/ZnS spectrum, other spectra are of other CdSe/ZnS reactions to show coverage of the visible spectrum…… 54

Figure 44. Absorption spectra overlaid on the emission spectra of Figure 43… 55

Figure **Page Number**

Figure 45. Plot of the difference in intensity between equal optical density samples of CdSe/TOPO and CdSe/ZnS……. 56

Figure 46. TEM image of quantum rods capped with TOPO…….. 57

Figure 47. Enlarged section of Figure 46 showing tetrapod and arrow shaped semiconductor nanoparticles…… 57

Figure 48. TEM image of a rod/dot mix…… 58

Figure 49. TEM image of CdSe/TOPO QDs with excellent monodispersity.. 58

Figure 50. TEM image of 5nm diameter SA capped quantum dots with good monodispersity and low aspect ratio …… 59

Figure 51. SA emission peak versus time plot showing predictions for two additional reactions that were performed and resulted in samples with emission wavelengths within less than 10nm of the target wavelength…….…… 61

List of Tables

Table		Page Number
Table 1.	Representative List of Colloidal QDs versus Matrix/QD Systems……..	7
Table 2.	Reactions for 3 sets of data for comparison of SA to DA……	22
Table 3.	Shifts in emission peak and FWHM……	36

1. Introduction and Motivation

Luminescent quantum dots (QDs) are zero-dimensional semiconductors that may be used in a wide array of fields and which will, along with rod and tetrapod nanoparticle semiconductors, see use in applications such as electro-optical devices, spectral bar coding, light filtering, and computing applications. Quantum dots, rods, and tetrapods all have diameters that fall below the material's Bohr-exciton radius, which is the characteristic distance between an excited electron and its hole within a given material. This confines the electron-hole pair and causes the particles to possess specific material properties, such as shifted emission spectra, which are distinctly different from bulk properties of the same semiconductor material.

QDs have been studied for approximately two decades with views toward the aforementioned applications as well as for the pure science aspects concerned with the physical, electronic, and non-linear optical properties that lie between the molecular and the bulk.[1,2] While quantum dots have dimensions that are on the order of nanometers, they still contain hundreds to thousands of atoms. Most of the QDs that have been studied to date are dispersed in a host matrix such as glass or a crystalline counterpart. The newest research is often being carried out using colloidal quantum dots that may be placed on a substrate in a self-assembly process to produce films, patterns, and wires.[3,4]

Colloidal quantum dots require a capping structure to charge-passivate the surface and eliminate defect behavior by surface atoms.[5] Capping structures are the means by which the quantum dots interact with their environment. With the correct capping structure, quantum dots may be made into sensors or incorporated into biological systems. For these reasons, an investigation into how to make cadmium selenide (CdSe) quantum dots with varied capping structures, particularly, how to make the robust ZnS capped CdSe variety for biological marker or polymer microsphere tagging applications, is of interest. The use of trioctylphosphine oxide (TOPO), stearic acid (SA), dodecylamine (DA), phenyl sulfone (PS), aminophenyl sulfone (APS) and other organic molecules as the capping structures of CdSe QDs during initial production of the nanoparticles is being investigated for this thesis. In the larger scientific scope, these capping structures could facilitate integration of CdSe QDs into biological or chemical sensing systems, polymeric systems, LEDs, photovoltaics and many other functional

applications.[6,7,8,9] Additionally, the inorganic capping structure zinc sulfide is under investigation. Such capping structures will be used as the primary ligands for high temperature, airless, organo-metallic based, colloidal synthesis of CdSe quantum dots. This project explores initial production of these differently capped quantum dots in order that future projects may incorporate them into applied systems.

2. Background to Quantum Dots: Physics

Traditional bulk material has atoms and their associated electrons, which are allowed to remain in their "natural" arrangement. Such bulk material may be considered a conductor, an insulator, or a semiconductor. Energy bands are a consequence of energy level mixing as many atoms are brought together in a crystal with every material having a unique electron energy band structure. The energy bands are separated by band gaps, or regions where "no wavelike electron orbitals exist."[10] A metal has at least one band that is partially filled, while an insulator has energy bands that are either filled or empty. A semiconductor, by contrast, is a material in which "all bands are entirely filled, except for one or two bands slightly filled or slightly empty."[10] Figure 1 shows how the bands are filled differently for metals, insulators, and semiconductors. Kittel defines band gaps as resulting from the interaction of the conduction electron waves with the ion cores of the crystal.[10]

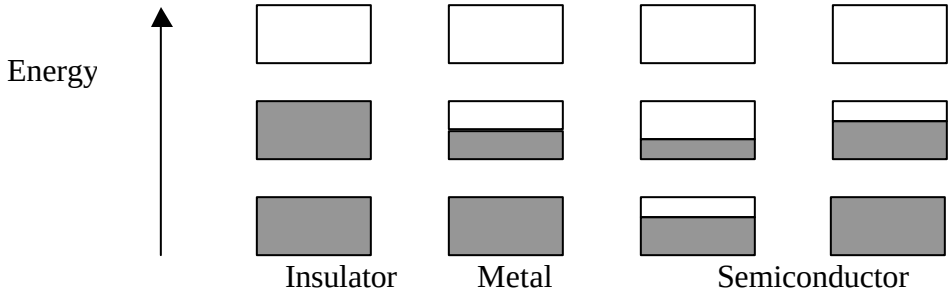

Figure 1. Schematic of electron occupancy of allowed energy bands for given materials.

Sandwiching a narrow-bandgap material between two large-bandgap materials creates quantum wells.[11] Such a sandwich confines electrons to movement between the two materials; thus, the energy levels of such a composite are quantized by the thickness

of the material. Electrons move between the full or semi-full valence band and the empty conduction band. Additionally, there is a shift in the absorption and emission spectra of the sandwiched material toward the blue due to increased self-energy. Quantum wires confine the energy level in a second dimension, causing photoexcited electrons and their corresponding holes to be spatially confined and making the energy states within the bands slightly compacted. Quantum dots confine this volume to an even greater extent, and cause the energy states to bunch together, thereby increasing the density of states and causing another shift of the emission wavelength.

Semiconductor nanostructures are so small that their electronic, optical, and physical properties deviate substantially from those of the bulk material. The size of the structure limits the exciton-Bohr radius of the bound electron-hole pairs, leading to altered electronic and optical properties, and causes high surface energy, which alters the physical properties.[12] The physical material is actually smaller than the natural exciton-Bohr radius, defined to be:

$$a_B = e_o h^2 / m_r e^2 \qquad \text{Eq. 1}$$

where e_o is the dielectric constant of the QD (at low frequencies), h is Planck's constant, and m_r is the reduced electron-hole mass.[12] The Schrödinger equation can be solved without Coloumb interaction for a spherical boundary condition that approaches the polyhedral surface of a quantum dot.[12] Such a solution is beyond the scope of this limited physics outline and shall be omitted here. However, the equations describing the electron energy levels in spherical quantum dots with infinite potential are of great importance because, together with the Schrödinger equation, they indicate the physical size dependence of the quantum confinement effect. Equations 2 and 3 stem from analysis of the Schrödinger equation and are used to find the energy levels of the hole and the electron, respectively, while Equation 4 indicates the energy of the system as a function of the sum of the electron and hole energy levels.

$$E^e = E_g + \frac{\hbar^2}{2m_e}\left(\frac{a_{n_e \ell_e}}{R}\right)^2 \qquad \text{Eq. 2}$$

$$E^h = -\frac{\hbar^2}{2m_h}\left(\frac{a_{n_h\ell_h}}{R}\right)^2 \qquad \text{Eq. 3}$$

$$\mathrm{E} = E^e + E^h = E_g + \frac{\hbar^2}{2m_e}\left(\frac{a_{n_e\ell_e}}{R}\right)^2 + \frac{\hbar^2}{2m_h}\left(\frac{a_{n_h\ell_h}}{R}\right)^2 \qquad \text{Eq. 4}$$

Note that in these equations $a_{n_e\ell_e}$ is the nth root of the ℓth order Bessel function for the electron while $a_{n_h\ell_h}$ is the nth root of the ℓth order Bessel function for the hole. The effective mass of the electron m_e and the effective mass of the hole m_h is different for each variety of semiconductor. Additionally, E_g is the band gap energy for the bulk semiconductor material.

The quantum confinement effect is what allows the tuning of absorption and emission wavelengths over the entire visible spectrum as a function of quantum dot size for CdSe. As is shown in Figure 2, the density of states changes from being continuous at all energy levels for a bulk material to becoming discrete transitions at certain energy levels for the quantum dot.

Furthermore, the quantum-mechanical wave functions of electrons and holes are confined within the limits of the material. Hence, when that confinement increases, the wave functions also become more confined.[12] Quantum confinement leads to altered emission lifetimes as well as altered luminescence quantum efficiency in quantum dots or rods.[13] Additionally, quantum confined structures exhibit a shifted band edge that allows for the production of varied emission peak wavelengths as dictated by the size of the confinement (i.e. the size of the quantum dot).

Within the previous theoretical discussion of energy levels and increasing confinement, several effects are omitted for simplicity's sake that must be mentioned here. They are homogeneous and inhomogeneous broadening effects that cause the theoretically discrete transitions to become Gaussian distributions of transitions. Homogeneous broadening is the result of phonon and other scattering effects that occur

during the excited electron's lifetime. Inhomogeneous broadening effects occur because when looking at a set of quantum dots there is a distribution of sizes and aspect ratios that translate into a small distribution of emission wavelengths rather than performing as a single discrete transition.

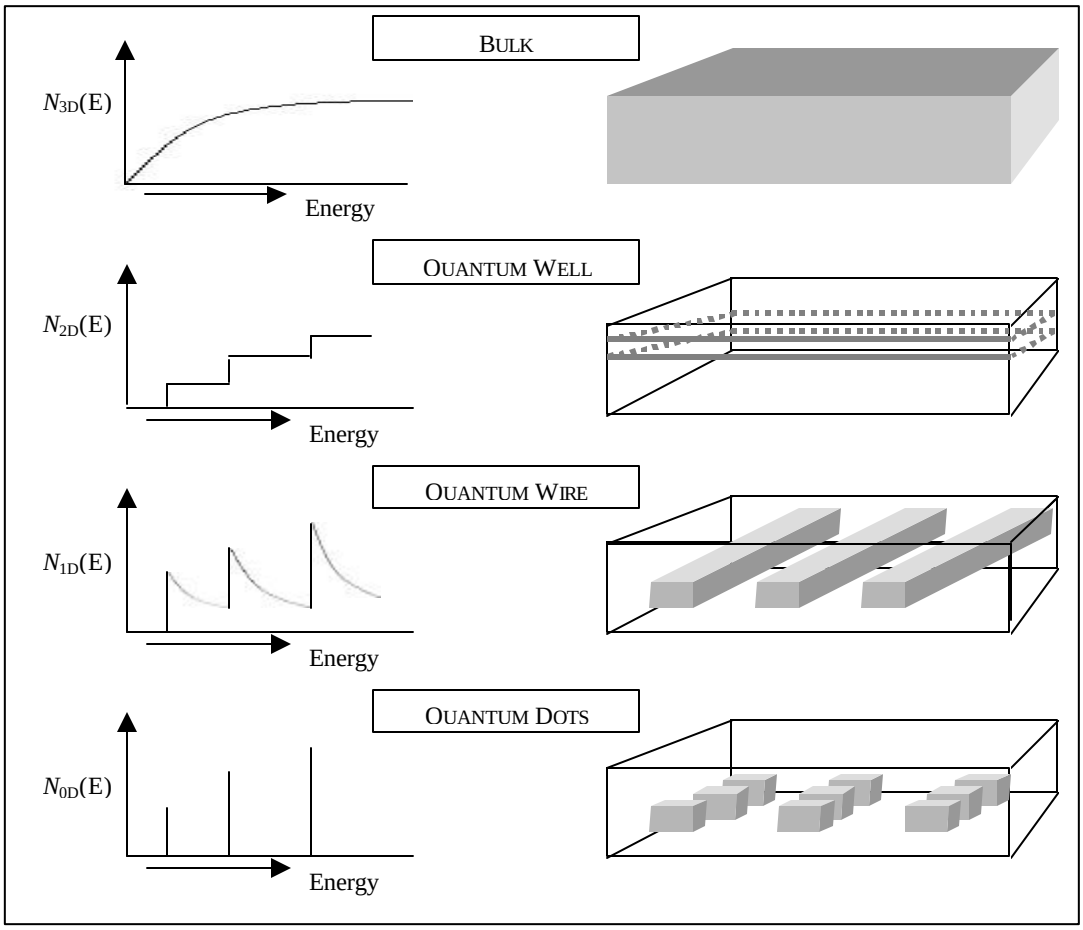

Figure 2. The progression of confinement and the effects on the density of states.

For promotion from one band to another to occur, an electron must absorb a photon of a given minimum energy. For an electron to jump from the valence band into the conduction band in CdSe, it must be excited by a high-energy photon such as that associated with ultraviolet light (for example, light with a wavelength of 365nm). Due to various scattering processes, including those mentioned in the paragraph above, during the excited electron's lifetime, electrons in the CdSe emit a photon from the bottom of the conduction band, within the visible spectrum (i.e. with less energy than was absorbed) as they jump back to the valence band.

Varying the length of the reaction and thereby adjusting the size of the CdSe quantum dots can produce nanoparticles with emissions covering the full spectrum of visible light. Size-tuning the emission wavelength occurs through confinement of the electron-hole pair within the QD structure as shown explicitly in Equation 4. This confinement of the electron-hole pair, as mentioned in the introduction, causes nanoparticle semiconductors to have material properties, the most obvious of which is the emission spectra, that differ from those of the bulk.

The emission photo shown in Figure 3 is of different-sized CdSe nanoparticles produced from the same reaction and, after cleaning, suspended in heptane. Notice how the emission spectra shift from blue to red. This shift corresponds to increasing reaction time (from left to right in the picture), which translates to increasing size of the nanoparticles. Hence, the larger the diameter of the material, the less the quantum confinement, and the more the material approaches bulk properties.

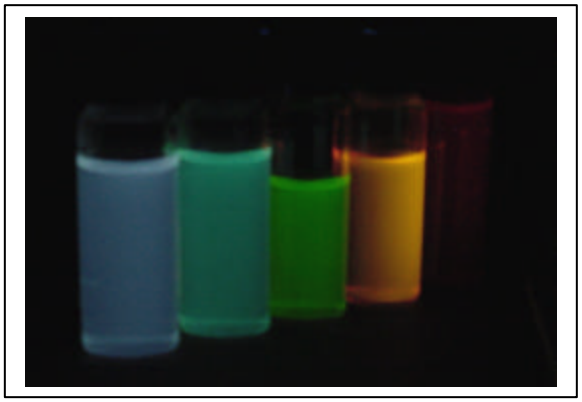

Figure 3. Emission spectra of different sized CdSe nanoparticles from the same reaction (Experimental results duplicating the work of Peng and Peng).[14]

3. The Colloidal Quantum Dot System

The advantages of a colloidal system over a matrix/QD system are many and varied. Three-dimensional interaction of quantum dots with their surroundings is desirable as it allows for applications such as tagging of DNA or aqueous monitoring for biological and chemical changes in a given environment. The colloidal system allows greater available surface area and environmental contact than the matrix/QD or substrate/QD system. The colloidal system also provides the ability to change the solvent

surrounding the quantum dots, deposit the dots through precipitation onto a substrate, or diffuse them into a polymer. Such flexibility makes bulk manufacturing of quantum dots desirable.

Quantum dots are being produced at the laboratory scale out of a variety of materials in accordance with the properties desired. Table 1 contains a sample list of quantum dots that are currently being produced, divided into colloidal and matrix/QD systems. As this paper deals exclusively with the colloidal system, references are provided for the matrix/QD systems, but they will not be discussed.

Table 1. Representative List of Colloidal QDs versus Matrix/QD Systems.

Colloidal	**Matrix/QD**
InP	GaAs[15]
GaP	None
$GaInP_2$	GaAs[15]
ZnS	Glass (SiO_2)[16]
ZnSe	Glass (SiO_2)[16]
PbSe	Phosphate Glass[17]
CdS	Glass (SiO_2)[18]
CdTe	Sodium Borosilicate (Sol-gel)[19]
CdSe	Glass (Sol-gel)[20]

3.1 Indium Phosphide, Gallium Phosphide, and Gallium Indium Phosphide

Indium phosphide (InP) quantum dots were first produced by the Micic group and shortly thereafter by the Alivisatos group.[21,22] The Alivisatos group used an indium chloride/$P(Si(CH_3)_3)_3$ reaction based on a modification of Micic *et al.*'s work that produced nanocrystals over a wide range of emission wavelengths with narrow size distribution and high crystallinity. Characterization techniques used by all groups include transmission electron microscopy for size and aspect ratio determination, powder x-ray diffraction for size and crystal structure determination, and fluorimetry / spectrophotometry for quantum yield determination.

Micic *et al.* expanded upon the work of Alivisatos to include InP, gallium phosphide (GaP), and gallium indium phosphide ($GaInP_2$) quantum dots.[23] The Micic

group used a combination of chloroindium oxolate, chlorogallium oxolate, and $P(SiMe_3)_3$ as precursors in a high temperature, high boiling-point, solvent based, airless reaction. Spectrophotometric work on these quantum dots characterized them as absorbing in the visible spectrum between 400nm and 700nm, with GaP covering the shorter wavelengths and InP the longer ones, while $GaInP_2$ was not sufficiently mono-disperse in size to allow spectrophotometric investigation.

Unfortunately, most of the early work with InP demonstrated through the low photoluminescent yield of all samples that there were a large number of surface trapped states where electron-hole non-radiative recombination could occur. Hence, Micic *et al.* found a hydrofluoric (HF) etch method by which one could remove what were essentially defects in the quantum dot surface structure and thereby greatly enhance the photoluminescent efficiency.[24] Weller *et al.* expanded upon Micic's work, while Zunger *et al.* explained that the surface traps quenching the luminescence of InP nanocrystals was related to In and P dangling bonds which provide surface states that are involved in the recombination process.[25,26] Weller *et al.* also explains that low photoluminescent efficiency is the result of inadequate surface passivation because TOPO cannot cap phosphorous, which may be remedied by the HF etching which removes the phosphorous atoms from the InP nanocrystal surface and leaves an indium rich surface to be capped by TOPO.

3.2 Zinc Sulfide and Zinc Selenide

Zinc sulfide (ZnS) QDs and zinc selenide (ZnSe) QDs have each been synthesized by numerous groups around the world; current research focuses on producing larger quantities, doping basic ZnS with manganese, lead (II), and cadmium, and varying the capping structures of the resulting quantum dots.[1,27,28,29] Kubo *et al.* are working to modify the surface chemistry of ZnS quantum dots doped with Mn.[27] The fact that doping studies have commenced on ZnS indicates that the ease with which ZnS is produced using the reverse micelle method has allowed for a much greater investigation and experimentation than other quantum dot types which require high temperature chemistry using organo-metallic precursors.

The reverse micelle method produces quantum dots using two different solvents to create micelles within which the reaction is contained. This procedure is easily performed on a laboratory benchtop, requires few large-scale pieces of equipment for reaction control or containment, and little temperature control. Furthermore, the relative stability and chemical inertness (with an appropriate capping group) of ZnS makes it an attractive quantum dot variety for environmentally friendly use. The attractiveness of ZnS has led to the invention of a simple, inexpensive, and reproducible procedure for the large-scale synthesis of ZnS nanoparticles by Rajesh Mehra's group.[30] The further advantage of the production technique is the water-soluble nature of the resulting nanoparticle powders. The method employed by Mehra *et al.* to achieve the water-solubility, though not directly applicable to CdSe, could be modified to allow for water-soluble CdSe quantum dots.

3.3 Lead Selenide

Lead selenide is one of the newer quantum dot types being produced and studied on a laboratory scale. The chemistry employed varies widely depending on the group producing the dots. Trindade *et al.* produces PbSe quantum dots using $Pb\{Se_2CN(C_2H_5)_2\}_2$ and $Pb\{Se_2CN(CH_3)(C_6H_{13})\}_2$ as single source precursors.[31] By dissolving these precursors into the high temperature coordinating solvent, tri-octylphosphine (TOP), and then using tri-octylphosphine oxide (TOPO) as the medium in which the reaction takes place, Trindade *et al.* were able to produce PbSe with a cubic structure.[31]

Murray *et al.* reported a high temperature co-precipitation approach in an organic solution of diphenyl ether and oleic acid, using lead acetate and a selenium/TOP stock solution.[32] This method seems a little less complicated than the Trindade approach as it required no synthesis of precursors and produced monodisperse, 6.0nm diameter, PbSe particles with less than 10% size distribution. Additionally, the Murray group produced diphenyl ether capped PbSe particles that could be self-assembled into films that were annealed to drive off the organic capping materials to leave PbSe monolayer films. This technique could conceivably be used with CdSe nanoparticles as well, but has yet to be applied broadly to nanoparticles.

3.4 Cadmium Sulfide

Cadmium sulfide (CdS) is often the nanoparticle semiconductor chosen first when starting a project because of the ease of its fabrication. There is no high-temperature, airless chemistry involved and no molten solvents. Instead, CdS QD fabrication employs a reverse micelle aqueous solution in which the micelle's size dictates the size of nanoparticle. Based on early semiconductor nanoparticle work performed by Kortan *et al.* in 1990 on CdSe and ZnS, Yang and Holloway found that various reverse micelle methods could be used to produce both plain CdS QDs and CdS QDs doped with Mn.[33,34] The difficulty with this method is that the resulting nanoparticle colloids are not monodisperse. The Gaussian distribution of nanoparticle sizes is quite large and hence, the emission spectra of the resulting quantum dot solutions are quite broad, with the best full-width half-maximum (FWHM) values being approximately 70nm (note FWHM measures the width of the emission curve at half of its full height).[34]

3.5 Cadmium Telluride

Cadmium telluride (CdTe) QD production has, until recently, generally been reported as a subset of CdSe preparation and hence, little independent information has been available about CdTe. Examples of such reporting include papers by Peng and Peng, Bawendi, and Talapin.[14,35,36]

Notable exceptions include Tang *et al.*'s work on CdTe nanowires and Talapin *et al.*'s work on CdTe synthetic approaches.[4,37] Tang's work emphasizes the growth of extremely long CdTe wires using CdTe QDs as building blocks. This approach is a rather novel means of building larger structures out of QDs using the material's dipole interactions rather than outside capping structures as the driving force for self-organization of the luminescent nanoparticle semiconductors. Alternatively, Talapin focuses on the synthesis of CdTe using a TOPO/dodecylamine combination solvent/capping structure, much as Peng's work demonstrated the same solvent combination worked for CdSe production (see below).

3.6 Cadmium Selenide

The model system for colloidal quantum dots produced by a high temperature, airless reaction method is cadmium selenide.[1] Early CdSe quantum dots were produced in 1993 by Alivisatos's group using organo-metallic chemical techniques. [38] Thereafter, other groups, including Hines's and Bawendi's, synthesized colloidal CdSe quantum dots by other means as well. [39,40] Furthermore, Hines's and subsequent groups such as Peng's investigated new capping structures for CdSe such as dodecylamine and stearic acid.

Cadmium selenide is interesting because it has unique optical properties in the visible spectrum. Through strict dimensional control, QDs can be produced to emit narrow color spectra that can be clearly distinct from one another at the full-width half maximum of the peak emission and have typical full-width half-maxima of only 25nm to 30nm. Because the color spectra do not overlap, one can increase the number of distinct colors, as compared to organic dyes, that are being detected simultaneously. The use of different emission colors and intensities as tags is called spectral multiplexing and may be applied to such applications as tagging of genes or proteins.[41,42] Figure 4 shows quantum dots that have been embedded in carboxyl modified polystyrene beads of 5µm diameter for exactly such an application. The three spheres, if correctly functionalized, could be used in DNA detection, or as chemical and biological sensors. Please see Appendix A for a paper describing work performed, in part, by the author on the subject of QD tagged microspheres used in DNA microarrays.

Figure 4. CdSe quantum dots embedded in polystyrene microspheres emitting at three distinct visible wavelengths simultaneously, all under the same ultraviolet light source.

3.6.1 Cadmium Selenide Structures

Cadmium selenide quantum dots have a wurtzite or zinc blende structure at room temperature, as shown in Figure 5 and Figure 6, respectively.[43] The structure of individual dots depends on the growth mechanism, pressure, and temperature applied. The surface tension produced as a result of the high surface to volume ratio inherent to nanoparticles distorts the surface of the nanoparticle, making it a nearly spherical polyhedron.

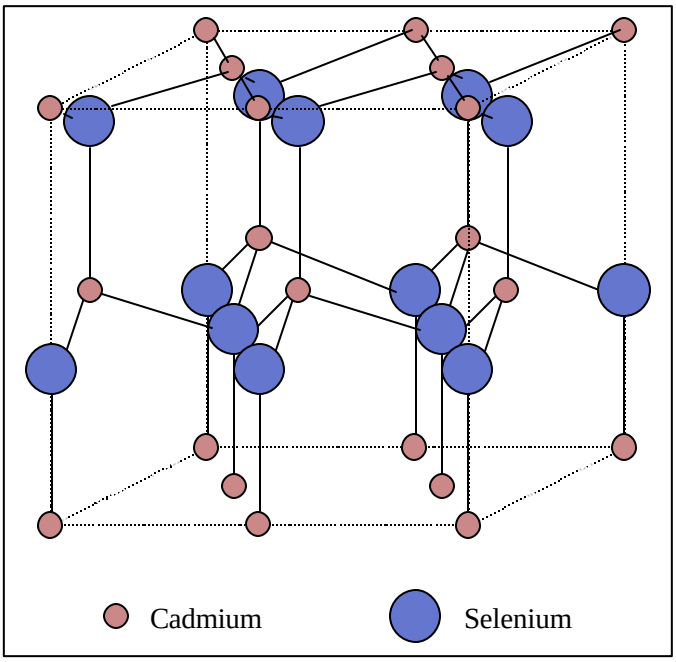

Figure 5. Schematic of wurtzite structure.

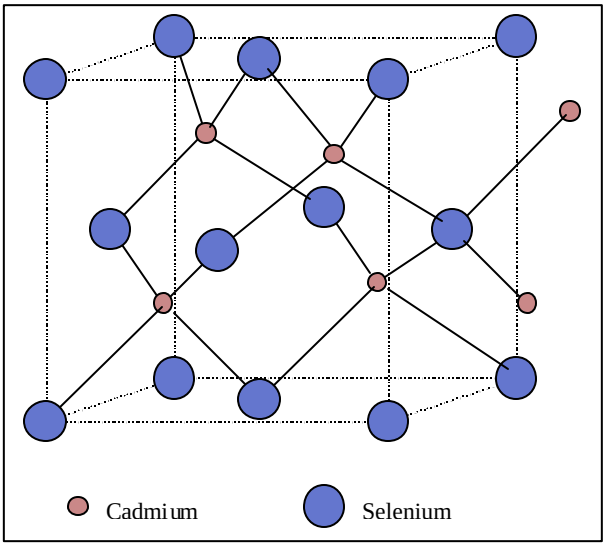

Figure 6. Schematic of zinc blende structure.

4. Chemistry

Almost all of the reactions to produce CdSe quantum dots use organo-metallic precursors and involve high temperature, solvent based, airless chemistry. A notable exception is the photo-initiated aqueous reaction chemistry presented by Zhu *et al.* in 2000.[44] For all synthetic routes, the goal is monodisperse, highly crystalline, colloidal quantum dots that exhibit the size-tuneable absorption and emission characteristics mentioned earlier.

In past trials, performed by the author for his senior honors thesis, cadmium oxide was heated under an argon blanket in 90% purity trioctylphosphine oxide (TOPO) and tetradecylphosphonic acid (TDPA) at 340°C until the color changed from dark red-brown to nearly colorless.[14] Simultaneously, selenium shot was stirred in trioctylphosphine (TOP) under argon until the selenium dissolved. The temperature of the Cd-TOPO solution was dropped to 270°C once the solution was nearly colorless. Once these steps were finished, the selenium solution was injected into the cadmium solution and the reaction began immediately; aliquots were removed at various time intervals. The various aliquots contained different sized nanoparticles according to the growth time in solution and hence, different emission peaks were achieved, as shown in Figure 7. The product of the reaction was washed with methanol and toluene and then stored in any of a variety of solvents such as heptane, hexane, dichloromethane, or toluene. The product was a quantum rod (or QD for the later reactions) coated in TOPO, which acts to "cap" the

particle and enhance luminescent yield by decreasing surface-related defect states (see section 4.1, below).

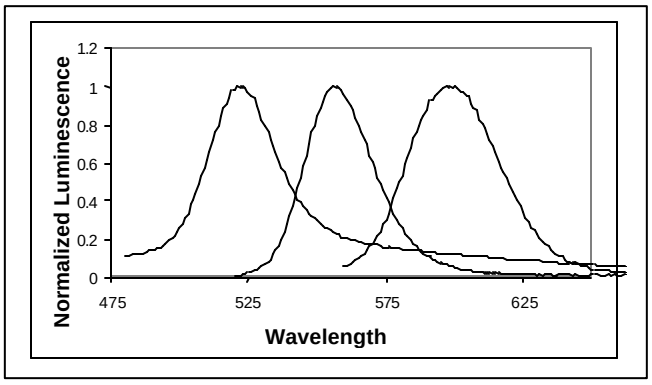

Figure 7. Spectra corresponding to the second, third and fourth vials shown previously in Figure 3; note how the spectra are clearly distinct at full-width half maximum. (Experimental work duplicating (in part) the work of Peng and Peng).

4.1 Capping Structures

4.1.1 Organic Capping Structures

The chemical composition and structure of materials capping cadmium selenide varies tremendously, as is necessary for a material that has so many possible uses. The capping structures are tailored to meet specific application based parameters such as water-solubility, chemical reactivity, or to keep particles from agglomerating. The easiest capping structures to produce (though by no means simple), and hence the most commonly produced, are those that also act as the solvent in which the organo-metallic reaction occurs. Such high boiling point, organic solvents abound; however, only a few have been tested. Of these, only TOPO has been thoroughly investigated over a wide range of production and subsequent environmental applications. Figure 8 shows the chemical structure of TOPO and Figure 9 shows a schematic of the capping structure/quantum dot interaction as proposed by Peng and Alivisatos.[5]

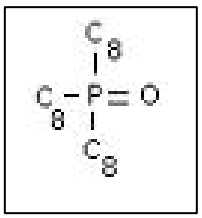

Figure 8. Trioctylphosphine oxide structure.

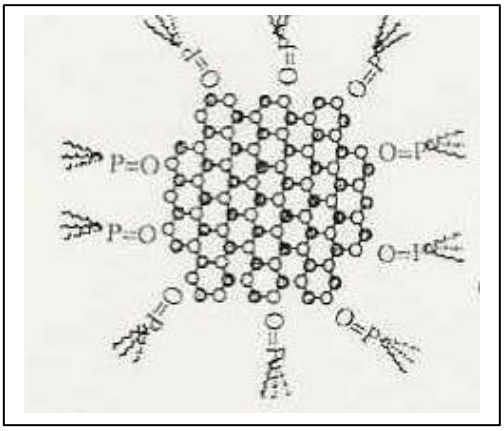

Figure 9. Peng and Alivisatos's schematic of how TOPO interacts with the surface of a CdSe quantum dot nanoparticle.[5] Reprinted with permission from J. Am. Chem. Soc. 1997, 119, 7019-7029. Copyright 1997 American Chemical Society.

Peng and Peng also described methods for other capping structures and provided some of the basis for the current work.[43] Peng and Peng briefly describe the stearic acid and dodecylamine reaction chemistries and provide some initial data on resulting emission and absorption spectra. Figure 10 shows the chemical structures of these two capping structures. Notice that dodecylamine does not have a double-bonded oxygen with which the quantum dot could potentially bond. The two free electrons on the nitrogen are likely to be what allow for interaction with the QD.

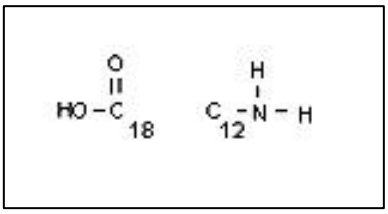

Figure 10. Chemical structures of stearic acid (left) and dodecylamine (right); Note: hydrogens are not shown in the carbon chains C_{18} and C_{12}.

4.1.2 Inorganic Capping Structures

Inorganic capping structures such as semiconductor materials and SiO_2 have also been proposed and tested. A wider band-gap semiconductor capping structure eliminates the surface-related defect states (dangling bonds) and confines charge carriers to the core material due to the band offset potential.[34] Further confinement allows for more of the

absorbed energy to be emitted as photons rather than dispersed as lattice vibrations and the elimination of the surface defect states reduces the amount of surface recombination of electron-hole pairs. SiO_2 structures are being explored for their possible uses as fully inert but porous shells for the optically active and biologically toxic semiconductor core.

Hines *et al.* was the first to report (1996) a successful semiconductor capping structure using a high temperature, airless chemistry approach, while Kortan *et al.* had reported such capping structures in 1990 using a reverse micelle approach. [39] Kortan reports on both CdSe capped with ZnS and ZnS capped with CdSe; however, the particles range over a fairly large set of sizes and, correspondingly, the photoluminescence ranges over the entire visible spectrum for a single sample. Using zinc sulfide as the capping structure, Hines produced core/shell particles with enhanced quantum yields and increased environmental stability. The zinc sulfide structure is now the best tested of the semiconductor capping structures, usually in a TOP/TOPO solvent. Yang and Holloway also report a reverse micelle method to produce a zinc sulfide capping structure.[34] The reverse micelle method often used to make CdS nanoparticles, is a low temperature, aqueous-based reaction described in section 3.4.

A method similar to the one used by Hines was employed by Peng, *et al.* to produce CdSe quantum dots capped with CdS. The CdSe/CdS quantum dots typically had shells of several atomic layers amounting to 0.7nm. Of particular interest in the Peng *et al.* work is the assertion that a CdSSe alloy is not formed, but rather a fully crystalline shell of CdS around the core of CdSe is grown epitaxially.

Gerion *et al.,* from Alivisatos's group, report a method of SiO_2 capping of ZnS capped CdSe quantum dots using silane precursors to form a network of siloxane bonds around the individual CdSe particles and eventually producing a SiO_2 shell. Figure 11 shows a schematic of the shell structure they proposed.[45]

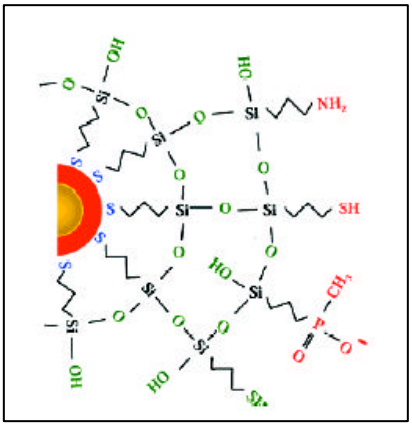

Figure 11. Schematic of SiO_2 capping of CdSe/ZnS structure with various functional groups as proposed by Gerion et al. Reprinted with permission from J. Phys. Chem. B 2001, 105, 8861-8871. Copyright 2001 American Chemical Society

Gerion reports, in another paper, that amino, carboxyl, and thiol groups may be introduced to the surface of such a shell, allowing for DNA attachment.[46] The SiO_2 capping allows for conjugation with DNA through well-understood mechanisms that may also be used to attach proteins and other organic molecules. Hence, a three-layer system is introduced, which provides both high quantum yield and good biological compatibility. SiO_2 capping also provides excellent stability over a wide range of pH and salt concentrations in water.

Overall, CdSe quantum dots with varied capping structures are useful in many applications. Three examples of such variation are trioctylphosphine oxide, dodecylamine, and stearic acid. With the correct synthesis methods and careful attention to the traits, such as melting point and boiling point, of each different capping structure, one is able to produce quantum dots with good monodispersity of size and hence, of emission wavelength.

5. Facilities and Equipment

For syntheses, standard airless chemistry procedures were followed. Safety equipment included ground-joint glassware for airless procedures, nitrile gloves for all work, high temperature gloves for hot work, half-mask respirators for all measurement work involving cadmium oxide, selenium powder, or toxic capping structures, and metal

or glass equipment for high temperature work. Furthermore, Tygon gas lines with a high-pressure regulator and argon or nitrogen were used for the purge equipment and a fume hood was necessary for exhausting all gaseous byproducts.

Originally, a standard piece of equipment in most chemical synthesis labs, the glass insulated heating mantle, was employed for providing the elevated temperatures, between 200°C and 400°C, necessary for the reactions described herein. However, through several demonstrative failed and non-repeatable reactions, a realization came about that a better, more reliable, and less fluctuating heat source was necessary. Additionally, after a number of glass encapsulated magnetic stir bars punctured the vessels in which they were stirring, an industrial stirrer was also deemed necessary. After quite a long search, a set of specially built polymer reactors was found that performed quite well. The building of such reactors was undertaken and the first molten bismuth bath reactor has been tested and performs well. The temperature stability that approximately 30 pounds of molten bismuth alloy affords is quite good and allows for stable long-time reactions without large fluctuations in temperature (the reactor that was built fluctuates less than 2 degrees over the period of a day) or loss of heat distribution (in glass insulated heaters a single filament may go out and leave a cold spot in the material around the round-bottom reaction flask).

Additionally, for the purifying and characterization of quantum dots, the following were necessary: microcentrifuge, micropipettes, ultrasonicating bath, transmission electron microscope, fluorimeter, spectrophotometer, and fluoroscope with ultra-violet excitation and full visible range emission capabilities. Because all waste produced was contaminated with cadmium, a waste stream protocol was established with Environmental Health and Safety. To decrease some of the costs of the project we arranged with Environmental Health and Safety to have some organic solvents and precursors delivered as they became available in surplus.

6. Procedure

The work for this project is based on the author's work performed previously during his undergraduate education. Major tasks included the test production of quantum dots with TOPO capping structure, the test production of quantum dots with varied

capping structures, the writing of procedures for each production scheme, a literature review and the TEM, fluorimetry, and spectrophotometry investigation of the QDs in heptane. The current project enlarges the investigation of specific test production reactions including dodecylamine (DA), stearic acid (SA), and phenyl sulfone (PS) and also investigates aminophenyl sulfone (APS), 4,4'dichlorodiphenyl sulfone, 4,4' difluorodiphenyl sulfone, sulfanilamide and zinc sulfide. Furthermore, the master's work expanded to include applications of quantum dots embedded in optical components, microspheres, and bulk polymers with final possible applications in DNA microarrays, lighting, and sensors. A bismuth bath reactor was constructed at the end of the project to facilitate future production of CdSe, InP, and other semiconductor nanoparticle materials.

6.1 Experimental Details

6.1.1 Materials

Trioctylphosphine oxide (TOPO, 90% and 99% pure), cadmium oxide powder, selenium shot, and trioctylphosphine (TOP, 95% pure) were purchased through Sigma-Aldrich. Tetradecylphosphonic acid was purchased through Alfa Aesar. Organic solvents (at minimum of HPLC grade) such as heptane, methanol, and toluene were purchased through Burdick and Jackson. Hexamethyldisilathiane, dimethylzinc, stearic acid, dodecylamine, and other capping structure components were purchased through Aldrich as well.

6.1.2 Procedural Safety

For each reaction, all equipment that was to be in direct contact with quantum dot containing material was cleaned and dried. Furthermore, all materials used in conjunction with the initial high temperature reaction were non-polymeric, high temperature and thermal shock resistant, as well as nonporous relative to the nanometer size scale of the quantum dots. All wastes were disposed of through the aforementioned waste stream set up with Environmental Health and Safety. A respirator was worn during the measuring of dodecylamine as it burns mucous membranes and cadmium oxide as it is a carcinogenic heavy metal. All work during reactions and cleanings was performed under a fully operational fume hood with the appropriate protective equipment in place.

6.1.3 Synthesis of TOPO Capped CdSe Quantum Dots

This synthesis was the basis from which all the other quantum dot work stemmed, both in the literature and in the work for this thesis. Early batches resulted in rods, which, while useful in their own right, were not the primary objective of this project. A full description of a typical rod-producing reaction is contained in Appendix B. In an attempt to decrease the aspect ratio of the quantum rods produced by the aforementioned method, the concentration of tetradecylphosphonic acid (TDPA) was varied and nearly monodisperse CdSe quantum dots capped with TOPO were synthesized. The TDPA concentration was varied from the original rod formulation (5.91 wt % of the TOPO weight) to 2.35 weight percent. However, it was found that the 90% purity of the TOPO was not sufficient. With 10% impurities in the TOPO, there were many possible compounds that always allowed rods to form. Impurities act to nucleate the necessary number of dots initially, while TDPA controls the growth surfaces on the semiconductor nanoparticles in a reaction, causing some surfaces to grow faster than others.[47]

Alivisatos *et al.* found that the role of hexylphosphonic acid (HPA) was to increase the growth rate of the (001) face of CdSe. Hence, by the fact that TDPA and HPA have an identical functional group and differ only by the carbon chain length, TDPA could be assumed to do the same, and Peng *et al.* demonstrated as much in 2001.[43] Upon the switch to 99% TOPO, 1.5 weight percent of TDPA produced excellent quantum dots following the time and temperature regime set up previously for rods. The reaction was run under airless conditions using argon or nitrogen as the purge gas and aliquots were taken on an approximately doubling scale (usually starting at 10 seconds, then 20, 45, 90, and so on) and typically quenched in methanol.

A typical reaction consisted of first producing a selenium stock solution by dissolving selenium pellets in trioctylphosphine over a period of an hour or so under moderate heat (i.e. 80 to 100 °C). TOPO, cadmium oxide, and tetradecylphosphonic acid were mixed and heated at 340°C, under argon or nitrogen, for approximately 1.5 to 2 hours (or until a nearly colorless solution was achieved). As with rods, the temperature was allowed to drop to 270°C, and the cooled selenium stock solution was injected and aliquots were taken, also as described for rods. If lower reaction temperatures were used,

the reaction occurred more slowly; if higher reaction temperatures were used, the reaction happened more quickly; 270°C was found to allow for a quick but controllable reaction. The resulting precipitates were washed multiple times with methanol to remove extra selenium and cadmium. The cleaned precipitate was suspended in toluene and then re-precipitated using methanol in order to remove excess TOPO. Usually, the quantum dots were stored in heptane, dichloromethane, hexane, or another organic solvent. The ratio of cadmium to selenium did not have to be altered; it remained at approximately 4:3.

6.1.4 Synthesis of Stearic Acid Capped CdSe Quantum Dots

Following upon the recent work of Peng *et al.*, stearic acid capped cadmium selenide quantum dots were synthesized using cadmium oxide as the cadmium-providing precursor.[43] The standard selenium stock solution mentioned above was used in this reaction as well, and the cadmium to selenium ratio was not altered. The stearic acid (SA) reaction kinetics were found to be extremely fast at the high reaction temperature of 270°C. The protocol described for TOPO capped dots above was therefore amended by decreasing the reaction temperature to allow for the collection of quantum dots over a wider range of sizes. The total reaction time was thus increased from approximately 12 minutes at 270 °C to one hour at 200°C. The quantum dots were, again, precipitated and stored in methanol.

6.1.5 Synthesis of Dodecylamine Capped CdSe Quantum Dots

Using Peng *et al.*'s recent work as a basis, dodecylamine capped cadmium selenide quantum dots were synthesized using cadmium oxide as the cadmium providing precursor.[43] The standard selenium stock solution mentioned above was used in this reaction as well and the cadmium to selenium ratio was not altered. Since this reaction has much slower reaction kinetics, the protocol described for TOPO capped dots was amended by changing the collection time between aliquots for all dodecylamine (DA) containing reactions to span over one hour, in order to allow for the collection of quantum dots over a wider range of sizes. Additionally, the reaction temperature was changed to 200°C from 270°C to account for the degradation of the DA at higher

temperatures. Dodecylamine capped quantum dots were precipitated and stored in methanol.

6.1.6 Comparison of Stearic Acid and Dodecylamine Capped CdSe in Terms of Reaction Rate

A comparison of SA and DA capped CdSe was undertaken in order to identify whether the use of different capping structures as ligands in the reaction that forms CdSe affected the production of the dots. In order to compare adequately, three different sets of data were collected. First, a set of reactions containing various percentages of SA (with the remainder TOPO) was developed. An analogous set was created for the DA capping structure. The third set of reactions was performed to rule out temperature variations as the reason for differences between the first and second sets. Each reaction in the third set contained a 95% SA/5% TOPO mixture but was performed at varying temperatures between 200ºC and 295ºC. The experimental setup is displayed below in Table 2. Collection times for sets one and two were one hour, while the collection time for set three was 12 minutes.

Table 2. Reactions for 3 sets of data for comparison of SA to DA.

Set 1: Varying percentage SA reactions performed at 200 ºC	Set 2: Varying percentage DA reactions performed at 200°C	Set 3: 95% SA / 5% TOPO reactions performed at various temperatures	
98% SA / 2% TOPO	98% DA / 2% TOPO	200 ºC	255 ºC
95% SA / 5% TOPO	95% DA / 5% TOPO	215 ºC	265 ºC
90% SA / 10% TOPO	90% DA / 10% TOPO	225 ºC	275 ºC
80% SA / 20% TOPO	80% DA / 20% TOPO	235 ºC	285 ºC
50% SA / 50% TOPO	50% DA / 50% TOPO	245 ºC	295 ºC

6.1.7 Synthesis of Phenyl Sulfone Capped CdSe Quantum Dots

Using Murray's recent work on PbSe capped with diphenyl ether as a starting point in looking for possible new capping structures, CdSe quantum dots with a phenyl sulfone capping structure were synthesized using the following procedure.[32] As shown in Figure 12, phenyl sulfone contains two double bonded oxygens that can interact with the surface of the quantum dot, similarly to stearic acid and TOPO, which each have only one such oxygen.

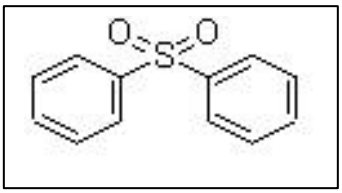

Figure 12. A schematic of the structure of phenyl sulfone.

The standard selenium stock solution mentioned above was used in this reaction as well, and the cadmium to selenium ratio was not altered. Since the kinetics were unknown for this reaction, a number of reactions at different temperatures were performed before 270°C was selected as the reaction temperature. The bath was pre-warmed to 280°C and the two-neck flask containing the reaction mixture was lowered into the bismuth bath. The red solution turned colorless almost immediately and the temperature was lowered to 270°C; the selenium stock solution was injected thereafter. Growth of the CdSe quantum dots ensued over a period of up to 8 hours, during which time aliquots were drawn out at approximately doubling intervals (45s, 1.5min, 3 min, 6 min, 12min, 24 min, etc.).

6.1.8 Synthesis of Aminophenyl Sulfone Capped CdSe Quantum Dots

Upon finding that phenyl sulfone acted as an excellent capping structure for CdSe quantum dot synthesis and passivation, other compounds were explored; 4-aminophenyl sulfone (APS) was one of these other compounds. As shown in Figure 13, the structure of aminophenyl sulfone is similar to phenyl sulfone, but has the additional primary amine groups attached to the phenyl rings. It is important to note that with this capping structure the amine *or* the double bonded oxygens can interact with the surface of the quantum dot.

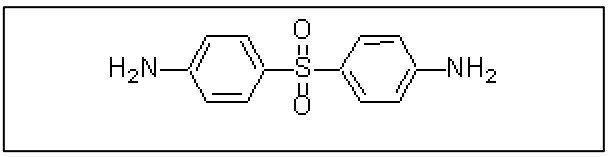

Figure 13. A schematic of the structure of 4-aminophenyl sulfone.

The standard selenium stock solution was used and the cadmium to selenium ratio remained unchanged. Since the kinetics were, again, unknown for this reaction, a number of reactions were performed at different temperatures and 230°C was thereby selected as the reaction temperature. The bismuth bath was pre-warmed to 230°C and the two-neck flask containing the reaction mixture was then lowered into the bath. The red solution turned colorless after approximately 10 minutes and the selenium stock solution was injected thereafter. Growth of the CdSe quantum dots ensued over a period of up to 6 hours during which time aliquots were drawn at time intervals similar to those for phenyl sulfone.

6.1.9 Synthesis of 4,4' Dichlorodiphenyl Sulfone and 4,4' Difluorodiphenyl Sulfone Capped CdSe Quantum Dots

Upon finding that aminophenyl sulfone acted as a viable capping structure for CdSe quantum dot synthesis and passivation, and upon realizing that the phenyl and aminophenyl sulfones both had a high density of electrons at the double bonded oxygens, reactions of 4,4' dichlorodiphenyl sulfone (ClPS) and 4,4' difluorodiphenyl sulfone (FPS) were undertaken to test whether compounds with lower electron densities at the double bonded oxygens would also cap CdSe. As shown in Figure 14 and Figure 15, the structures of 4,4' dichlorodiphenyl sulfone and 4,4' difluorodiphenyl sulfone are very similar to aminophenyl sulfone, but have chlorines and fluorines, respectively, in place of the amines, attached to the phenyl rings.

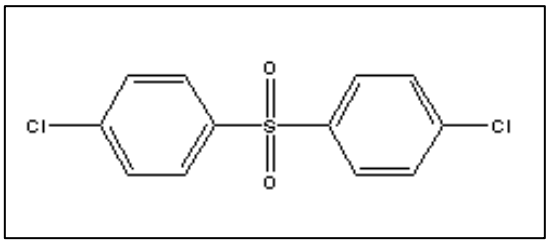

Figure 14. The structure of 4,4'-dichlorodiphenyl sulfone.

It is important to note that the strong electronegativity of the atoms actually draws the electron density away from the center of the molecule and toward the respective chlorine or fluorine, making the oxygens less reactive than in the aminophenyl or phenyl sulfones. With this in mind, the reactions were performed expecting very different results, including the possible lack of formation of semiconductor nanocrystals.

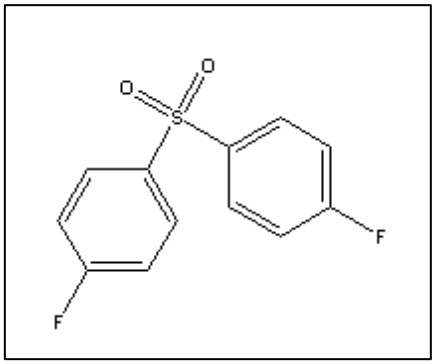

Figure 15. The structure of 4,4'-difluorodiphenyl sulfone.

The standard selenium stock solution was used and the cadmium to selenium ratio remained unchanged. Since the kinetics were expected to be different for these reactions, the boiling point for each material was determined and the reactions were performed below these temperatures. The final reaction temperatures for both FPS and ClPS were 250°C. The bath was pre-heated to 250°C and the two-neck flask was lowered into it. The red solution turned colorless and the selenium stock solution was injected thereafter. In the case of FPS, heavy condensation recrystallization of the sulfone occurred at the top of the flask, indicating a possible loss of the material from the reaction. However, the FPS

reaction was allowed to take place over a period of an hour during which time aliquots were drawn at the doubling time intervals described earlier, in an attempt to grow CdSe quantum dots. It must be noted that the possible loss of some of the material from the reaction should be taken as an unknown in repeating the reactions, but that the effect seems negligible. The ClPS reaction occurred at a much faster rate of 3 minutes for the entire reaction.

6.1.10 Synthesis of Sulfanilamide Capped CdSe Quantum Dots

Since the production of CdSe capped with symmetric sulfones succeeded, the next logical step was to investigate asymmetric sulfones. As a test case, sulfanilamide was selected for the possible additional benefit of containing two amine groups to which structures could be attached while the sulfone caps the quantum dot. The structure of sulfanilamide is shown in Figure 16.

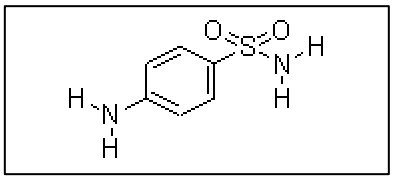

Figure 16. The structure of sulfanilamide.

A typical reaction for sulfanilamide capped CdSe consisted of the following generalized procedure. The standard selenium stock solution was used and the cadmium to selenium ratio remained unchanged. Since the kinetics were expected to be different for these reactions versus reactions of the symmetric sulfones, the boiling point of sulfanilamide was determined and the reaction temperature set at 205°C. The bath was pre-heated to 205°C and the two-neck flask was lowered into it. The red solution turned colorless in approximately 10 minutes and the selenium stock solution was injected thereafter. The reaction was allowed to take place over a period of several hours during which time aliquots were drawn.

6.2 Synthesis of Zinc Sulfide Capped CdSe Quantum Dots (CdSe/ZnS)

The synthesis of CdSe/ZnS nanoparticles is a more lengthy and involved process than any of the above. This is primarily due to the necessity of a second injection of material, ZnS precursor, and the fact that the components of that precursor are more hazardous and environmentally sensitive. However, the resulting nanoparticles are preferred for several reasons. Of primary importance is the increased quantum yield and hence, increased luminescence as compared to TOPO capped dots. Furthermore, the zinc sulfide capped CdSe surface may be considered smoother because it does not have the hydrocarbon chains creating a pseudo surface above the actual surface. Hence, it diffuses much more easily into polymers. Additionally, CdSe/ZnS is the base quantum dot structure upon which glass capping is performed, which makes the material chemically inert but still optically active, a very important characteristic for DNA or cell tags. (Organically capped quantum dots may still be chemically toxic to cells or living organisms.)

Preparation for the CdSe/ZnS synthesis reaction is a three-step process. First, a standard CdSe/TOPO reaction is prepared; the standard reactants are used and the selenium stock solution is prepared as a second step. The third step involves dissolving hexamethyldisilathiane (sulfur precursor) and dimethylzinc (zinc precursor) into TOP in a fully airless and waterless environment with argon purged syringes and flasks. This solution must be made fresh for every reaction. Additionally, with the high toxicity of dimethylzinc and the extreme stench of hexamethyldisilathiane, all work must be carried out in a fume hood without any removal of materials that come in contact with either substance unless in a sealed container.

Production of CdSe/ZnS begins with a standard TOPO reaction that is started at 340°C. Once colorless, the temperature is lowered to 310°C, selenium stock solution is injected, and the temperature is dropped to 300°C for initial CdSe core particle growth. After some growth time, the ZnS precursor solution is injected over a period of one to two minutes to allow for formation of the shell structure. The temperature is immediately dropped to approximately 100°C for the remainder of the reaction to anneal the particles and grow thicker ZnS shells on the CdSe cores. The product of the reaction is quenched in methanol and purified according to the procedures described earlier for CdSe/TOPO.

6.3 Characterization of Resulting Quantum Dots

Emission, absorption, size, and shape characterization of the material produced through the above reactions was undertaken using standard techniques for fluorimetry, spectrophotometry, and transmission electron microscopy, respectively. Through these techniques one was able to determine the quality of each reaction, and whether any mistakes were made during the synthesis that led to other shapes or aggregation of the particles. Additionally, the simple test of whether or not the particles suspended in certain organic solvents was used as a "go / no-go" test of samples to indicate whether a mistake was made during purification.

6.3.1 Fluorimetry

Emission spectra were taken using a Photon Technology International (PTI) fluorimetry system and quartz cuvettes. Standard fluorimetry techniques were employed in the investigation of the emission properties of the CdSe nanoparticles; please see Appendix C for the general procedure employed in the investigation of samples. A fluorimeter is designed to detect the fluorescence or photoluminescence of a sample. The fluorimeter is equipped with a wide spectrum light source that is limited by a monochromator that adjusts the wavelength of light allowed to pass through to the sample for excitation purposes. For a simple diagram of the setup, please see Appendix C. A colloidal sample of CdSe material produced according to the above procedures and usually suspended in toluene or heptane, was excited at a single wavelength of 300nm to 400nm, depending on the sample. Note that the use of a single excitation wavelength was a limitation of the fluorimetry setup and not of the CdSe nanocrystals, as they will photoluminesce as a function of a broad range of excitation wavelengths below the band-gap. Normally, ultra-violet wavelengths were employed because they supplied higher excitation energy, which led to correspondingly higher emission intensity from the CdSe quantum dots.

The sample's emission is detected and measured using a photomultiplier tube (PMT), allowing a quantitative analysis of the photoluminescence of the sample. For the type of investigation required, however, the emission intensities were normalized in order

to account for concentration variations between samples. Hence, data that looked like Figure 17 was normalized to produce the plots in Figure 18.

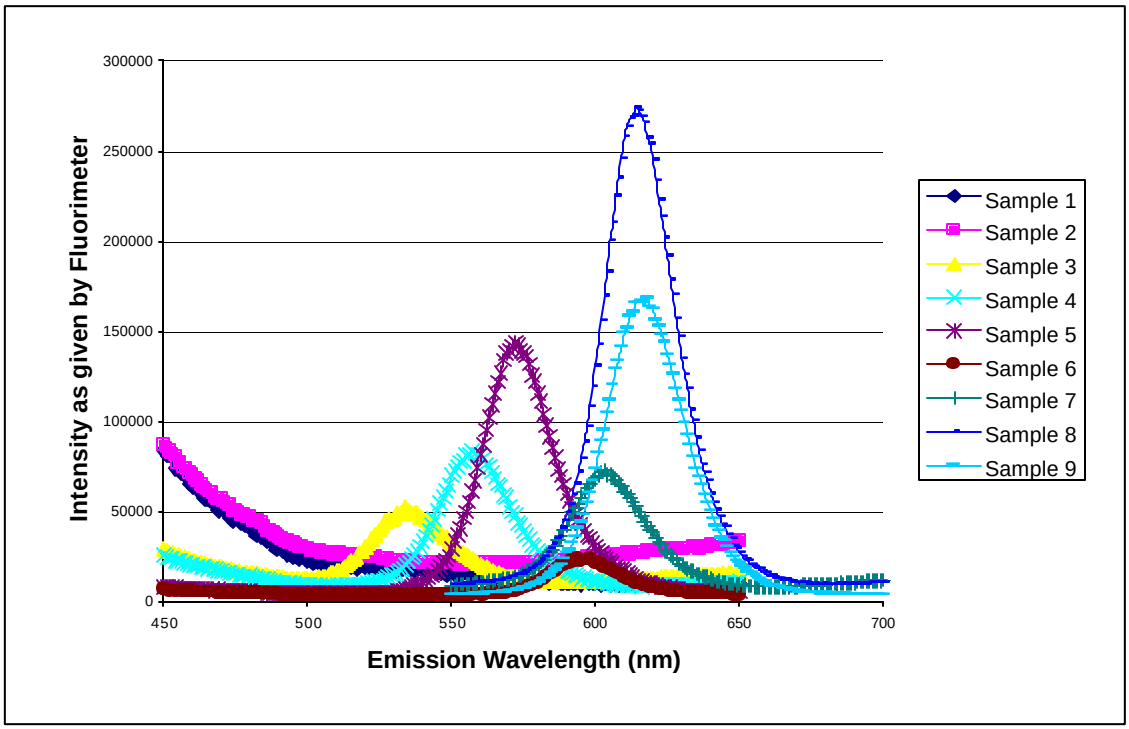

Figure 17. Photoluminescence data for a stearic acid reaction, as received from the fluorimeter, showing intensities relative to the most intense sample in the set.

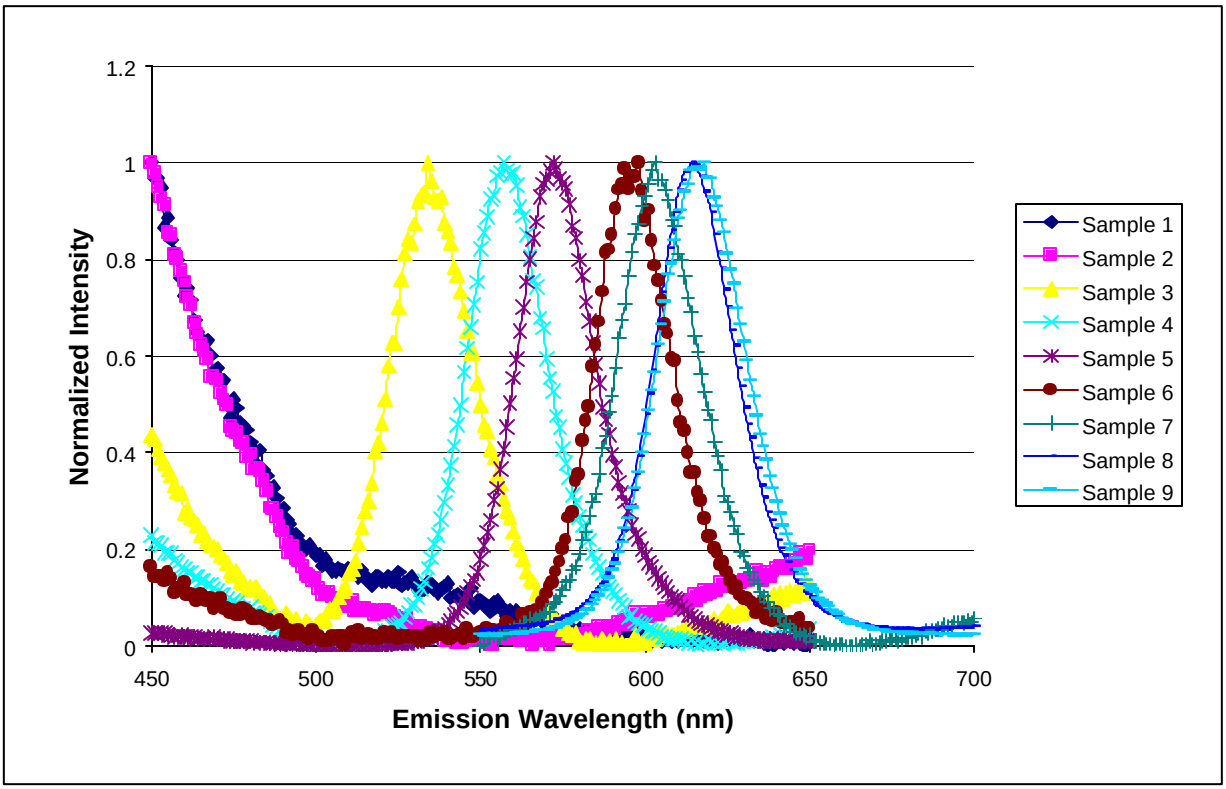

Figure 18. The same data as Figure 17, but with normalized intensity.

Of particular importance to note is the fact that sample 6 in Figure 17 is nearly lost amongst the other plots and very difficult to read, while in Figure 18 the same sample clearly has a peak at approximately 600nm; the normalization is important as it allows for an easier comparison of peak emission and FWHM values. Since the relative emission intensity values were rendered meaningless by the fact that concentrations of CdSe in each solution varied and proved difficult to measure for each sample due to retained extraneous capping structure, the loss of this information by the normalization process was deemed insignificant. However such data would be useful if the concentrations of quantum dot material could be standardized for each sample.

While the peak values that may be taken directly from the normalized plots provide an indication of the size of the quantum dots (remember that the diameter of the particle directly effects the emission wavelength of the dot, hence wavelength and dot size are correlated), the FWHM values provide information about the monodispersity of the sample. Hence, Figure 19 shows plots of two different samples, both with normalized intensity, but with very different full-width half maximum values. Curve 1 has a FWHM

value of approximately 27nm while Curve 2 has a FWHM value of approximately 70nm. Curve 1 has a narrow FWHM indicating a greater monodispersity than Curve 2, with the broader FWHM, because the size distribution of the quantum dots is what leads to a range of individual emissions that the fluorimeter collects and displays as a Gaussian distribution (inhomogeneous broadening). Additional reasons for the Gaussian distribution include dots with slight aspect ratios and the homogeneous broadening effects discussed in the section below.

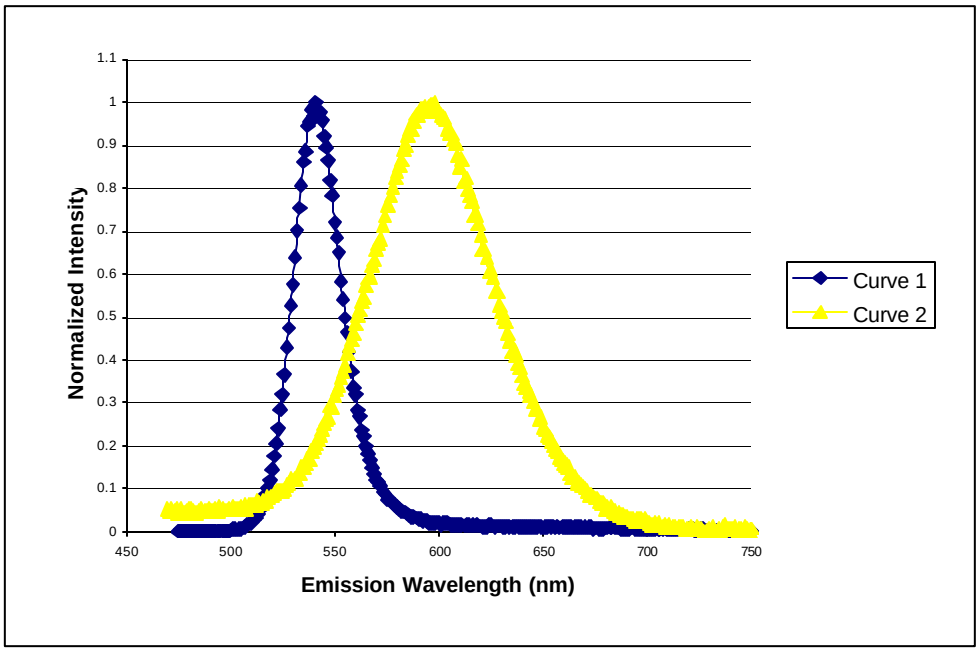

Figure 19. Full-width half maxima differences: an indication of quantum dot size distribution differences.

An additional indication that the material being produced in each reaction is a quantum confined rather than an organic material is the fact that one may excite the material anywhere below the band edge in terms of wavelength or above the band edge in terms of energy. An easy demonstration of this was made using a CdSe/APS sample and exciting it at different wavelengths and seeing if the emission peak shifted. As shown in Figure 20, the emission peak did not shift at all and was preserved over a range of 100nm of excitation. When compared to standard organic dyes, where there is a single optimal excitation wavelength, the excitation window of QDs is vastly different. The fact that QDs may be excited anywhere below the band edge in terms of wavelength means that a

set of QDs emitting at different wavelengths may all be excited by a single source of ultra-violet light.

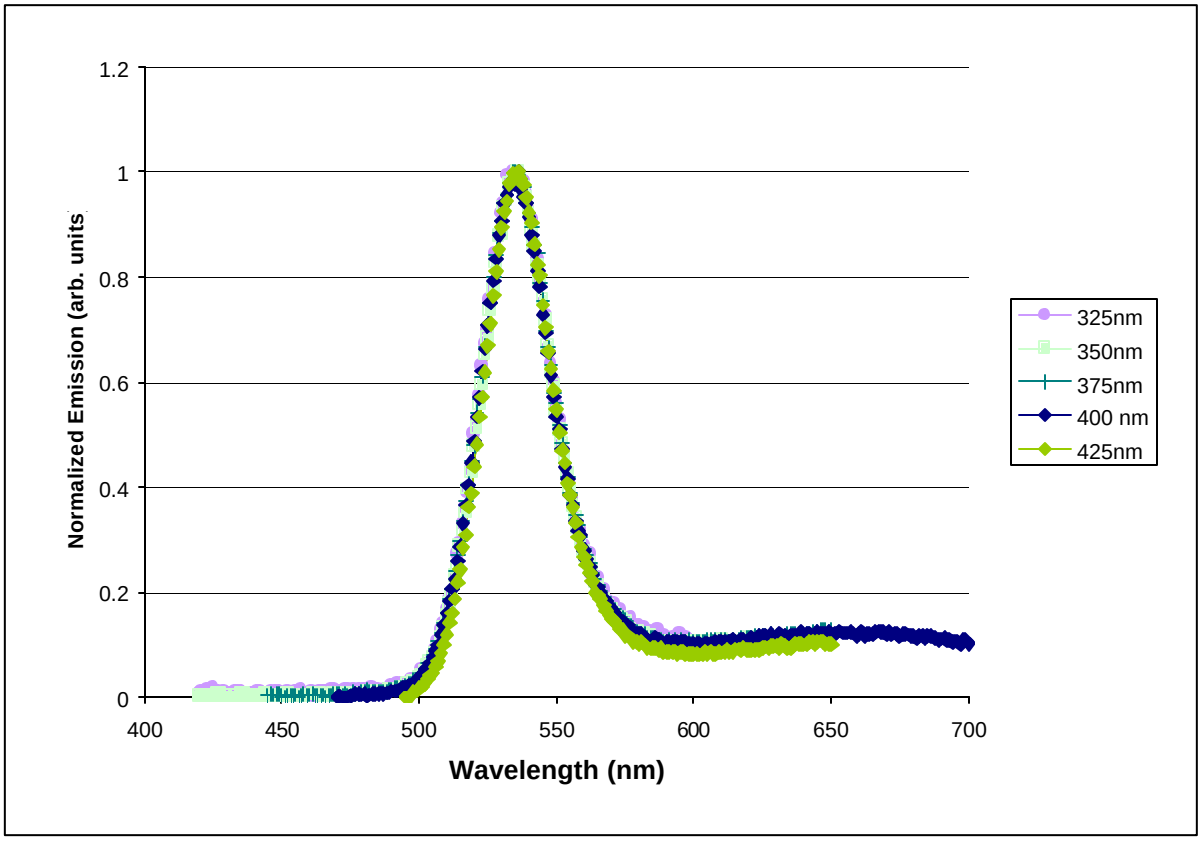

Figure 20. Demonstration of CdSe QD emission consistency over a broad range of excitation wavelengths.

6.3.2 Spectrophotometry

Spectrophotometry is a means by which the absorption of the sample is measured, indicating where the band-edge of the material lies on the absorption/excitation spectrum. All spectrophotometry was performed using a Hewlett-Packard model 8452A diode array spectrophotometer and quartz cuvettes. The strength of absorption is an approximate method of measuring how much of the material is suspended in the sample. However, with quantum dots difficulties arise from the variety of sizes.

Typically, the machine is first calibrated with a blank sample of the chosen solvent. Then, a colloidal sample is placed into the cuvette and placed into the sample chamber. A pulse of wide-spectrum light is passed through the sample and the resulting absorption is collected and the blank sample is subtracted out. Since the Hewlett-Packard

model spectrophotometer collects data down to 300nm and the TOPO capping structure actually absorbs in that region, as shown in Figure 21, the absorption peaks below 300nm must be removed. The data, once normalized, shows very distinct absorption bands of the CdSe quantum dot, as shown in Figure 22.

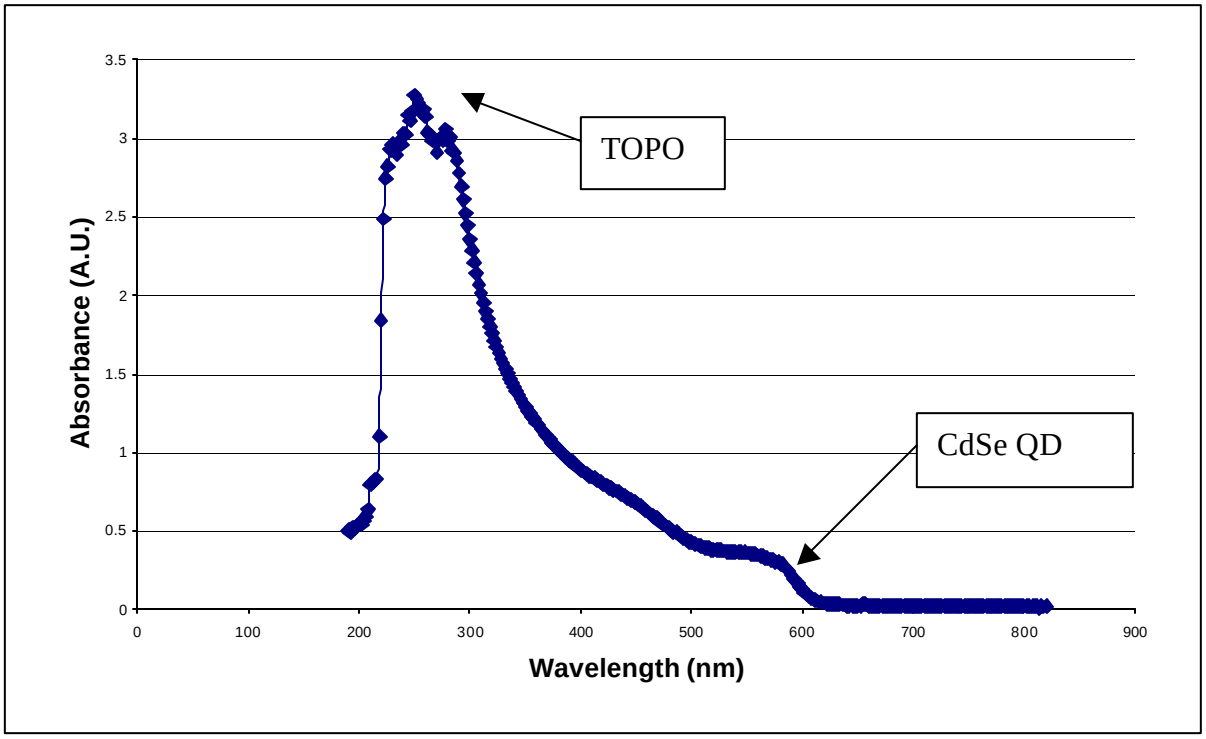

Figure 21. Absorption spectrum of a CdSe/TOPO sample before normalization and deletion of TOPO absorption.

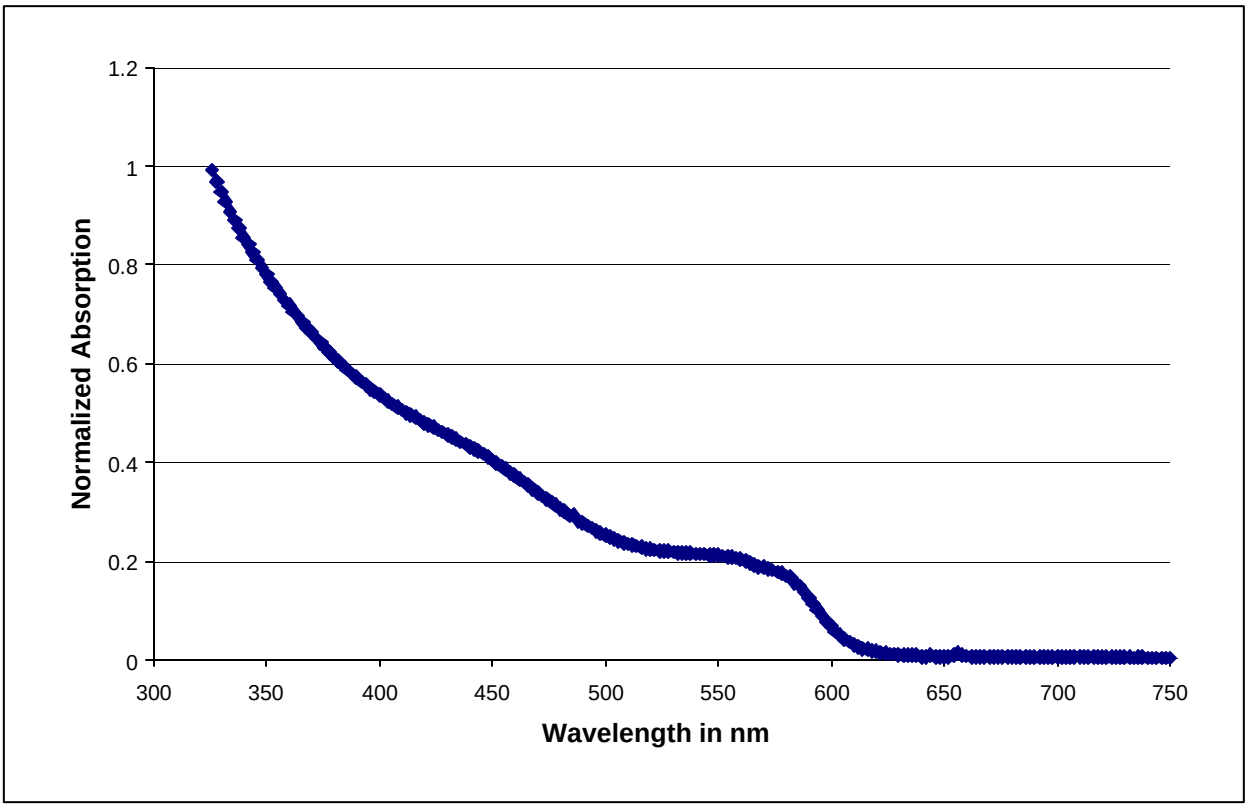

Figure 22. Absorption spectrum of the same CdSe/TOPO sample as Figure 21, but after normalization and deletion of TOPO absorption.

Rather than showing two or three distinct peaks, as would be expected from theoretical calculations for a zero-dimensional semiconductor structure (QDs are an example of such structures), homogeneous and inhomogeneous broadening effects cause the smoothing of the peaks into a continuous structure, such as the one in Figure 22.

Homogeneous broadening effects occur due to phonon and other scattering effects.[12] Inhomogeneous broadening effects occur due to the particles having different sizes; the size distribution may be approximated by a Gaussian distribution.[12] In order to take into account different inhomogeneous broadening for different samples, Gaussian distributions with different widths must be assumed. The larger the width of the distribution, the more continuous the quantum confined transitions become. Hence, rather than seeing multiple discrete peaks in Figure 22, as one would expect from theory, one actually sees one semi-discrete peak with a few extra "bumps" toward the high-energy, short-wavelength, side of the main peak.

6.3.3 Size Selective Precipitation

One of the main methods to decrease the FWHM is size selective precipitation. This effect occurs with every sample that is purified, causing spectra taken from two identical samples that were purified at different times to show slightly different peak emissions and FWHMs. However, the effect may be magnified if done intentionally. Size selective precipitation occurs when the CdSe quantum dots are precipitated out of toluene suspension using methanol. One adds methanol to the toluene solution until it becomes cloudy and then centrifuges the sample. The precipitate is the large dots while the solution still contains the smaller dots. If this method is employed several times, the FWHM of the sample will be decreased substantially. An example of the results of this method is shown in Figure 23, where the broadest of the spectra is the emission of the sample as it was taken and quenched directly into toluene, the second broadest spectrum is the sample in heptane after the first purifying procedure, and the narrowest spectrum is the sample after it has been re-precipitated out of heptane and resuspended in toluene.

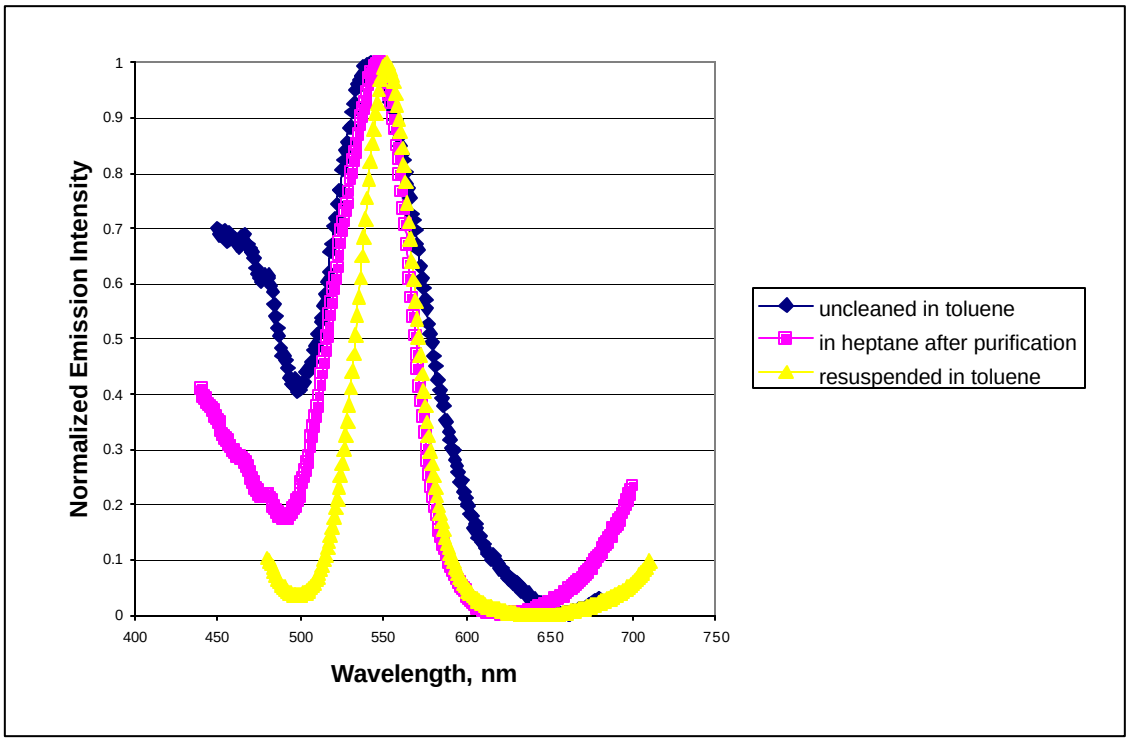

Figure 23. The emission of size selective precipitated samples, performed to decrease FWHM.

As the figure shows, each successive step causes one to lose some of the dots. The first step leads to a loss of both the smallest and largest QDs, while the second step

causes the loss of the smallest QDs. In all steps, the largest QDs settle out while the smallest QDs remain suspended in solution. In this example, the change in FWHM is quite impressive and there is also a small shift in peak emission, as indicated in Table 3. Such results are typical of the size selective procedure and provide a means to further narrow the as-produced emission FWHM and the size distribution of dots. It should also be mentioned here that through refinements of the production technique, the size-selective precipitation technique may be rendered unnecessary for most samples. For most of the work shown herein, size-selective precipitation was not employed, but the technique is described here because it is often mentioned in literature.

Table 3. Shifts in emission peak and FWHM.

Sample	Peak (nm)	FWHM (nm)
CdSe/ZnS uncleaned in toluene	542	68
CdSe/ZnS in heptane after purification	548	53
CdSe/ZnS resuspended in toluene	552	38

6.3.4 Transmission Electron Microscopy

Transmission electron microscopy investigation of CdSe is an effective method of determining or verifying size and shape uniformity of the QDs within a sample. Additionally, when a reaction behaves in an odd fashion or produces precursors that emit broadly in the visible spectrum, TEM provides a method for discerning whether or not QD material was actually produced. One can "see" and photograph the material, or rather its shadow. In TEM, an electron beam is focused on a monolayer of dried out QDs on a 200 mesh copper grid coated in carbon (i.e. the QDs are no longer a colloidal suspension). Electrons pass through the CdSe QDs at a slower rate than through the plain carbon grid, and hence, a shadow is detected by the film when it is exposed for the purpose of taking a photograph. Unfortunately, at the high magnifications necessary for observation of the 3-10nm diameter QDs, the resolution is often not very good, but does at least indicate that a certain kind of material was produced, such as dots, rods, or other shapes.

Additionally, the pictures taken through TEM provide a good means of ascertaining aspect ratios and comparing samples. Scanning the pictures into digital format can allow for enlargements of certain QDs to look at individual shapes. However, the original picture must be of high resolution and of very clearly defined QDs for such enlargement to be effective.

7. Results

7.1 Fluorimetry and Spectrophotometry Investigation of CdSe

7.1.1 TOPO Capped CdSe Quantum Dots

Trioctylphosphine oxide (TOPO) capped quantum dots of CdSe composition were produced in a single run using 1.5 wt % (of the TOPO) of the stabilizer, TDPA. Samples were pulled out over a period of 44 hours at growing intervals (approximately doubling early on and then every 4-6 hours). The result, as shown in Figure 24 , was a group of samples that spanned the range of possible colors for CdSe; from blue (484 nm) to red (666 nm) peak emission wavelengths under ultra-violet excitation. In this graph, the full-width half maximum (FWHM) of each curve varies between approximately 28nm and approximately 50nm. This variation is only noticeable in this set of data because of the long reaction time. However, it is important to note that even at the high end, 50nm FWHM (all the way to the right in the set shown in Figure 24), quantum dots are still far better than most organic dyes in terms of FWHM. Of particular importance for applications are emission colors that are distinct. Distinct, in this case, is defined as separated at the full-width half maximum of the emission curve. Hence, by this definition, one is able to discern curves from Figure 24 that would be distinct from one another and cover virtually the entire spectrum as in Figure 25. Additionally, a representative absorption plot was taken using the spectrophotometer. The plots shown in Figure 26 show the absorption and emission spectra for the sample, indicating that the material absorbs directly up to the band-edge.

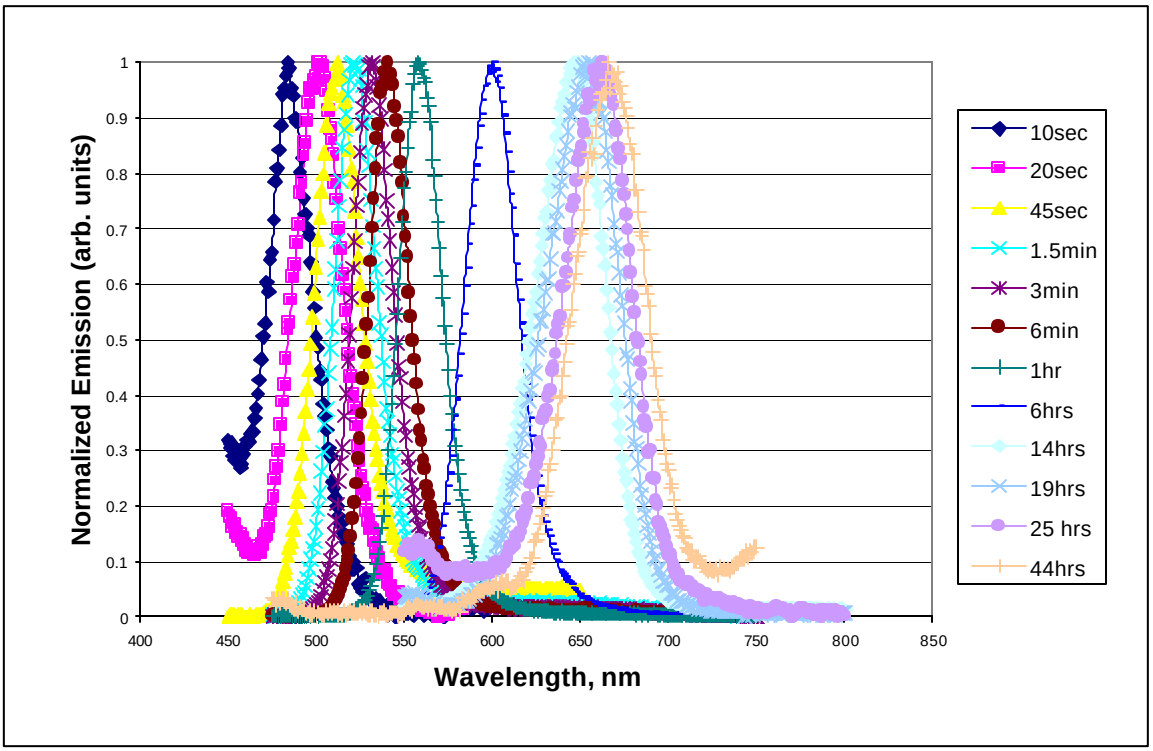

Figure 24. The full array of emission colors as sampled from a single 44 hour reaction of CdSe quantum dots capped with TOPO.

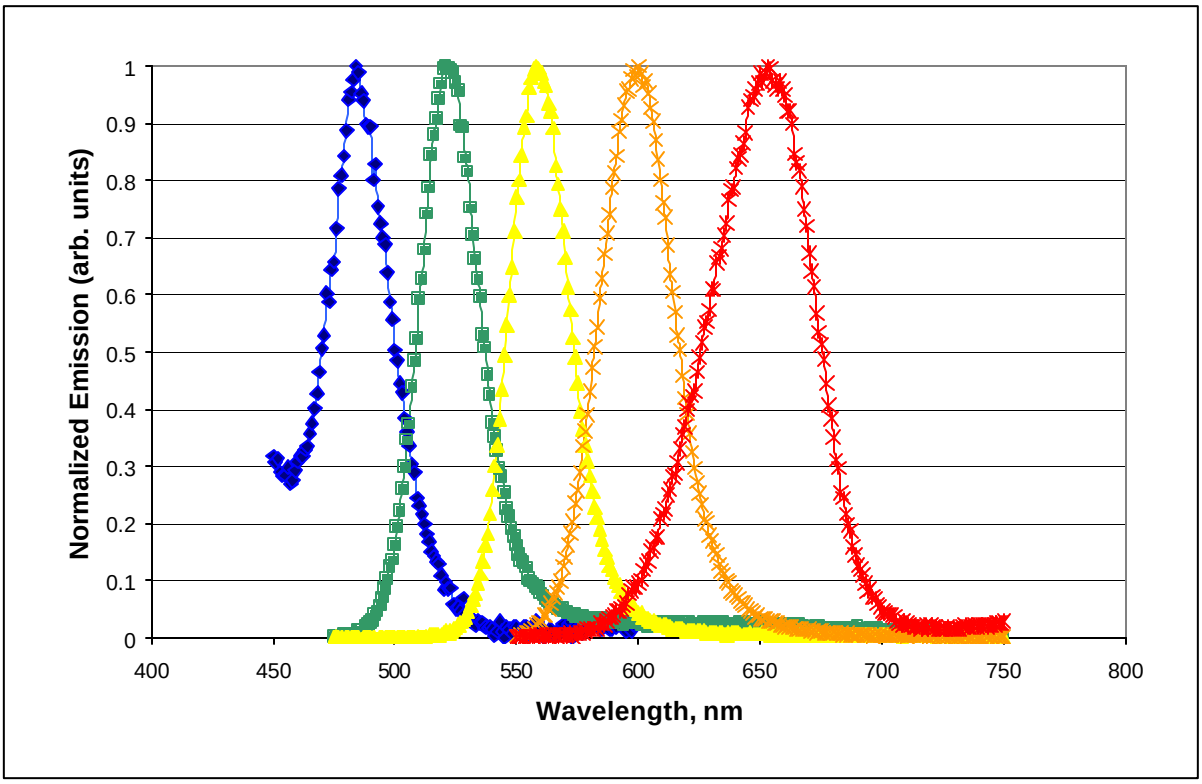

Figure 25. Distinct emission colors and time progression of quantum dot growth during reaction.

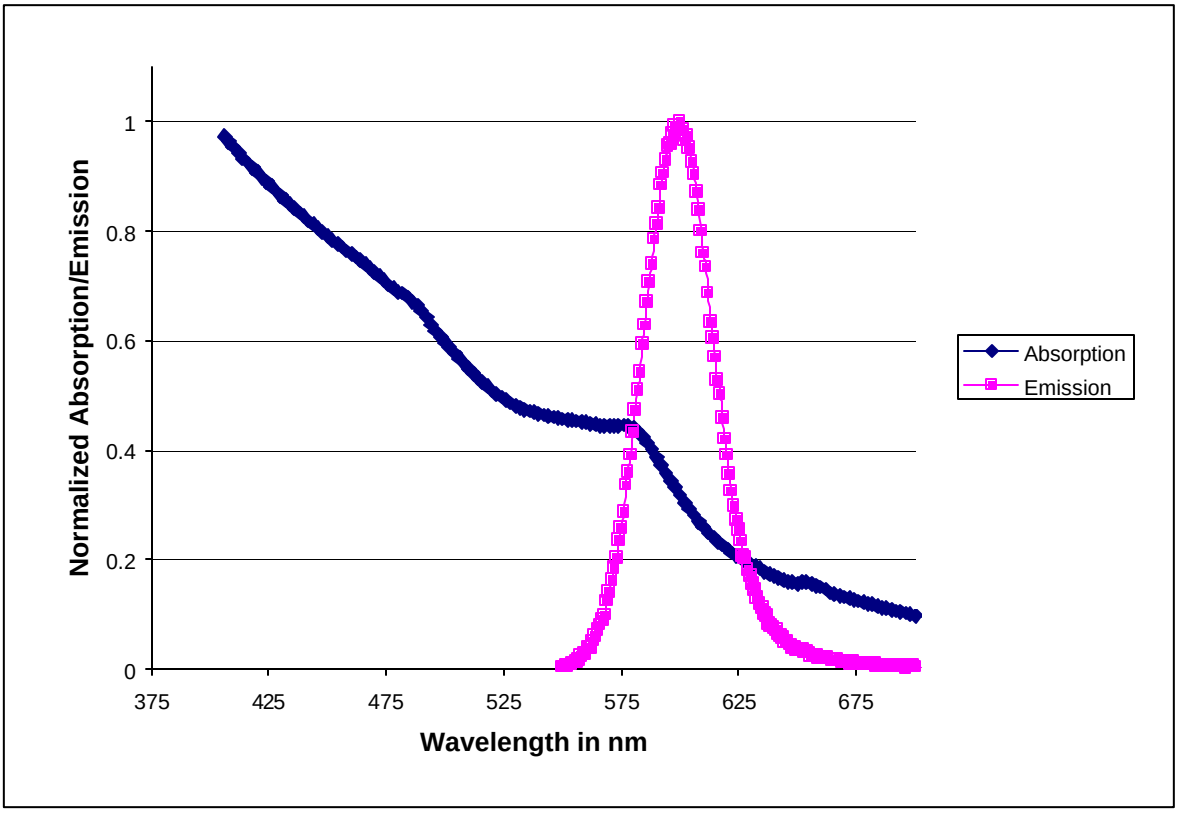

Figure 26. Absorption and emission plots for the 6 hour sample from Figure 25.

7.1.2 Stearic Acid Capped CdSe Quantum Dots

Stearic acid capped CdSe quantum dots were produced shortly after the TOPO capped ones. Samples were, again, taken over the span of a single reaction with doubling time intervals, though only up to 12 minutes; this reaction was much faster than any of those previously performed and required close attention to sampling times. As seen in Figure 27, the stearic acid (fatty acid) capped QDs also exhibit emission curves that span the visible light spectrum from the low 500nm to the low 600nm range. Such a range of emission was found to be in accordance with the literature.[43] Additionally, unlike the TOPO reactions, the stearic acid reactions produced quantum dots with consistent FWHM values across the spectrum, a trend that is visible in Figure 27. Recently performed reactions indicate that stearic acid reactions, when performed at lower temperatures, also yield blue-emitting quantum dots with emission wavelengths as low as 480nm. Hence, stearic acid capped dots can also be made to cover the entire visible

spectrum. Additionally, the 12-minute sample in Figure 27 yielded a representative absorption spectrum that is shown in Figure 28.

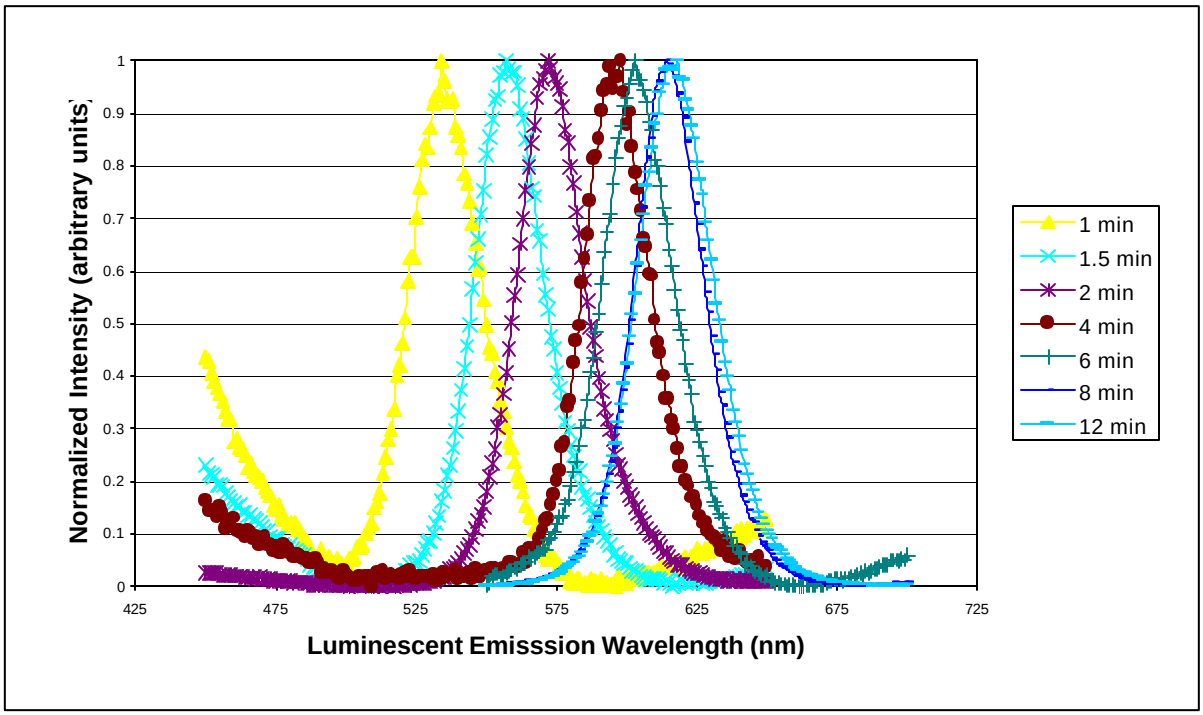

Figure 27. Stearic acid capped quantum dots' luminescent emission spectra under ultraviolet excitation.

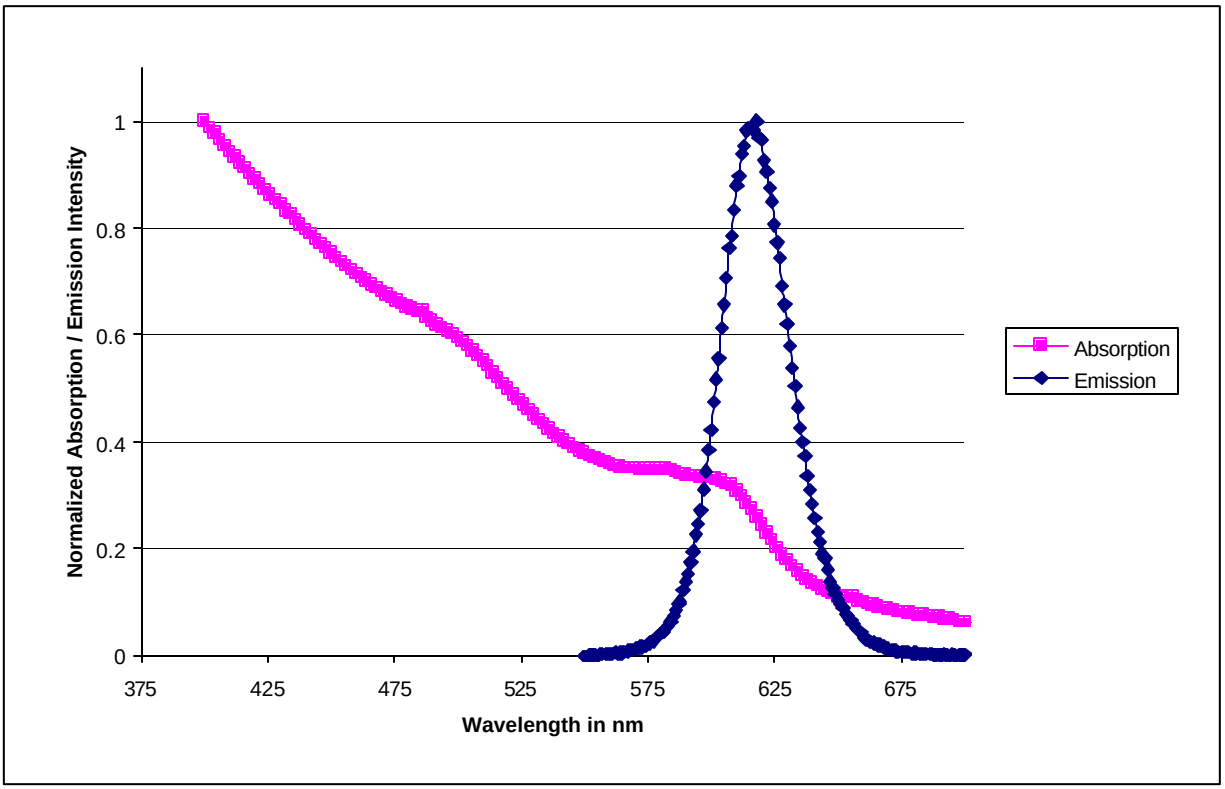

Figure 28. Absorption and emission of the 12 minute sample from Figure 27, representative of the entire set.

7.1.3 Dodecylamine Capped CdSe Quantum Dots

Dodecylamine capped CdSe quantum dots were successfully produced. Samples were taken as described for stearic acid, but this time over a period of approximately one hour in order to capture more of the spectrum. This reaction is slower than for stearic acid, but faster than for trioctylphosphine oxide. The resulting emission spectra from a 50% dodecylamine reaction are shown in Figure 29. The second sample, at 2 minutes and 10 seconds, produced such low concentrations that in order to record an emission spectrum, the baseline had to be raised on the fluorimeter (i.e. the shutters needed to be opened further), creating the noisy looking data, even when normalized. Later samples, however, provided clean, sharp peaks with excellent FWHMs and absorption peaks such as the one for the 40 minute sample shown in Figure 30.

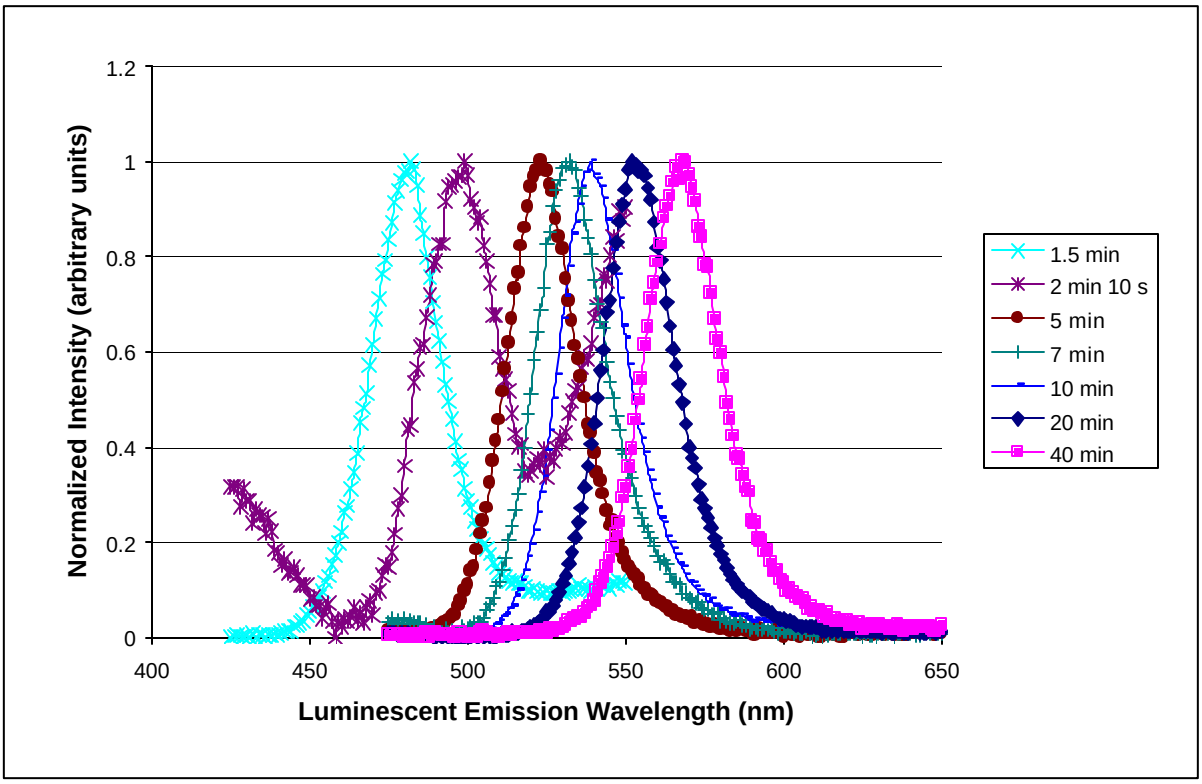

Figure 29. 50% dodecylamine capped quantum dots' luminescent emission spectra under ultraviolet excitation.

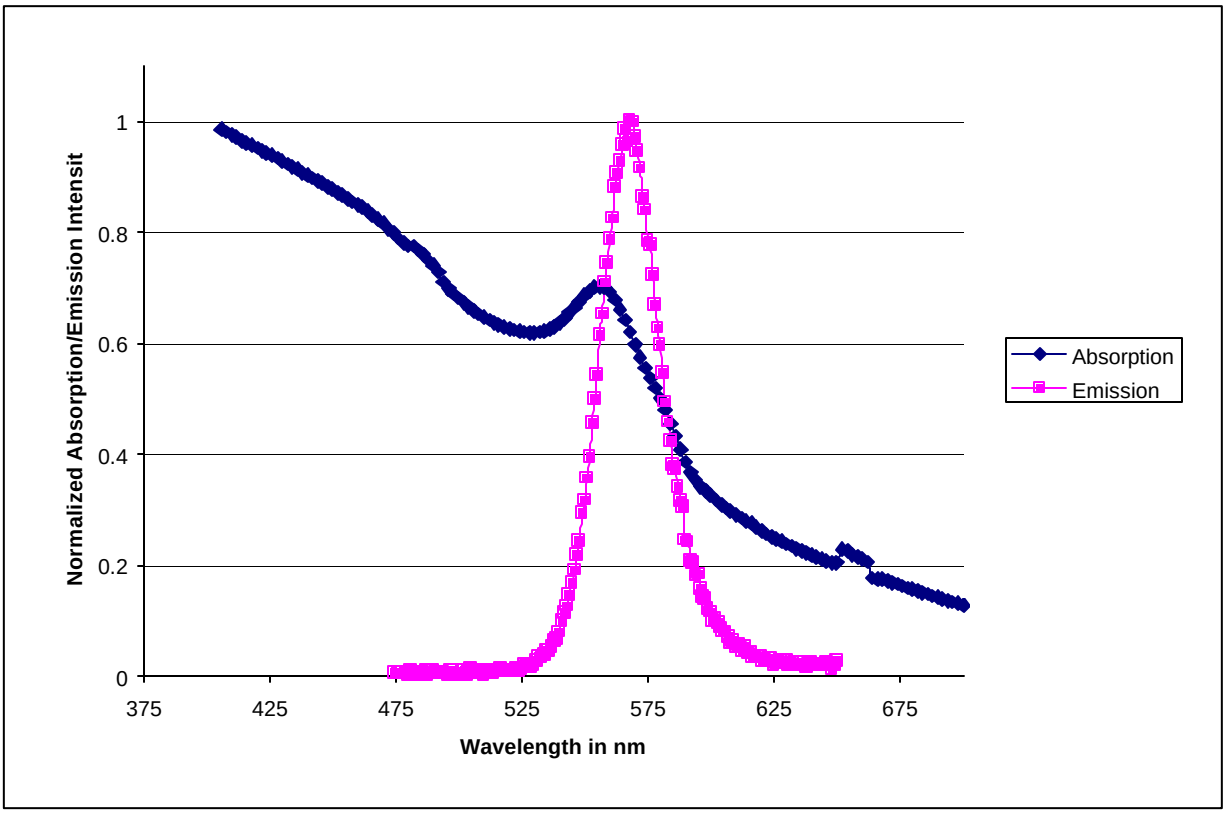

Figure 30. Absorption and emission spectra for the 40 minute sample of Figure 29, 50% CdSe/DA.

7.1.4 Comparison of Stearic Acid and Dodecylamine Capped CdSe Quantum Dots

The comparison of SA to DA capped CdSe produced large amounts of data through a time consuming process of running the numerous reactions outlined in the procedure section. Each of the 20 or so reactions also required fluorimetry to be performed on each of the 8-10 samples per reaction. The resulting emission peaks for each of the samples was recorded and plotted against reaction time; the plot points for each reaction were then connected to form a graph. The graphs were overlaid to allow for comparison between reactions of a given type. The resulting data plots are shown in Figure 31 and Figure 32 for the stearic acid and dodecylamine reaction sets, respectively. The slopes of different parts of each of the graphs are indicative of the speed of the reaction. Of interest in all of these reactions is the fact that there seems to be a point at which the reaction changes speed. For each reaction of a given capping structure type, this "break point" seems to be relatively independent of the percentage of capping structure included in the reaction as well as being independent of temperature, as all reactions were performed at the same temperature of 200ºC.

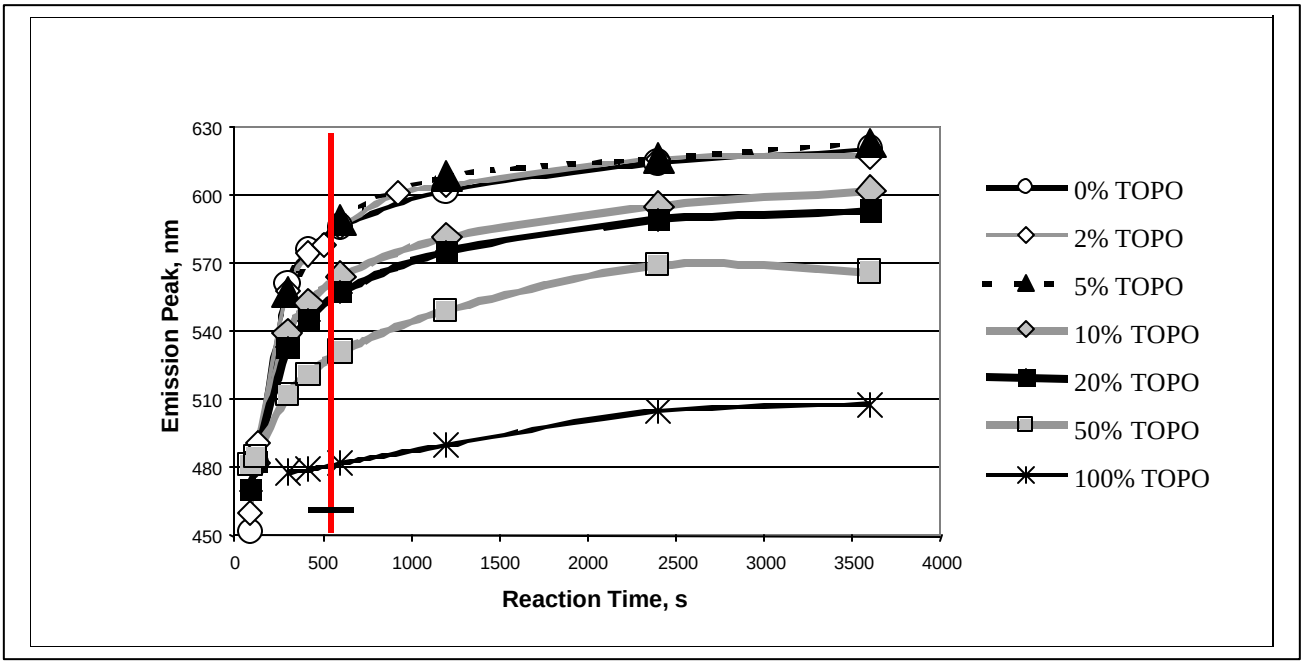

Figure 31. Plot of emission peaks of varied percentage of TOPO/SA reactions versus reaction time.

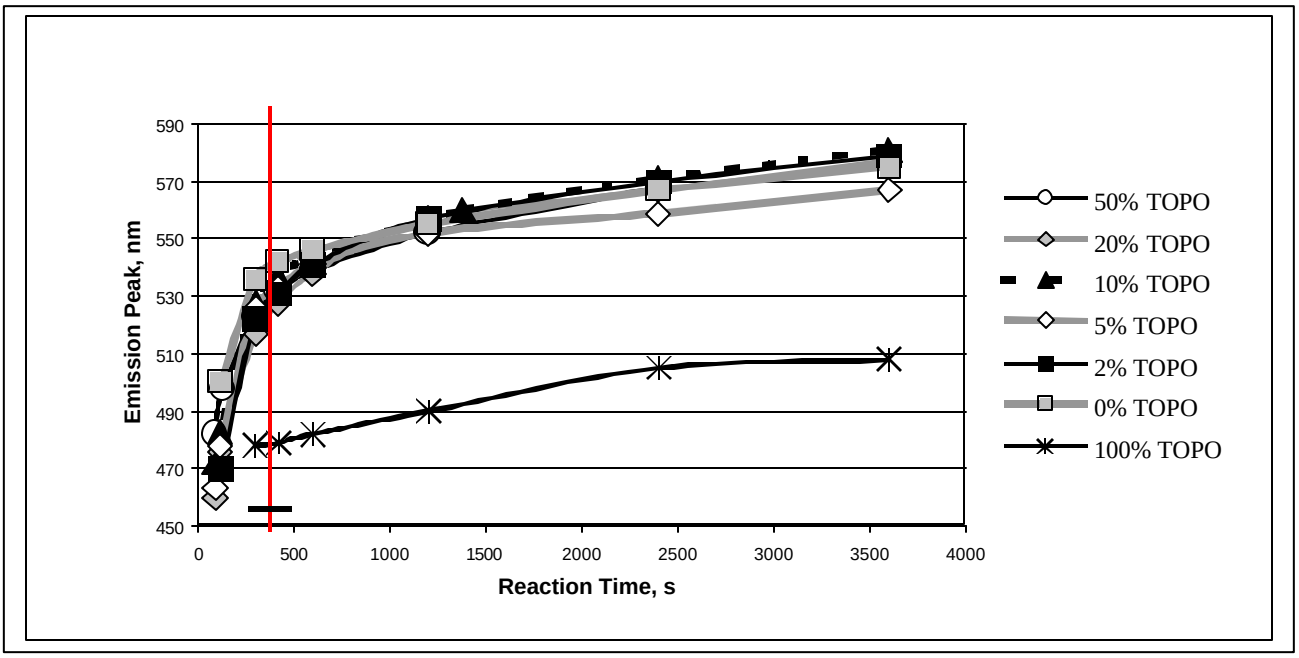

Figure 32. Dodecylamine reaction plots of emission peak versus time.

The breakpoint is defined as the intersection point of two straight lines created by the main legs of each curve. The red vertical line in each of Figure 31 and Figure 32 indicates the average breakpoint for the set of reactions, while the black perpendicular bar indicates the range of breakpoints found. Note that the average and range of breakpoints does not include the baseline 100% TOPO reaction, because that reaction remained constant for both sets.

Furthermore, to insure reproducibility, the reactions were performed a second time. Precise temperature control was found to be of great importance in order to attain reproducibility and required the third part of the comparison to be performed in order to rule out temperature effects and insure that the observed effects were a result of changing the capping structures. Figure 33 contains plots of 95% SA/5% TOPO reactions, each of which was at a temperature between 200ºC and 295ºC, as indicated. Each reaction was performed according to the general guidelines outlined in the procedures section.

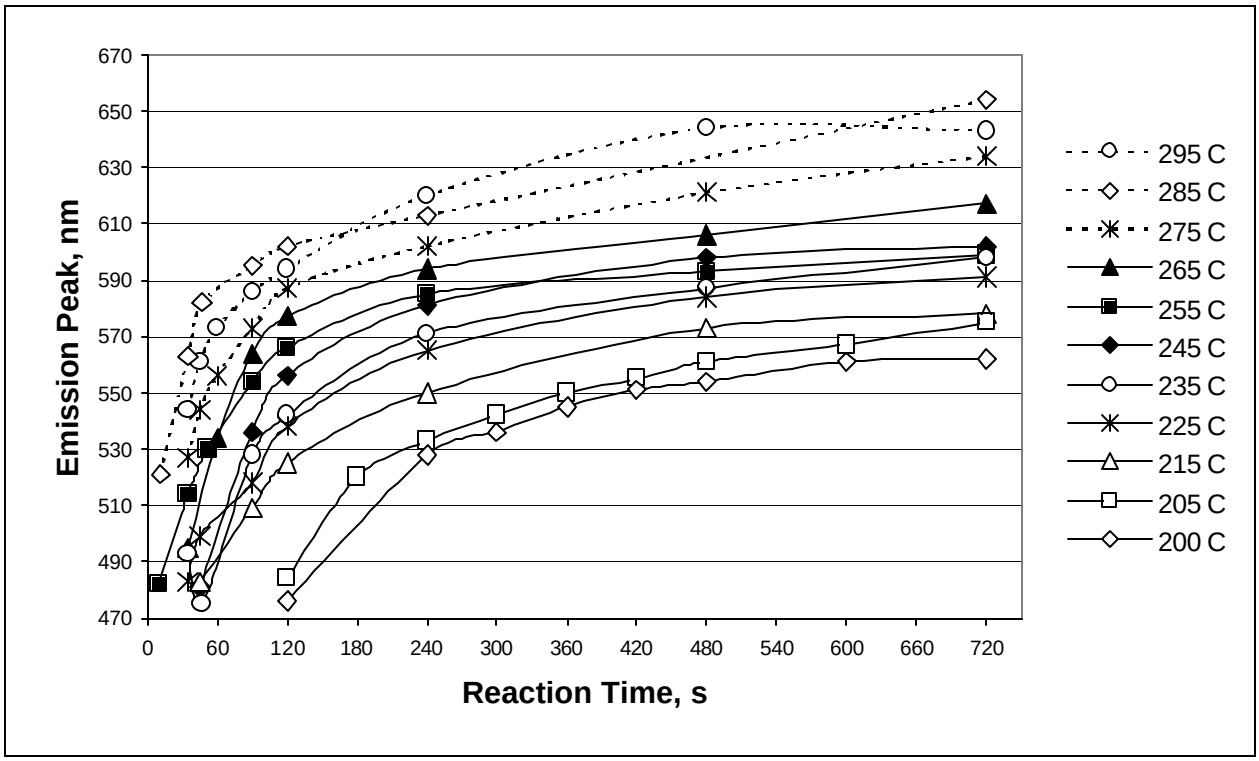

Figure 33. 95% SA/5%TOPO reactions performed at different temperatures; plots of emission peak versus time.

In the stearic acid and dodecylamine reactions the breakpoint did not definitively shift due to reaction temperature. The breakpoint did, however, shift relative to emission wavelength due to the difference in the type of capping structure. Hence, the stearic acid reactions produced QDs reliably that emit in the 560nm-620nm wavelength range while the dodecylamine reactions, over the same time period, produced QDs which emit in the 530nm-580nm wavelength range. The range is selected by the fact that the respective reactions had slowed enough to reliably be able to withdraw samples that produced the correct quantum dot size, which in turn produced the planned wavelength. This indicates that the kinetics are faster for the stearic acid reaction than for the dodecylamine reaction for reasons other than reaction temperature. Further investigations will be necessary to determine the reason for such a large difference in reaction kinetics for such seemingly similar reactions. The finding, however, is useful in the production of quantum dots, as this information seems to indicate that certain capping structures will produce certain sized semiconductor nanoparticles more easily than others. Hence, the stearic acid reaction produced dots that emitted in the orange-red region of the spectrum more easily

and reproducibly than the green-yellow region of the spectrum where dodecylamine produced dots.

7.1.5 Phenyl Sulfone Capped CdSe Quantum Dots

The previously unreported synthesis of phenyl sulfone capped CdSe quantum dots was successfully performed in the laboratory. Samples were taken, as described for stearic acid, but this time over a period of approximately one-half hour. This reaction is very similar to that of trioctylphosphine oxide. As with all of the reactions for new capping structures, initial test reactions were performed using 50% TOPO and 50% new capping structure, in this case phenyl sulfone. Such a reaction is performed in order to determine whether the material is compatible with the other constituents of the reaction and to see if the material acts as a nucleation inhibitor rather than a capping structure. Hence, for most reactions both a 50% and a 100% sample were performed numerous times to show repeatability. The resulting emission spectra from the phenyl sulfone 50% reaction are shown in Figure 34 while those for a 100% reaction are shown in Figure 35. Though these spectra look similar, the only way to tell whether the reactions were, in fact, similar, is to plot the emission peaks against the reaction time. Doing this produces Figure 36, where it is clear that the reactions are very similar, even though the 100% reaction was only run for 12 minutes and the 50% for 8 hours. Additionally, absorption spectra for the samples indicated strong absorption and, again, demonstrate the purity of the samples, with each of the three peaks in Figure 37 indicating a different discrete electron-hole state with corresponding homogeneous and inhomogeneous broadening effects creating a Gaussian distribution around each peak absorption wavelength.

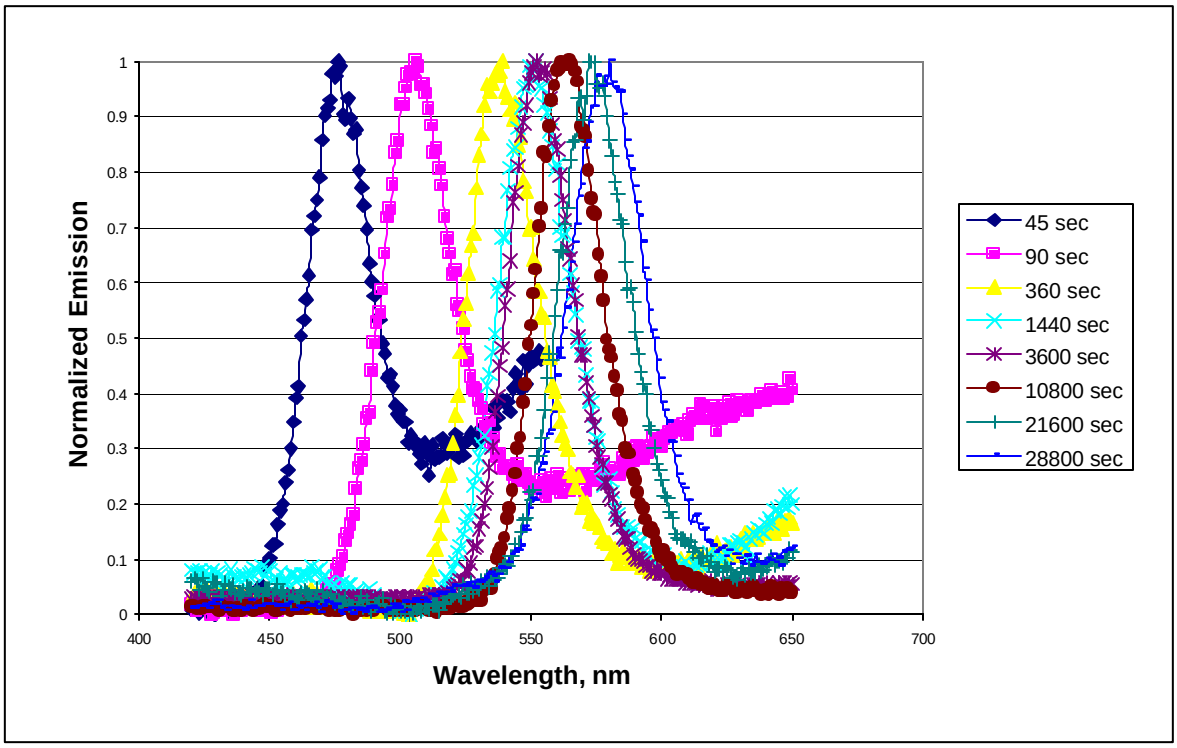

Figure 34. 50% Phenyl sulfone/ 50% TOPO capped quantum dots' luminescent emission spectra under ultraviolet excitation.

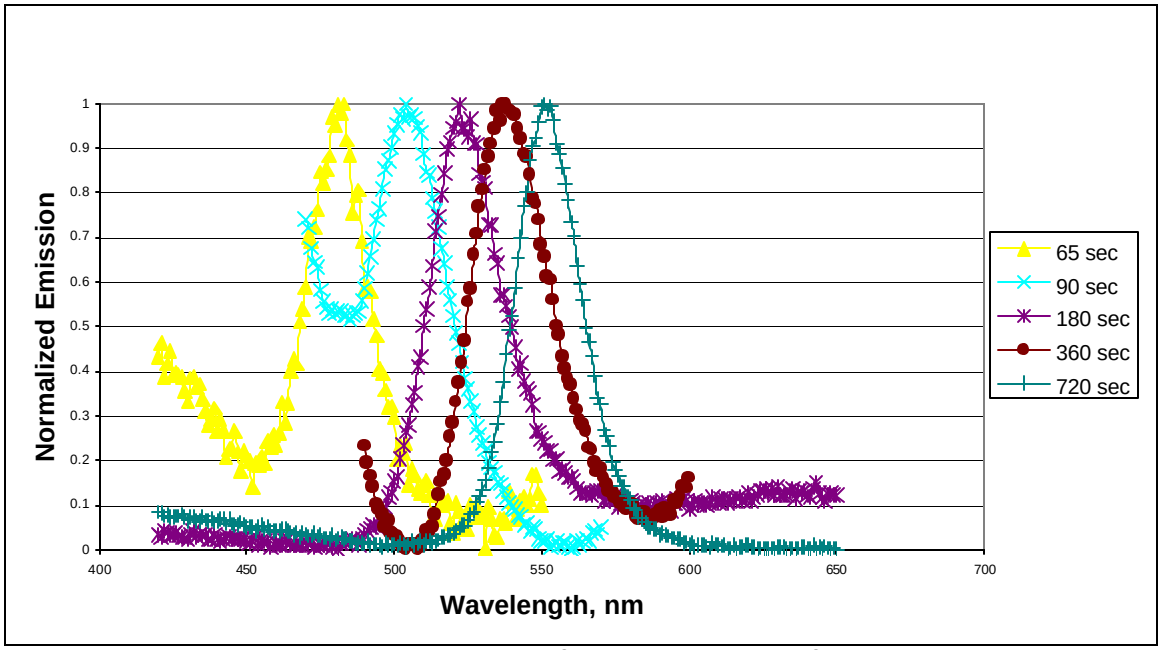

Figure 35. Emission spectra from 100% phenyl sulfone capped CdSe.

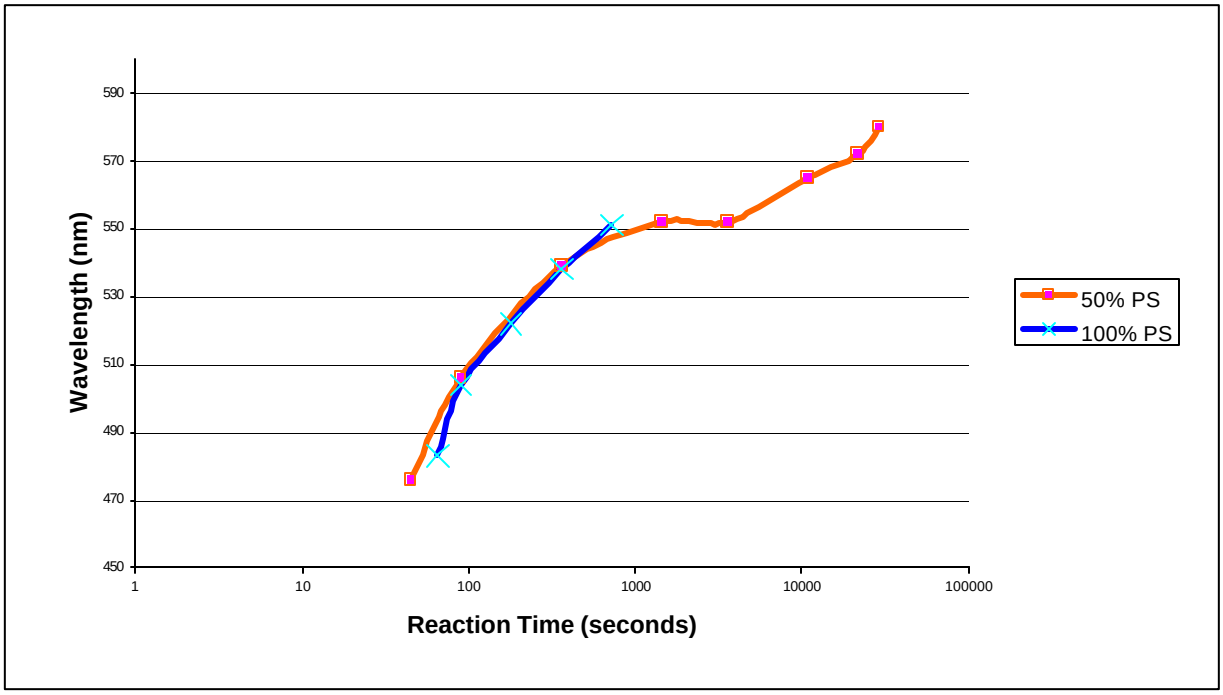

Figure 36. Reaction time vs wavelength plot, showing the similarity between 50% and 100% phenyl sulfone reactions. Note that the reaction time axis is in log form for better visibility of the graph.

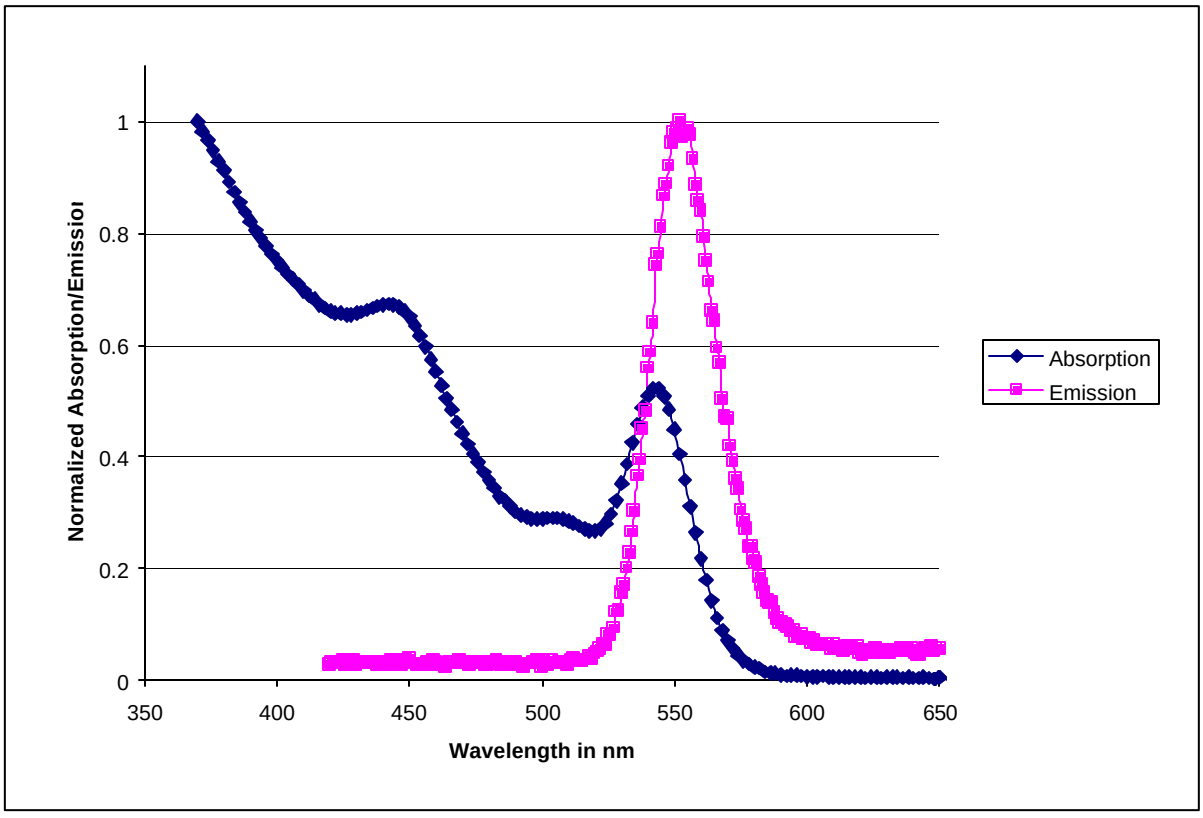

Figure 37. Absorption and emission spectra for the one hour sample in Figure 34, 50% CdSe/PS.

7.1.6 Aminophenyl Sulfone Capped CdSe Quantum Dots

The idea to use aminophenyl sulfone (APS) as a capping structure stemmed from the excellent results obtained using phenyl sulfone. The aminophenyl sulfone reactions produced very bright material, even as freshly produced, without purification. The resulting emission spectra, shown in Figure 38, indicate the speed with which the reaction occurs, even at 230°C.

Additionally, it was found that quenching the APS reaction from 230°C to room temperature in methanol produced the quantum dots for which the spectra in Figure 38 are shown. However, the quenching of the exact same dots in toluene produced material that did not emit at all. This fact is currently being investigated.

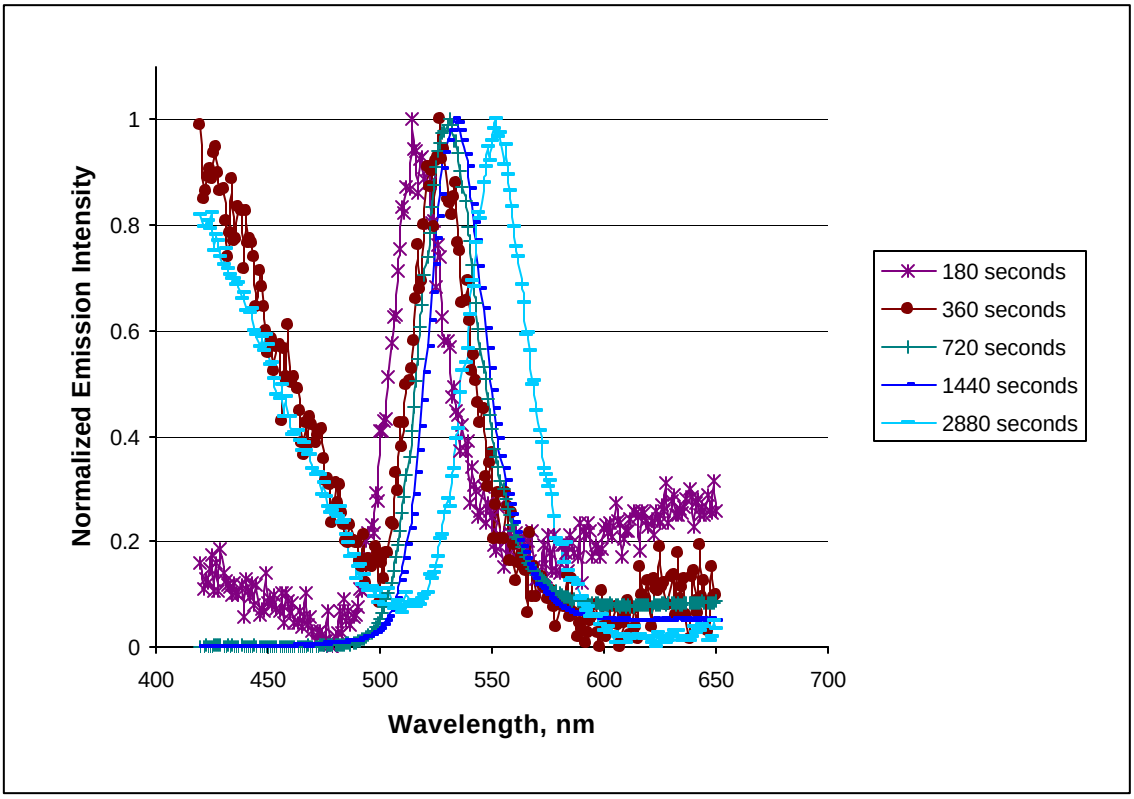

Figure 38. A 100% aminophenyl sulfone reaction produced quantum dots luminescing with the above emission spectra under ultraviolet excitation. Note that the "noisy" data is due to extremely small sample quantities.

Additionally, absorption spectra of the samples were taken and showed very nice absorption, as seen in the representative plot of the 1440 second sample in Figure 39, similar to how CdSe/TOPO QDs would normally absorb. Furthermore, the ability to find

such a distinct absorption peak indicates that the material may be made in concentrated enough form for storage and applications where high doping with QDs would be necessary. Figure 39 also shows the emission spectrum for the representative sample from the 100% CdSe/APS reaction.

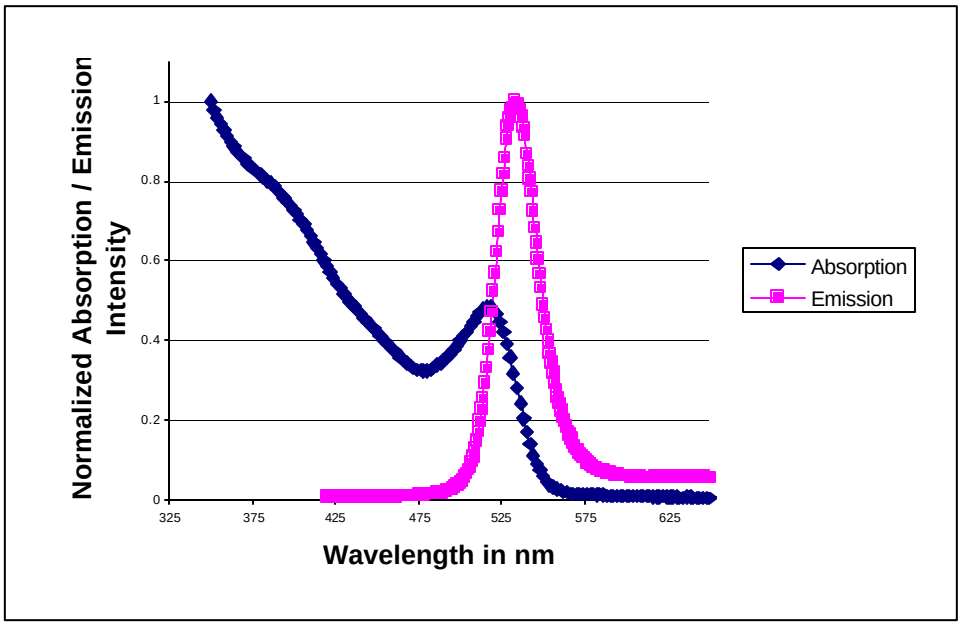

Figure 39. Absorption and emission plots of a representative 100% CdSe/APS sample taken at 1440 seconds.

7.1.7 4,4'-Dichlorodiphenyl Sulfone and 4,4'-Difluorodiphenyl Sulfone Modified CdSe Reactions

These preliminary reactions performed as expected, oddly. The standard CdSe reaction was definitely greatly modified by the presence of either 4,4'-dichlorodiphenyl sulfone (ClPS) or 4,4'-difluorodiphenyl sulfone (FPS). Further investigation is necessary, but it seems that these varieties of sulfones may actually limit the reaction to such an extent that only one size of QD is produced.

The ClPS/TOPO reaction produced very little CdSe material, if any, by visual inspection, and the fluorimetry results indicated as much. Appendix D contains the original plots of the data, which are very noisy and show little structure over all ten samples, while Figure 40 contains a single representative emission spectrum of the last sample in the reaction, pulled from the reaction at 188 seconds.

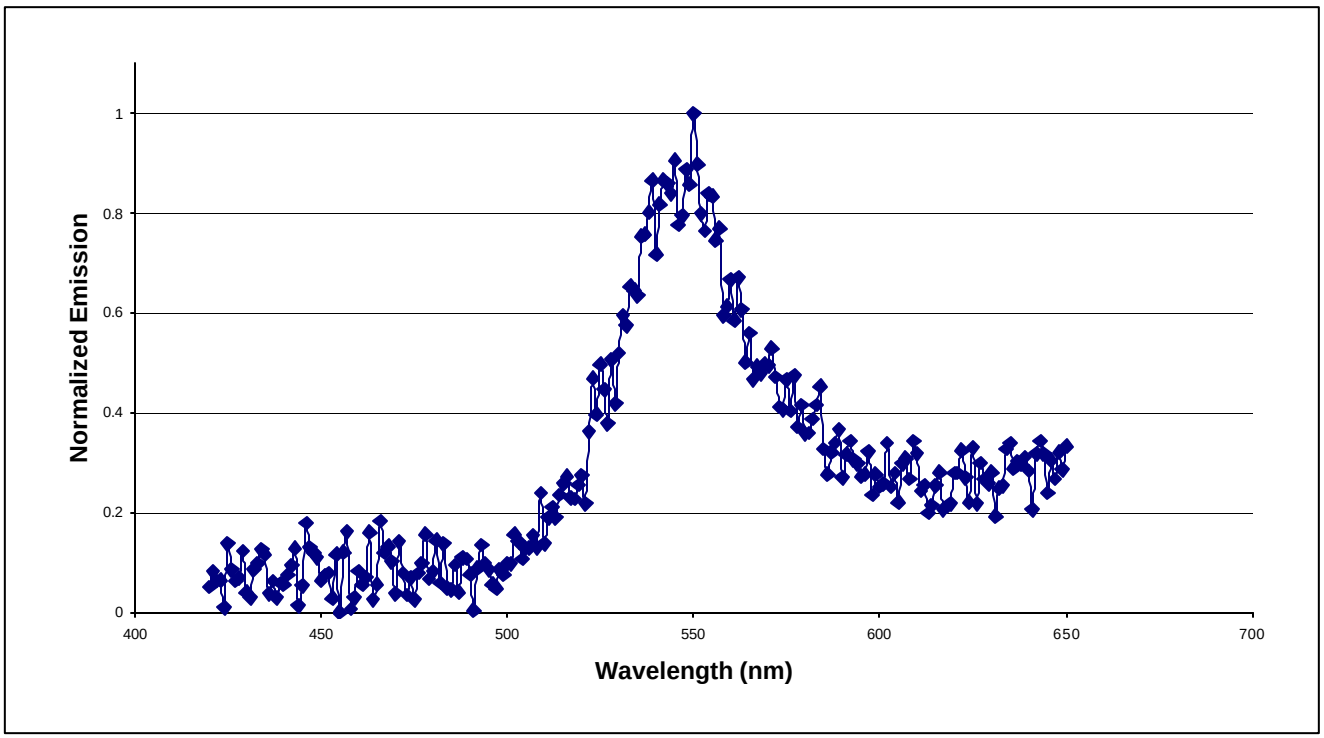

Figure 40. The final sample from a 50% ClPS reaction indicates the presence of some CdSe.

This plot is a good example of what one often must start with when looking at new capping structures/reaction modifiers; initial reactions and even the first set of reactions are plumbing the unknown areas of a reaction mechanism to find when QDs form and then determine at what rate). Though the plot is rather noisy, the general trend is easily followed, and there definitely seems to be some CdSe QDs that were produced from the 50% ClPS/TOPO reaction. This plot was of some encouragement, unfortunately, the 100% 4,4'-dichlorodiphenyl sulfone reaction which was run for 150 seconds, indicated that no QD material was produced. Again, the reader is directed to Appendix D for the plot. In many ways, this data seems to support a hypothesis outlined earlier, that the chlorine atoms draw electron density away from the center of the molecule, where the reaction with the surface of the dot takes place; hence, no CdSe QD-forming reaction actually occurs.

The 50% FPS/TOPO reaction produced very different results in that it produced 9 QD samples, taken at different reaction times, but all exhibiting only one emission peak, at approximately 585nm, with little variation. Appendix D shows the emission plots for all nine samples, while Figure 41 shows a single representative plot at half an hour.

Incredibly, the reaction took place over 45 minutes, indicating that though heating continued, the reaction to grow the CdSe QDs was actually limited by the presence of FPS to a very specific QD size. Whether FPS binds with the QD surface or with the free selenium-TOP molecules remains to be investigated, but the reaction indicates that there might be a way to limit reactions with the addition of an inhibitor.

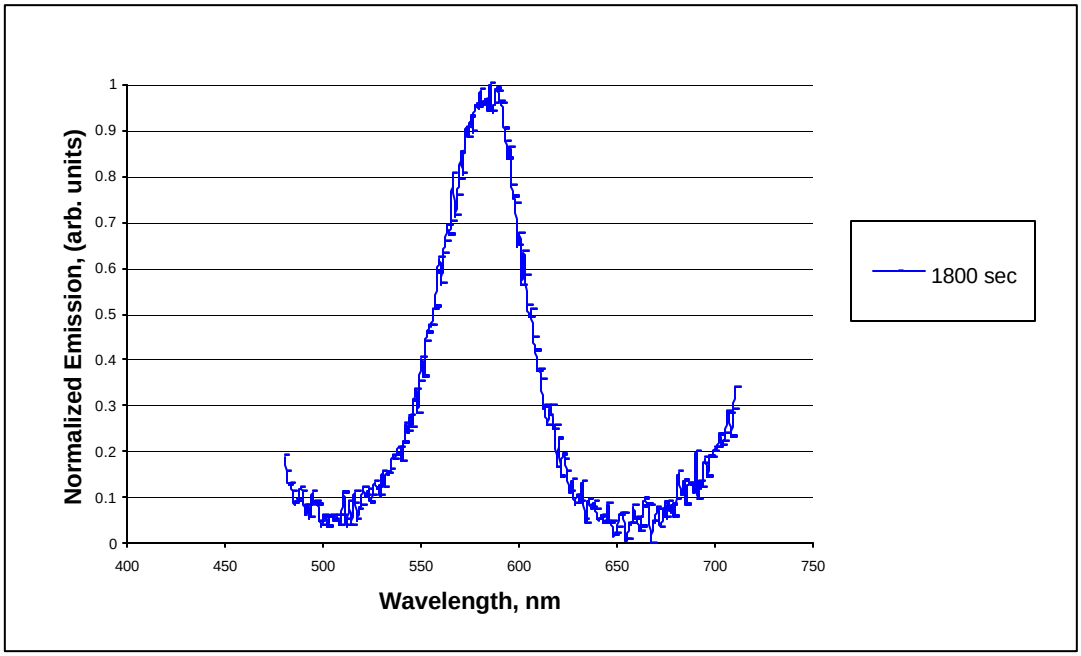

Figure 41. A representative plot of the 30-minute sample of the 50% FPS/TOPO reaction emission, indicating that inhibition of the reaction is occurring when the QDs reach a certain size.

The 100% FPS reactions also gave only the vaguest indication of having produced anything quantum dot related at an emission wavelength of 450nm – smaller than anything previously produced (a plot of the data is provided in Appendix D). Hence, a thorough investigation of emission wavelength as a function of percentage of FPS is necessary to draw any conclusions about the effects of FPS as an inhibitor of the CdSe QD synthesis reaction. However, both the 50% and 100% FPS reaction results support the hypothesis that FPS limits the reaction to a very specific QD size and hence, limits the possible emission wavelength, providing exciting opportunities for tailoring reactions to specific sizes with less worry about reaction length.

7.1.8 Sulfanilamide Modified CdSe Quantum Dot Reactions

As was mentioned earlier, sulfanilamide (SAM) is an asymmetric sulfone with two amine groups available for further chemistry, and it therefore provides very different reaction mechanisms for the production of CdSe quantum dots. Surprisingly, the sulfanilamide reactions performed in a fashion reverse from that for ClPS or FPS, in that the 100% SAM reaction actually slowed the QD reaction down tremendously, while the 50% SAM reaction did not produce any tangible QD product. For plots of the emissions of all the samples taken from these reactions, please see Appendix D.

For the 100% SAM reaction, after initial nucleation of the particles, growth continued extremely slowly for several hours. The emission plot, shown in Figure 42, indicates that the first sample that produced any QD material, taken at 1 hour, actually produced little QD product and hence, the baseline on the fluorimeter was turned up quite high to collect the data. However, later samples became better defined and had only slightly shifted peak wavelengths. Over a period of 3 hours, the peak wavelength only shifted a total of 5nm, however each successive sample did shift toward longer wavelengths. Additional investigations will be necessary, but, with two sulfone reactions performing similarly in terms of their ability to inhibit the reaction, a hypothesis for further study could be made concerning the phenomenon.

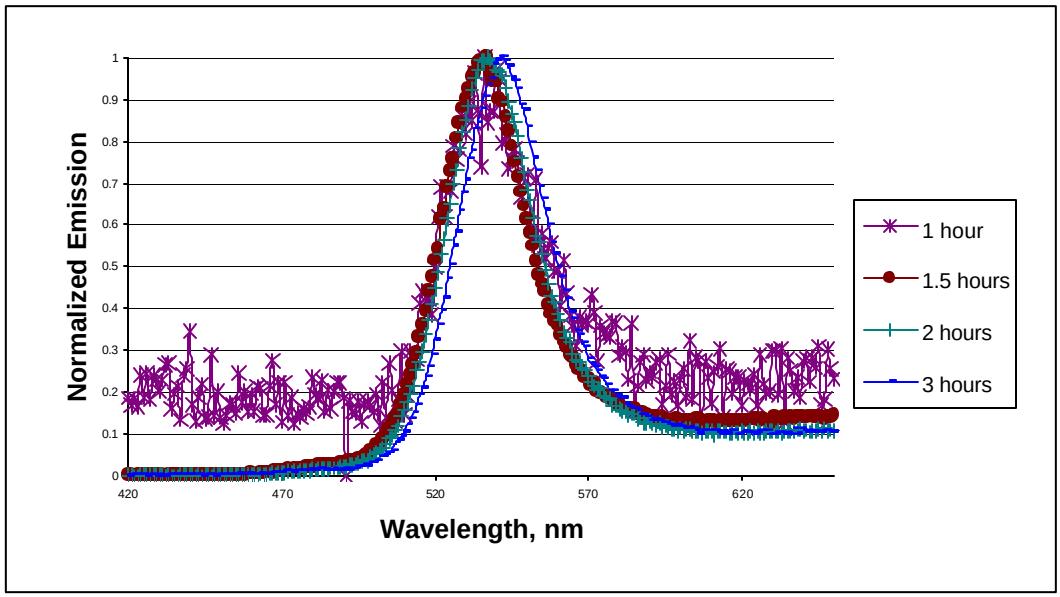

Figure 42. 100% Sulfanilamide reaction samples that indicate inhibited nucleation and growth.

7.2 Zinc Sulfide Capped CdSe Quantum Dots (CdSe/ZnS)

After a number of mistrials due to a lack of temperature control during the annealing process, CdSe/ZnS was produced in large quantities. Each reaction produces only one dot size, which means that only a single absorption/emission curve per reaction is possible. Of particular interest are the extremely bright samples that were achieved with relatively low concentrations of material. For example, a yellow-green emitting quantum dot sample was produced in which ~2uL of saturated sample in heptane added to 3 mL of heptane produced the emission peak at 556nm shown in Figure 43. The other emission peaks are for CdSe/ZnS reactions performed with the intent of reaching the colors indicated. Note how the FWHM becomes considerably larger as the reactions become longer. Additionally, because all of the reactions produced large single samples at the end, there was plenty of material on which to perform spectrophotometry and the resulting normalized absorption plots are shown in Figure 44. The broad emission curve labeled C Emission in Figure 44 and its corresponding absorption curve labeled C Absorption indicate that defocusing of the QD size distribution is occurring. This sample is a candidate for the size selective precipitation technique, but was left as produced to show how reactions tend to defocus as the size of the QDs becomes large.

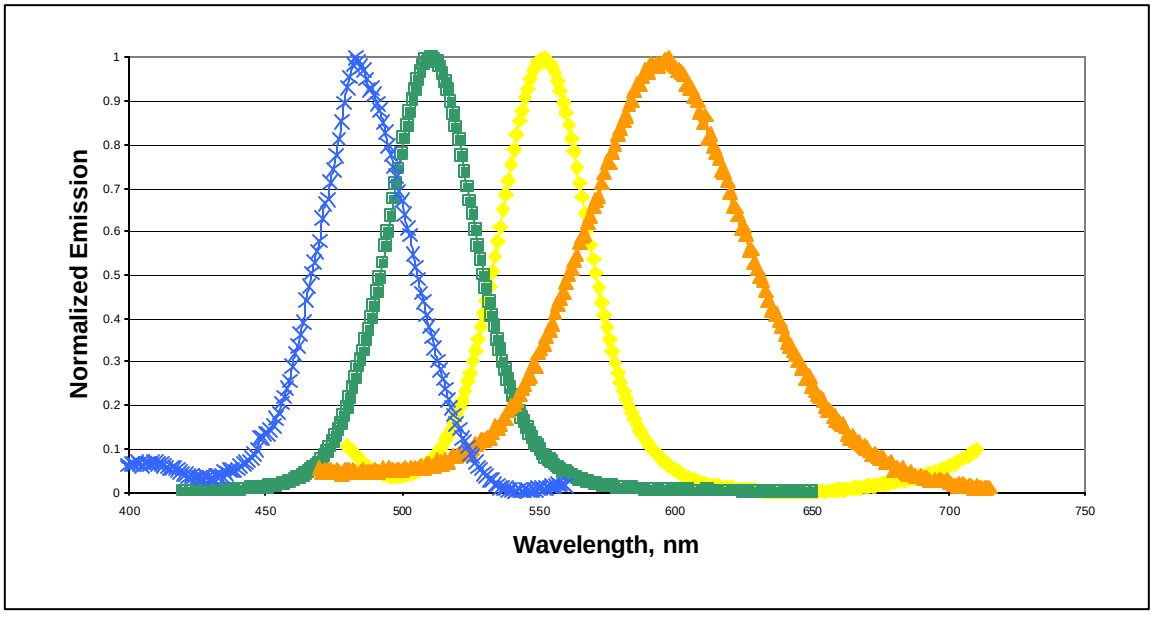

Figure 43. Yellow spectrum is the 556nm emitting CdSe/ZnS spectrum, other spectra are of other CdSe/ZnS reactions to show coverage of the visible spectrum.

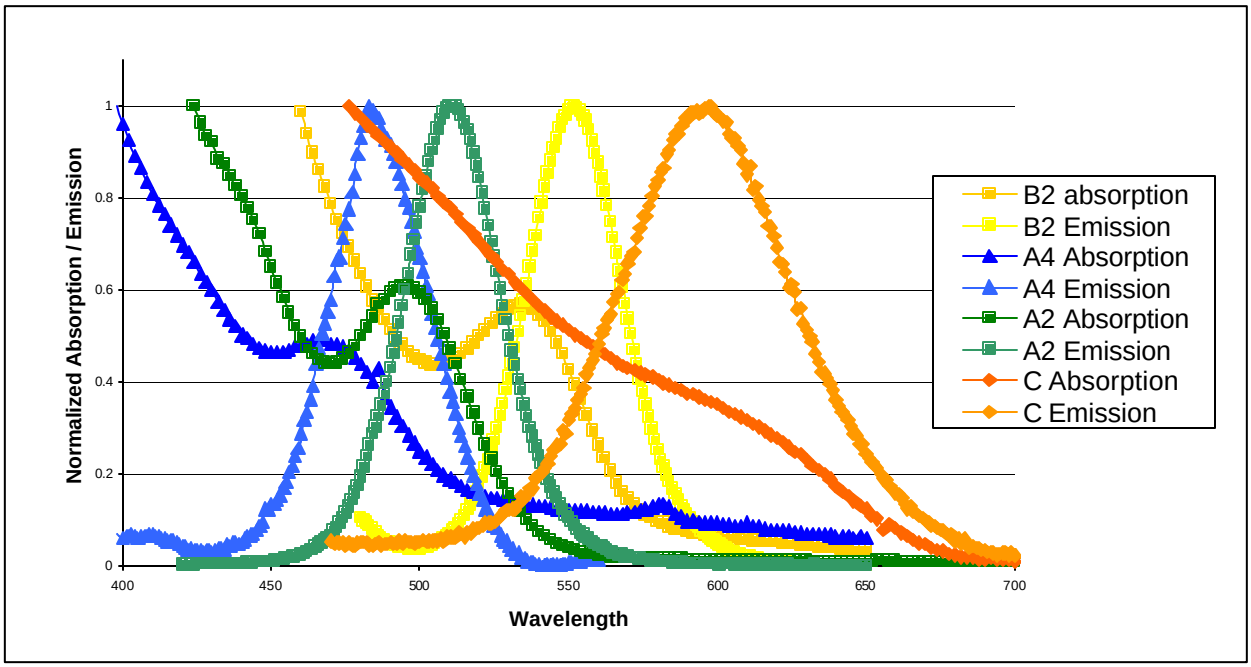

Figure 44. Absorption spectra overlaid on the emission spectra of Figure 43, note that reaction C did not absorb very well.

As Hines's group found in the early 1990s, the CdSe/ZnS core/shell particles produced here have significantly brighter emissions, meaning that there is a much higher conversion of input energy to output energy. This conversion translates to higher quantum yield. To test this, two cuvettes were filled with concentrated CdSe/TOPO and CdSe/ZnS samples with similar emission wavelengths of approximately 600nm (within 5nm of each other) and their optical densities were equilibrated. The resulting emission intensities, shown in Figure 45, indicate that the CdSe/ZnS sample has an emission intensity of greater than double that of CdSe/TOPO! Hence, the addition of a thin shell of ZnS capping reduced the number of surface defects that, in turn, reduced the occurrence of surface recombination of electron-hole pairs and thereby increased the quantum yield significantly.

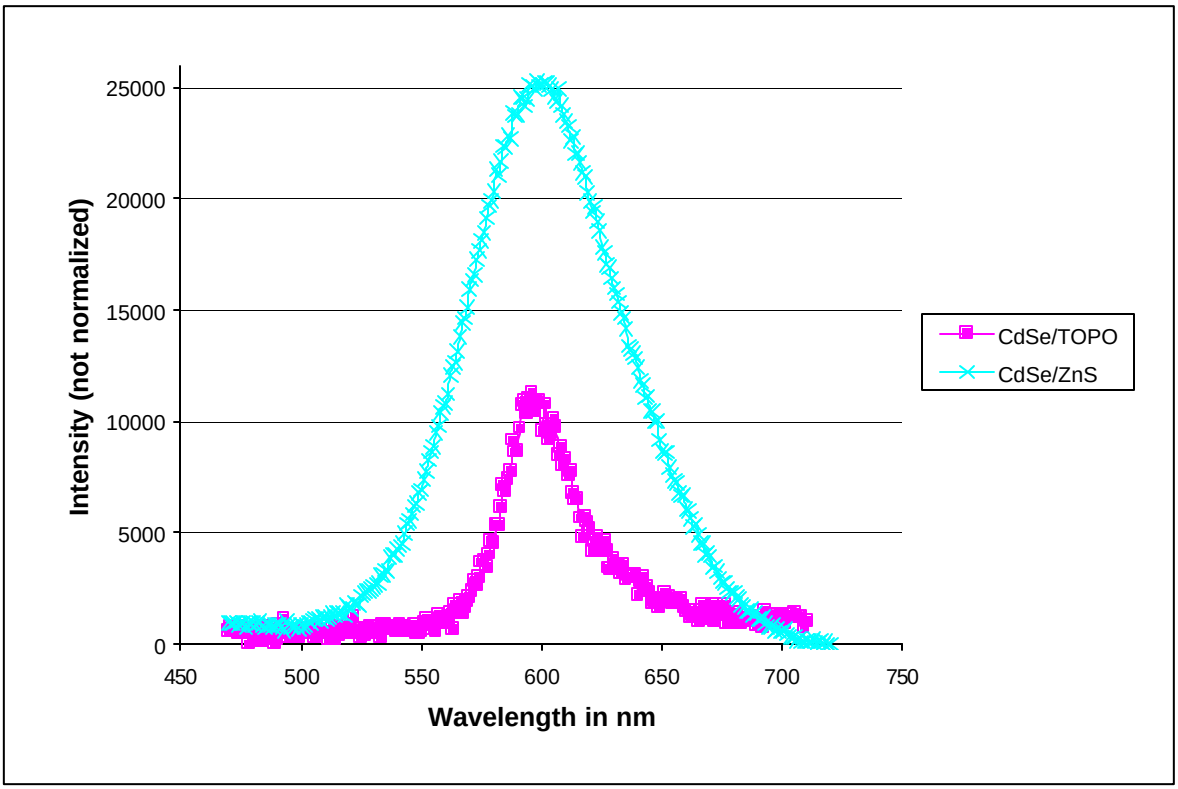

Figure 45. Plot of the difference in intensity between equal optical density samples of CdSe/TOPO and CdSe/ZnS.

7.3 Transmission Electron Microscopy (TEM) Results and Discussion

Though all of the above reactions have been investigated using TEM, the contrast of such small material without an energy filtering apparatus on the microscope is difficult to capture in printable format. However, a picture of almost every type of reaction has been taken, and a few representative pictures are presented below.

7.3.1 CdSe/TOPO – Rods, Dots, Tetrapods, and Other Shapes

Originally presented in the author's honors thesis, Figure 46 shows rods in quantity. As indicated by the length scale at the upper left of the TEM picture, these quantum rods are approximately six to eight nanometers in length and one to two nanometers in diameter, creating a significant aspect ratio.

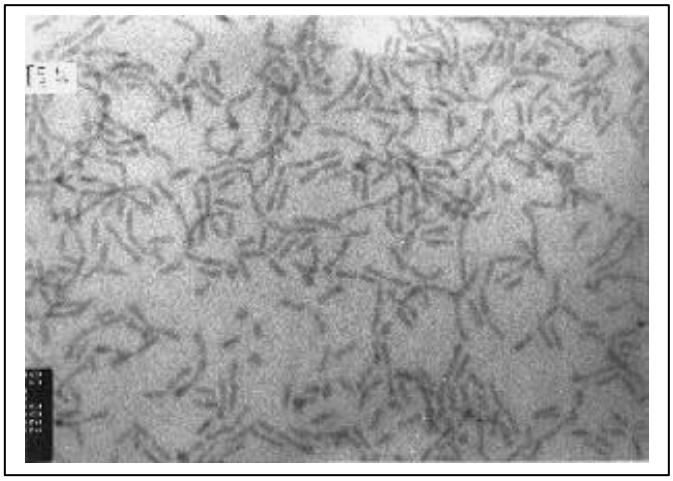

Figure 46. TEM image of quantum rods capped with TOPO.

Additionally, upon further investigation of the sample shown above, tetrapods and teardrops were found to have been produced. Alivisatos *et al.* reported on such material in 2000.[47] The arrows in Figure 47 point to arrows and tetrapod shaped CdSe nanoparticles in an enlarged portion of Figure 46. Such structures occur due to variations of monomer concentration with reaction time and may be segregated out using the size selective precipitation techniques described earlier. Uses for these different shapes are currently being explored.

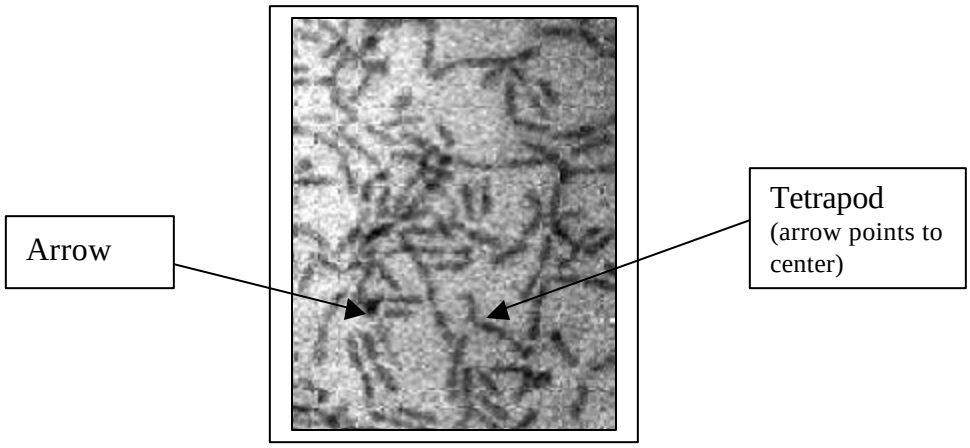

Figure 47. Enlarged section of Figure 46 showing tetrapod and arrow shaped semiconductor nanoparticles.

Figure 46 and Figure 47 may be compared to Figure 48 and Figure 49, which contain TEM pictures of QDs in a mixed size sample and rather monodisperse QDs, respectively. All of the TOPO capped CdSe structures are produced with the same type of standard CdSe/TOPO reaction, changing only the TDPA stabilizer concentration.

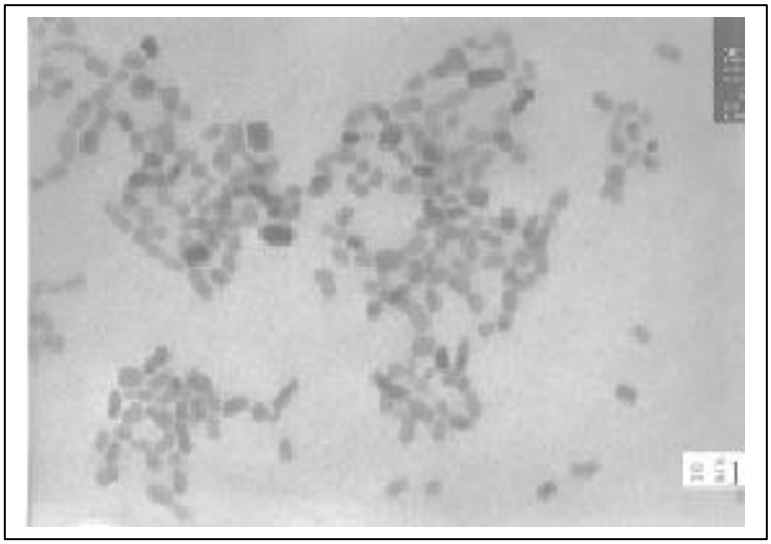

Figure 48. TEM image of a rod/dot mix, note the 10nm size bar on the lower right.

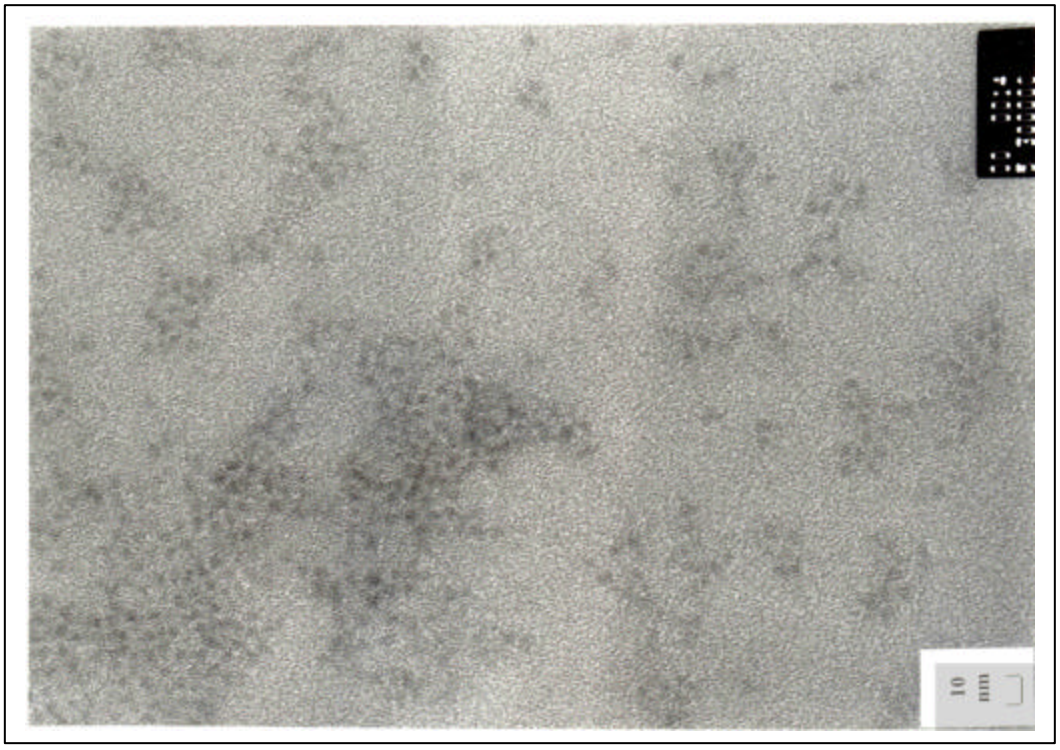

Figure 49. TEM image of CdSe/TOPO QDs with excellent monodispersity, size bar indicates diameters of approximately 5nm (magnification 300,000x).

7.3.2 CdSe/SA TEM Results

The high speed of the CdSe/SA reaction caused some initial concern as to the homogenous nature of the sample achieved. However, first fluorimetry and then TEM confirmed that the CdSe/SA reaction produced excellent QD material. As shown in Figure 50, a TEM image of the stearic acid capped material confirms that the material is actually monodisperse quantum dots with only slight aspect ratios. Additionally, as the QDs self-assemble, the spacing between them indicates that an organic material is likely to be capping the QDs. This inference may be made on the observation that the spacing between the inorganic QDs in Figure 50 is rather regular. Since TEM cannot be used to observe homogenous materials with non-crystalline structures, the capping structure would not be visible in the pictures taken using this microscopy technique, however, the spacing is an indication of the presence of a capping structure.

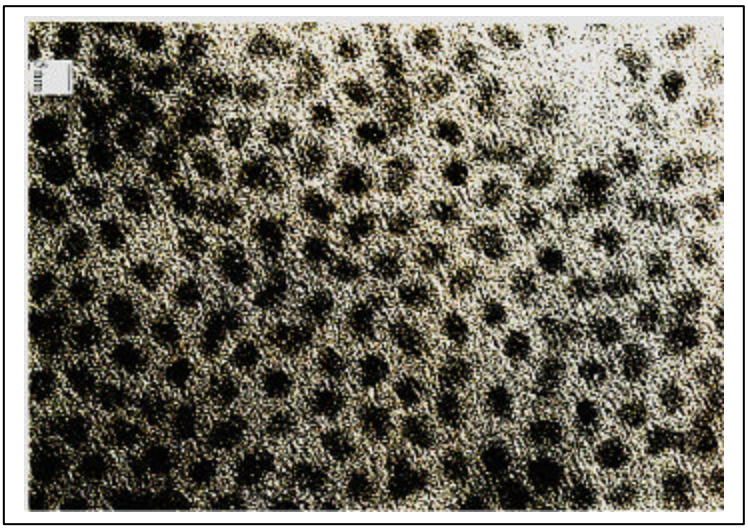

Figure 50. TEM image of 5nm diameter SA capped quantum dots with good monodispersity and low aspect ratio (magnification approx 1.6million x).

7.4 Predicting Quantum Dot Emission from Reaction Length

Over the course of the work performed and herein described, a useful but simple method was found for predicting how long a reaction needed to run before being quenched in order to attain a specific wavelength. This method was particularly useful for such capping structures as PS, APS, SA, and TOPO, which were often requested for other projects and needed to be produced in quantity to emit at a specific wavelength.

The method is highly temperature dependent and requires a reaction setup that is reproducible. However, with these guidelines in place, single injection reactions may be made to produce quantum dots reliably within a 10-15nm range of the target wavelength.

To begin, one needs to run a fixed reaction with 6-10 samples taken in the growth region that produces light emitting nanoparticles when excited by ultra-violet light. Once the reaction is completed and cleaned, fluorimetry data needs to be collected and emission peaks recorded. Once these peaks are known, a graph may be plotted such as the line labeled "original reaction" in Figure 51. As an example of this technique, a ½ hour long CdSe/SA reaction was used to produce particles with emission peaks such that the curve in Figure 51 was produced. The extra dot at 14.2 minutes (852 seconds) on the plot indicates where another reaction, which was planned to have an emission wavelength of 585nm from the plot below, actually produced dots emitting at 584nm. Hence, the prediction worked. An additional test of the forecasting ability of such a graph ensued and a best-fit line labeled "Log. (original reaction)" was added to predict an emission wavelength of 628.7nm at one hour. A reaction was run to one hour and the peak emission wavelength was recorded as 619nm, also shown on the graph in Figure 51. Hence, the actual value is only 10nm off the predicted value; this is within the aforementioned 10-15nm range of the target wavelength.

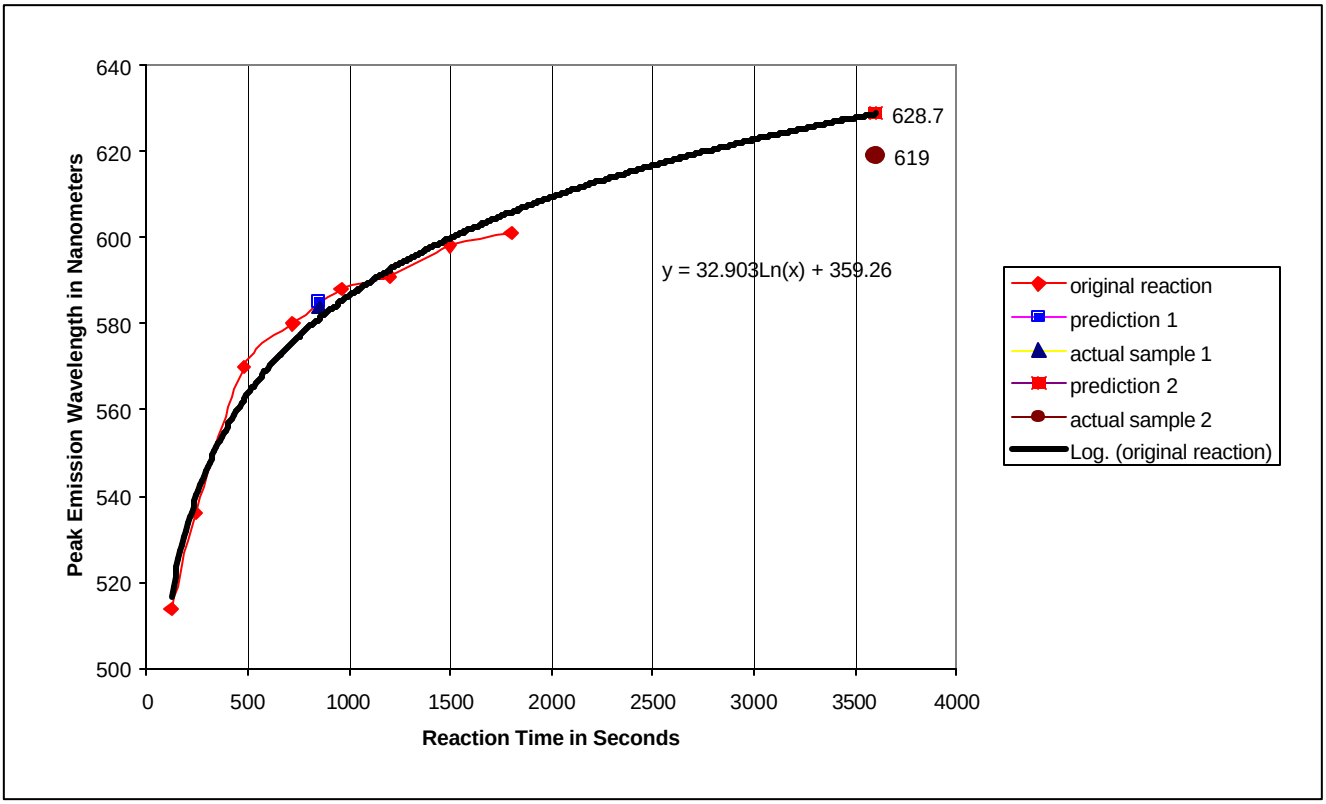

Figure 51. SA emission peak versus time plot showing predictions for two additional reactions that were performed and resulted in samples with emission wavelengths within less than 10nm of the target wavelength.

Toward the long-wavelength end of the spectrum, where the quantum confinement effects become weaker because the material approaches the bulk, the growth times usually become extremely long or one is unable to achieve the wavelength altogether. Additionally, this procedure is only good for predicting single injection, single temperature reactions. For reactions such as ZnS capping of CdSe, there are multiple injections and multiple temperatures; hence, the procedure must be refined for predicting emission wavelengths for these more complex reactions.

8. Discussion of Objectives and Results

This project began with the background laid down by the author's previous investigation of a standard reaction that produced quantum dot structures of CdSe capped with trioctylphosphine oxide, stearic acid, or dodecylamine. This work was built upon thorough temperature range investigations of SA and TOPO, as well as a determination of whether the percentages of SA and DA versus TOPO affected any aspect of the reactions to produce CdSe capped with either structure, independent of temperature effects on reaction kinetics.

Thereafter, the reaction mechanisms were extended to the investigation of phenyl sulfone, aminophenyl sulfone, 4,4'-dichlorodiphenyl sulfone, 4,4'-difluorodiphenyl sulfone, and sulfanilamide. This meant tailoring the reactions found in the literature that dealt with TOPO capping to match these new potential capping structures and determining the reaction kinetics with respect to growth time and limitations.

The modified TOPO reaction that was described above was used as the baseline from which other capping structure reactions were designed. The quantum dot-producing reactions were designed to be less toxic than the original ones Alivisatos, Hines, and others used in the early 1990s, in which dimethyl cadmium was employed as the cadmium precursor. Instead, CdO was used in the modified reaction. The standard TOPO reaction can be made to be a rather long one, as indicated by the 44-hour peak in Figure 24, but it produces uniform material and is reproducible. The reproducibility of this CdSe/TOPO reaction was tested using fluorimetry and transmission electron microscopy to look at emission spectra and size/shape uniformity over a number of reactions. Hence, the data from the TOPO capping reactions are what acted as the baseline comparison for all of the remaining reactions. Of particular interest with respect to these comparisons is the fact that certain capping structure types and even certain reaction temperatures within a capping structure type do not produce red-emitting quantum dots before bulk material is produced.

Additionally, the products of the TOPO reactions allowed for early investigation into environmental and solvent-based effects. Environmentally, quantum dots' emission is quenched when large shifts in pH, melting, or oxidation occur. These environmental conditions occur rarely during standard quantum dot production and cleaning, but need to be remembered for applications and further modifications where environments may change suddenly in terms of pH, temperature, and availability of oxygen. Solvent-based effects are generally limited to whether the quantum dot material remains suspended in the solvent or not. Generally, nonpolar solvents allow the TOPO capped quantum dots to suspend nicely, while polar solvents do not allow such suspension into colloidal form. This is important information when looking at cleaning of samples and performing both spectrophotometry and fluorimetry analysis of samples.

Concerning the techniques used for quantum dot investigation, standard TEM, spectrophotometry, and fluorimetry sufficed for these early investigations into large numbers of quantum dots. However, more in depth, single quantum dot investigations should be the next step. These could be carried out using a high-resolution transmission electron microscope and looking at lattice fringes to indicate the crystal structures. Fluorimetry, while good for large sets of quantum dots suspended in solvents as were produced for this project, is not designed for single quantum dot investigations. Much more sensitive detectors are necessary, or a system designed to look at single molecule fluorescence, such as a femto-second laser system outfitted with photon counting capabilities. Over the next year, the author will be spending time with Dr. Ulrike Woggon's group in Dortmund, Germany for exactly such investigations.

Furthermore, x-ray photoelectron spectroscopy (XPS), a surface investigation technique, could be used to investigate the surface of the CdSe to see if oxidation is occurring over time in samples that have been stored for long periods (months or years). XPS in conjunction with standard x-ray powder diffraction (XRD) also allows for the investigation of ZnS capping of CdSe because the ZnS signature will be dominant in XPS while CdSe will dominate XRD. These techniques are only now becoming viable for the work contained herein due to the sample size necessary for standard techniques. The current focus in this area is to scale up current production to allow for the employment of such techniques.

Throughout the many reactions that have been run for this project, a number of simple but very important discussion points have been uncovered concerning the procedure for all reactions. Firstly, the initial sample time at which quantum dots are present depends on the reaction kinetics (as determined by temperature, type of capping structure, etc). This means that initial reactions often act to probe the unknown to find the "speed" with which the reaction occurs. Often only a single sample out of ten will prove that a reaction has produced something promising. The next reaction's sample times must be tailored around the time at which the previous reaction has produced the promising sample, and so on.

Furthermore, to create excellent reproducibility between reactions, at least 10 seconds (preferably 15 seconds) are necessary between samples. Such a time interval

allows the operator enough time to perform the simple task of withdrawing an aliquot from the reaction carefully and safely (the reaction takes place at over 270°C). Safety is a key issue during all work with toxic material, especially when it is hot and in liquid form. This requirement may induce limitations in the type of quantum dots produced, however, only automated sampling could overcome the time constraints related to manual sampling.

Lastly, the reaction temperature and subsequent resetting thereof is extremely important in terms of reproducibility. Experience shows that a few degrees difference in the reaction temperature leads to a lack of reproducibility that can be devastating. This is due to the small size of the particles being produced. A change of a single monolayer of atoms in terms of the diameter of the particle is measured in tens of nanometers in the emission spectrum. Such sensitivity to temperature means that temperature stability and reproducibility are one of the most important variable aspects of every reaction.

9. Summary

Overall, the investigation of the production of CdSe quantum dots, of different capping structures, and of various reaction modifications has been quite successful. With few setbacks, CdSe QDs were produced with a variety of capping structures. Some of the important techniques learned include airless, high-temperature CdSe QD syntheses, toxic material handling, equipment building and monitoring, fluorimetry, spectrophotometry, and TEM.

The goal of reproducing the published data on stearic acid and dodecylamine was accomplished and an expansion of the investigations up until then ensued. The final and main goal of beginning an investigation of new capping structures and reaction modifiers has been successfully initiated with excellent prospects. Finally, the quantum dots that have been produced in this project are now ready for application based research or single quantum dot investigation. These materials have been produced, purified, characterized, and stored in such a way that they are ready for immediate use in future projects.

10. Future Work

In the future, other varieties of quantum dot materials will be investigated. Of particular interest are PbSe and InP and, in the distant future, AlN. This repertoire of nanoparticle semiconductor synthesis experience should allow for the production of quantum dots covering the spectrum from the near-ultra-violet to the infrared in terms of emission spectra.

Additionally, entraining quantum dots into various materials and creating either *in situ* sensors or luminescent materials poses many interesting challenges and exciting opportunities. In the biological labeling and tagging field, quantum dots have recently been touted in *Science* and other journals as a means to employ nanomaterials in a very significant way. [48] Future work in this area will be interdisciplinary in an extreme sense, bringing engineers, applied scientists, and theorists together to solve the next challenges and answer the next questions.

References

[1] Yoffe,A.D. “Semiconductor quantum dots and related systems: electronic, optical, luminescence and related properties of low dimensional systems.” *Advances in Physics*. Vol. 50, No. 1, 1-208, Taylor and Francis, 2001.

[2] Micic, O.I. H.M. Cheong, H. Fu, A. Zunger, J.R. Sprague, A. Mascarenhas, and A.J. Nozik. “Size-Dependent Spectroscopy of InP Quantum Dots.” *J. Phys. Chem. B.* 1997, 101, 4904-4912.

[3] Vossmeyer, T., S.Jia, E. Delonno, M.R. Diehl, S.-H. Kim, X. Peng, A.P. Alivisatos, and J.R. Heath. “Combinatorial approaches toward patterning nanocrystals.” *Journal of Applied Physics*. Vol. 84, Number 7, 1998. pp. 3664-3670.

[4] Tang, Zhiyong, Nicholas A. Kotov, Michael Giersig. “Spontaneous Organization of Single CdTe Nanoparticles into Luminescent Nanowires.” *Sicence*. Vol. 297 (#5579): pp. 237-240.

[5] Peng, Xiaogang, Michael C. Schlamp, Andreas V. Kadavanich, and A.P. Alivisatos. “Epitaxial Growth of Highly Luminescent CdSe/CdS Core/Shell Nanocrystals with Photostability and Electronic Accessibility.” *J.Am.Chem.Soc.* 1997, 119, 7019-7029

[6] Lee, Jinwook, Vikram C. Sundar, Jason R. Heine, Moungi G. Bawendi, and Klavs F. Jensen. “Full Color Emission from II-VI Semiconductor Quantum Dot-Polymer Composites.” *Advanced Materials Communications*. 2000, *12* No. 15, August 2.

[7] Parak, W.J., D. Gerion, D. Zanchet, A. S. Woerz, T. Pellegrino, C. M. Micheel, S. C. Williams, M. Seitz, R. E. Bruehl, Z. Bryant, C. Bustamante, C. R. Bertozzi, A. P. Alivisatos. "Conjugation of DNA to silanized colloidal semiconductor nanocrystalline quantum dots" *Chemical Materials* 14 (5): 2113-2119.

[8] Han, Mingyong, Xiaohu Bao, Jack Z. Su, and Shuming Nie. “Quantum-dot-tagged microbeads for multiplexed optical coding of biomolecules.” *Nature Biotechnology*. Vol. 19, July 2001.

[9] Huynh, Wendy U., Janke J. Dittmer, William C. Libby, Gregory L. Whiting, and A. Paul Alivisatos. “Controlling the Morphology of Nanocrystal-Polymer Composites for Solar Cells.” *Advanced Functional Materials*. 2003, *13*, No. 1 January.

[10] Kittel, Charles. Introduction to Solid State Physics. 5th ed. New York: John Wiley and Sons, 1976.

[11] Singh, Jasprit. Modern Physics for Engineers. New York: John Wiley and Sons: 1999.

[12] Peyghambarian, Nasser, Stephan W. Koch, and Andre Mysrowicz. Introduction to Semiconductor Optics. Englewood Cliffs: Prentice Hall, 1993.

[13] Overney, Rene M. and Scott E. Sills. "Constrained Systems: Caught Between Dimensions." Interfacial Properties on the Submicron Scale. 7 May, 2002. Site may be found at http://depts.washington.edu/nanolab/publications/dimension.pdf.

[14] Peng, Z. Adam and Xiaogang Peng. “Formation of High-Quality CdTe, CdSe, CdS Nanocrystals using CdO as Precursor.” *J. Am. Chem. Soc.* 2001, *123*, 183-184.

[15] Fantini, A. Phillipp, F. Kohler, C. Porsche, J. Scholz, F. “Investigation of self-assembled InP-GaInP quantum dot stacks by transmission electron microscopy.” *Journal of Crystal Growth*. v 244 n 2 October 2002. p 129-135.

[16] Jan, Ja-Chin, Shou-Yi Kuo, Sun-Bin Yin, and Wen-Feng Hsieh. “Temperature Induced Stress of ZnSe Quantum Dots in Glass Matrix Thin Films Grown by Pulsed Laser Deposition.” *Chinese Journal of Physics.* Vol. 39, No. 1, Feb. 2001. p 90-97.

[17] Lipovskii, A. E. Kolobkova, V. Petrickov, I. Kang, A. Olkhovets, T. Krauss, M. Thomas, J. Silcox, F. Wise, Q. Shen, and S. Kycia. “Synthesis and Characterization of PbSe quantum dots in phosphate glass.” *Appl. Phys. Lett.* 71 (23), 8 December 1997. p. 3406-3408.

[18] Banerjee, Sharmila; Sen, Pratima. “Optical Gain in an Inhomogeneous Distribution of CdS Quantum Dots Embedded in Glass Matrix.” *Journal of Nonlinear Optical Physics and Materials and Physical Computation* 10, no. 3 (2001): 355-370.

[19] Chia, Connie, Kao, Yu-Hua. Xu, Yuhuan Mackenzie, John D. “Cadmium telluride quantum dot-doped glass by the sol-gel technique.” Proceedings of SPIE - The International Society for Optical Engineering. v 3136 1997. p 337-347.

[20] Ou, Duan Li., Seddon, Angela B. “Cadmium selenide quantum dot doping of organic-inorganic hybrid materials derived by sol-gel processing.” Proceedings of SPIE - The International Society for Optical Engineering. v 3136 1997. p 348-357.

[21] Micic, Olga I., Calvin J. Curtis, Kim M. Jones, Julian R. Sprague, and Arthur J. Nozik. "Synthesis and Characterization of InP Quantum Dots." *J.Phys.Chem.* 1994, *98*, 4966-4969.
[22] Guzelian, A.A., J.E.B. Katari, A.V. Kadavanich, U. Banin, K. Hamad, E. Juban, A.P. Alivisatos, R.H. Wolters, C.C. Arnold, and J.R. Heath. "Synthesis of Size Selected, Surface-Passivated InP Nanocrystals." *J. Phys. Chem.* 1996, *100*, 7212-7219.
[23] Micic, O.I., J.R. Sprague, C.J. Curtis, K.M. Jones, J.L Machol, and A.J. Nozik. "Synthesis and Characterization of InP, GaP, and $GaInP_2$ Quantum Dots." *J. Phys. Chem* 1995, *99*, 7754-7759.
[24] Micic, O.I., H.M. Cheong, H. Fu, A. Zunger, J.R. Sprague, A. Mascarenhas, and A.J. Nozik. "Size-Dependent Spectroscopy of InP Quantum Dots." *J. Phys. Chem.B*. 1997, *101*, 4904-4912.
[25] Talapin, D.V. A.L. Rogach, H. Borchert, S. Haubold, M, Haase, and H. Weller. "Colloidal Synthesis of Monodisperse Luminescent InP Nanocrystals." Indium Phosphide and Related Materials Conference, 2002. IPRM. 14th *Proceedings.* pp. 593-596.
[26] Fu, H., A. Zunger, *Phys. Rev. B* Vol 56, p. 1496, 1997.
[27] Kubo, T. Isobe, T. Senna, M. "Enhancement of photoluminescence of ZnS:Mn nanocrystals modified by surfactants with phosphate or carboxyl groups via a reverse micelle method." *Journal of Luminescence*. v 99 n 1 August 2002. p 39-45.
[28] Bol, Ageeth A. Meijerink, Andries. "Luminescence of nanocrystalline ZnS:Pb2+." Materials Research Society Symposium - Proceedings. v 667 2001. p G471-G476.
[29] Kulkarni, S K. Winkler, U. Deshmukh, N. Borse, P H. Fink, R. Umbach, E. "Investigations on chemically capped CdS, ZnS and ZnCdS nanoparticles." *Applied Surface Science*. v 169-170 Jan 2001. p 438-446.
[30] Kho, Richard, Claudia L. Torres-Martinez, and Rajesh K. Mehra. " A Simple Colloidal Synthesis for Gram-Quantity Production of Water-Soluble ZnS Nanocrystal Powders." *Journal of Colloid and Interface Science*. 227, 561-566 (2000).
[31] Trindade, Tito, Olinda C. Monteiro, Paul O'Brien, and Majid Motevalli. "Synthesis of PbSe nanocrystallites using a single-source method. The X-ray crystal structure of lead (II) diethyldiselenocarbamate." *Polyhedron* Vol. 18, Issues 8-9, 12 March 1999, pp 1171-1175.
[32] Chen, Feng, Kevin L. Stokes, Weilie Zhou, Jiye Fang, and Christopher B. Murray. "Synthesis and Properties of Lead Selenide Nanocrystal Solids." Mat.Res.Soc.Symp.Proc.Vol 691, 2002, Materials Research Society.
[33] Kortan, A.R., R. Hull, R.L. Opila, M.G. Bawendi, M.L Steigerwald, P.J. Carroll, and L.E. Brus. "Nucleation and Growth of CdSe on ZnS Quantum Crystallite Seeds, and Vice Versa, in Inverse Micelle Media." *J. Am. Chem. Soc.* **1990**, *112*, 1327-1332.
[34] Yang, Heesun, and Paul H. Holloway. "Enhanced photoluminescence from CdS:Mn/ZnS core/shell quantum dots." *Applied Physics Letters.* Vol. 82, Number 12. American Institute of Physics, 2003.
[35] D.V. Talapin, S.K. Poznyak, N.P. Gaponik, A.L. Rogach, A. Eychmueller. "Synthesis of surface-modified colloidal semiconductor nanocrystals and study of photoinduced charge separation and transport in nanocrystal-polymer composites." *Physica E: Low Dimensional Systems and Nano-structures*. Vol. 14, Issues 1-2, April 2002. pp 237-241.
[36] Murray C., Norris D., Bawendi M., "Synthesis and Characterization of Nearly Monodisperse CdE (E=S, Se, Te) Semiconductor Nanocrystallites." J. Am. Chem. Soc., 115, (1993).
[37] Talapin, D.V., Stephan Haubold, Andrey L. Rogach, Andreas Kornowski, Markus Haase, and Horst Weller. "A Novel Organometallic Synthesis of Highly Luminescent CdTe Nanocrystals." *Journal of Physical Chemistry B.* 2001, *105*, 2260-2263.
[38] Goldstein, A N. Echer, C M. Alivisatos, A P. "Melting in semiconductor nanocrystals." *Science*. v 256 n 5062 Jun 5 1992 p 1425-1427
[39] Hines, Margaret A., Phillippe Guyot-sionnest. "Synthesis and Characterization of Strongly Luminescing ZnS-Capped CdSe Nanocrystals." *J.Phys. Chem.* 1996, 100, 468-471.
[40] Danek, M. Jensen, K F. Murray, C B. Bawendi, M G. "Preparation of II-VI quantum dot composites by electrospray organometallic chemical vapor deposition." *Journal of Crystal Growth*. v 145 n 1-4 Dec 2 1994. p 714-720.
[41] Meissner, Kenith. "Development of Fluid-based Microarray Technology Using Microspheres and Quantum Dots." Application for an Individual Allocation from American Cancer Society Institutional Research Grant, 2001.

[42] Meissner, K.E., E. Herz, R.P. Kruzelock, and W.B. Spillman. “Quantum dot-tagged microspheres for fluid-based DNA microarrays.” phys. stat. sol. (c) **0**, No. 4, 1355– 1359 (2003).
[43] Qu, Lianhua, Z. Adam Peng, and Xiaogang Peng. "Alternative Routes toward High Quality CdSe Nanocrystals." *Nano Letters* Vol. 1 No. 6, American Chemical Society, 2001.
[44] Zhu, Junjie, Xuehong Liao, Xiaoning Zhao, Jun Wang. “Photochemical synthesis and characterization of CdSe nanoparticles.” *Materials Letters*. 47 (2001) 339-343.
[45] Gerion, Daniele, Fabien Pinaud, Shara C. Williams, Wolfgang J. Parak, Daniela Zanchet, Shimon Weiss, and A. Paul Alivisatos. “Synthesis and Properties of Biocompatible Water-Soluble Silica-Coated CdSe/ZnS Semiconductor Quantum Dots.” *J. Phys. Chem. B.* **2001**, *105*, 8861-8871.
[46] Parak, W.J., D. Gerion, D. Zanchet, A. S. Woerz, T. Pellegrino, C. M. Micheel, S. C. Williams, M. Seitz, R. E. Bruehl, Z. Bryant, C. Bustamante, C. R. Bertozzi, A. P. Alivisatos. "Conjugation of DNA to silanized colloidal semiconductor nanocrystalline quantum dots" *Chemical Materials* 14 (5): 2113-2119.
[47] Manna, Liberato, Erik C. Scher, and A. Paul Alivisatos. “Synthesis of Soluble and Processable Rod-, Arrow-, Teardrop-, and Tetrapod-Shaped CdSe Nanocrystals.” *J. Am. Chem. Soc.* 2000, 122, 12700-12706.
[48] Chan, Warren C. and Shuming Nie. “Quantum Dot Bioconjugates for Ultrasensitive Nonisotopic Detection.” Science. 25 September 1998 Vol 281.

Appendix A

Paper: “Quantum dot-tagged microspheres for fluid-based DNA microarrays”

Includes pages 70 – 74 (unnumbered).

phys. stat. sol. (c) **0**, No. 4, 1355–1359 (2003) / **DOI** 10.1002/pssc.200303092

Quantum dot-tagged microspheres for fluid-based DNA microarrays

K. E. Meissner[*,1], **E. Herz**[1], **R. P. Kruzelock**[2], and **W. B. Spillman, Jr.**[1]

[1] Optical Sciences and Engineering Research Center, Virginia Polytechnic Institute and State University, Blacksburg, VA 24061, USA

[2] Virginia Bioinformatics Institute, Virginia Polytechnic Institute and State University, Blacksburg, VA 24061, USA

Received 30 September 2002, accepted 2 December 2002
Published online 3 July 2003

PACS 87.80.–y, 85.35.Be, 87.14.Gg

Quantum dot-embedded microspheres offer a promising technology for the development of a fluid-based DNA microarray to replace current biochip microarray technology. The narrow emission and long lifetime from the quantum dots (QD's) is ideal for dense spectral multiplexing. Also, the QD's may all be excited by a single source. To implement this solution, we have fabricated CdSe quantum dots following published procedures and embedded them in polystyrene microspheres. As a first step in this development, we have investigated the use of a flow cytometer in analyzing the encoded microspheres. We demonstrate the use of a microsphere-based DNA detection system and investigate the readout of quantum dot-tagged microspheres. We also discuss some of the inherent limitations and difficulties of using such a system to address the need for a high-throughput readout for spectral multiplexing for fluid-based DNA microarrays.

1 Introduction DNA microarray technology can be used for comparative genome hybridization, polymorphism analysis, gene mapping, evolutionary studies, mutation detection, compound screening and optimization, toxicity screening, as well as gene expression profiling. Specifically, microarrays provide a powerful high-throughput system that allows for large-scale analysis of gene expression, genetic alterations, and signal transduction pathways, providing a valuable tool for disease diagnostics, prognostics and therapeutics. Prototype gene expression microarrays emerged as experimental platforms in the late 1980s [1, 2]. In most cases, hybridization was performed on membranes, but in 1992, E. Southern's laboratory reported a method to covalently attach oligonucleotides on a glass surface [3]. On this foundation, the first glass cDNA expression microarrays were built [4]. Conventional biochip technology consists of robotically printing oligonucleotides or cDNA clone inserts onto a glass slide. One or more fluorescent-labeled cDNA probes are then generated from the samples to be compared and hybridized to the surface. A laser is used to excite the dye labels and the resulting fluorescent intensities are acquired using a laser confocal fluorescent scanner. The resulting ratio of fluorescent intensities forms the basis for further meta-analyses such as clustering. These spatially multiplexed systems have provided a firm foundation for genetic analysis, but suffer from a number of weaknesses.

Microsphere-based arrays are a significant first step toward overcoming many of these design limitations inherent to conventional microarray technologies. Rather than giving each target gene a positional signature on a biochip, the identity of a gene can be determined by the spectral signature of a micro-

[*] Corresponding author: e-mail: kmeissne@vt.edu, Phone: +01 1 540 231 2512, Fax: +011 540 231 6642

 1610-1634/03/00007-1355 $ 17.50+.50/0

Table 1 Basic comparison of typical biochip DNA microarray with microsphere-based microarray. The biochip microarray is based on 150 μm diameter spots. The element surface area defines the surface area of each array element (spot or microsphere).

	sample volume (•l)	packing fraction (%)	element surface area (•m^2)	total array elements	total target area (cm^2)
biochip	20	14.5 (by area)	17691	15000	2.7
microsphere	20	15.5 (by vol.)	12.6	877000000	111

sphere. The use of functionalized microspheres permits hybridization to take place in the more controlled environment of a test tube. Gene expression profiles are estimated as the microspheres are passed through a high speed readout system such as a flow cytometer. Table 1 demonstrates the advantage of using many smaller array elements in a microsphere-based system. Here, a standard biochip microarray is compared with a system based on 2 •m diameter microspheres. The sample volume and packing fraction are essentially the same in the two cases. The effects of using many smaller probing elements will produce far better statistical data on the target population. Microsphere-based systems would be compact, relatively inexpensive, easily automated, and offer a viable means to identify individuals with physiological disorders such as cancer, diabetes, and cardiovascular disease.

The introduction of high-throughput technologies will permit us to pose questions about how genes and gene products collaborate to affect the outcome in complex diseases like cancer. Current biochip microarrays do not include the number of replicates needed to distinguish small relative changes in gene expression versus normal genetic variability. A microsphere based system, as demonstrated above in Table 1, would allow for the necessary number of replicates, decrease the signal to noise ratio, and broaden the detection limits.

2 Experimental details

2.1 Production of CdSe/ZnS core/shell quantum dots CdSe/ZnS core/shell nanocrystals were synthesized and their core size estimated at 3.9 nm using previously reported methods [5, 6]. The addition of the ZnS capping structure shifted the emission wavelength approximately +15 nm indicating an increased diameter of approximately 7 nm [7]. Briefly, trioctylphosphine oxide (TOPO), CdO, and a stabilizer were heated under argon in a two-neck flask. After approximately forty minutes at 340 °C the solution turned colorless and Se-trioctylphosphine (Se/TOP) stock solution was added. At the desired emission wavelength, the reaction mixture was allowed to cool to approximately 300 °C and a Zn/S/TOP solution was injected in five half-milliliter portions evenly spaced over 100 seconds. The Zn/S/TOP solution was produced using hexamethyldisilathiane, dimethylzinc, and TOP as precursors [8]. The temperature was allowed to drop to 100 °C and the reaction continued for 1 hour thereafter. The CdSe/ZnS product was precipitated using methanol and resulted in the spectra shown in Fig. 1.

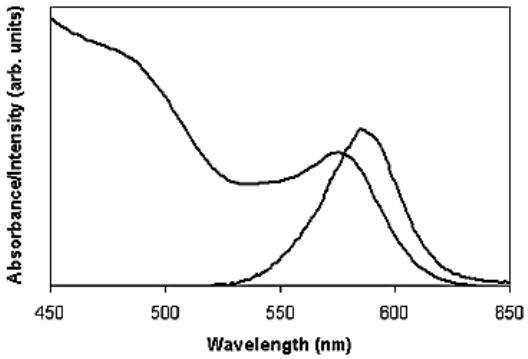

Fig. 1 Absorbance and emission spetra from the CdSe/ZnS quantum dots used in this work.

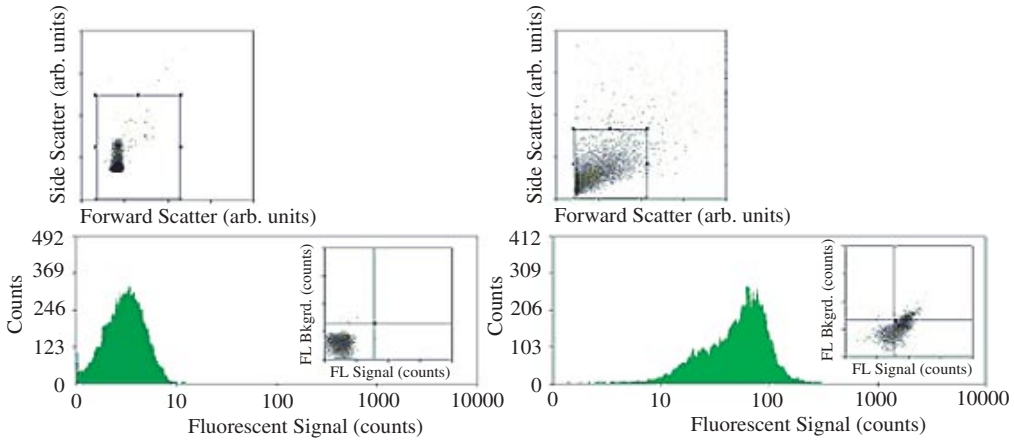

Fig. 2 (online colour at: www.interscience.wiley.com) Flow cytometer data from polystyrene microspheres without hybridized DNA targets (left set of graphs) and with DNA targets (right set of graphs). Set of graphs includes a histogram of fluorescent return from fluorescein (large graphs at bottom), graph of flourescein flourescence versus fluorescence in a background wavelength band (inset), and graph of forward scatter versus side scatter (top graphs).

2.2 Infusion of polystyrene spheres with CdSe/ZnS quantum dots Polystyrene microspheres were infused using modifications of previously reported methods [9]. Typically, the microspheres were swelled using a 95% butanol/5% chloroform solution to which was added a suspension of CdSe/ZnS quantum dots in heptane. After 20 minutes of constant shaking, the solution was centrifuged and the spheres resuspended in phosphate buffer solution.

2.3 Attachment of DNA to microspheres DNA oligonucleotides were attached to the surface of CdSe/ZnS nanocrystal-infused carboxylated microspheres through an aqueous procedure using the manufacturer's preferred method. Most commonly, approximately 5 million spheres were surface activated using 1-ethyl-3-(3-dimethylaminopropyl)-carbodiimide (EDC); amino-modified oligonucleotides were added and allowed to react with the activated surface. The microspheres were washed and placed in a phosphate buffer solution for storage and characterization of attachment.

2.4 Flow cytometer Flow cytometers measure the properties of cells or cellular-sized particles in suspension as they flow through a laser beam in single file. The measurement system is triggered by a scattering event. The flow cytometer then measures forward scatter intensity, side scatter intensity and emission intensity in a number (usually 3 or 4) of wavelength bands.

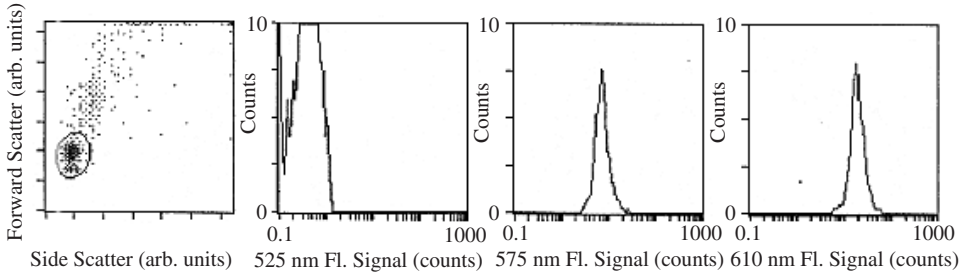

Fig. 3 Flow cytometer data from single color polystyrene microspheres. The leftmost graph shows the scattering profile and grouping. The three graphs to the right are histograms showing emission events in three wavelength bands ($\Delta\lambda = 10$ nm FWHM). The quantum dot emission peak at 590 mn accounts for the signals on both the 575 nm and 610 nm channels.

3 Results and discussion The first step in demonstrating the viability of a DNA microarray based on polystyrene microspheres process involved testing the hybridisation of target DNA to probe DNA attached to the microspheres. Here we isolated total RNA from mouse embryonic stem (ES) cells. A T75 flask of mouse ES cells and the fibroblast feeder cells on which they were grown was added to 5 ml of TRIZOL. 1 ml of chloroform was added and the organic and aqueous phases were separated by centrifugation. Total RNA was precipitated with isopropanol and resuspended in DEPC water. 5 μg of total RNA, the amount of total RNA that we use in our microarray experiments, was used for reverse transcription, dye primer fluorescein labeling and microsphere hybridisation [10]. Fluorescein-labeled pools of cDNA were hybridized to GAPDH specific oligonucleotide probes coupled to the surface of unstained 5.5 μm microspheres. Hybridisation experiments were performed as described [11]. As shown in Fig. 2, a robust signal was detected after a 2 h hybridisation. The mean of the fluorescent signal detected from the fluorescein-tagged DNA increases by more than one order magnitude. The background signal in the unused wavelength band increases slightly due to leakage from the fluorescein. Additionally, the scattering profile of the microspheres is significantly different suggesting that we have successful hybridisation. Because the hybridisation time is much shorter than typical for biochip microarrays (~16 h), the microsphere hybridisation efficiency appears to be superior.

After confirming the efficacy of microsphere-based DNA microarrays, we explored the use of quantum dots to label the microspheres. Since the detectors on a flow cytometer are not correlated, multicolor tests are not possible at this time. The CdSe/ZnS quantum dots (whose absorption and emission spectra were shown in Fig. 1) were infused into 5.5 •m diameter polystyrene microspheres as described and run through a flow cytometer. The results are shown in Fig. 3. Here, a tight grouping of events is observed in the scatter graph and chosen for analysis (as indicated by the circle). Events outside this tight grouping are generally due to multiple microspheres in a droplet or other anomalous droplet behavior. The three wavelength channels show signals from 10 nm bandpass filters centered at the labelled wavelengths. The 525 nm channel has only 0.2% of the selected events occurring above the background level set with undoped microspheres. As expected, the 575 nm and 610 nm channels both show a strong signal due to the quantum dots in the microspheres and capture 99.6% and 99.8% of the selected events, respectively. This demonstrates the ability to use a flow cytometer for high speed readout of a microsphere-based microarray.

Finally, the ability of the flow cytometer to differentiate intensity levels from the microspheres was tested. Two sets of microspheres were infused with different densities of quantum dots and mixed in phosphate buffer solution. The results are shown in Fig. 3. Two distinct peaks are observed in both the 575 nm and 610 nm channels. Here, a similar tight grouping of events was observed in the scatter graph with 91.9% of the grouped events being above the background level for the 610 nm channel. The higher peak comes from identical microspheres to those used in Fig. 4. Thus, the PMT detector voltage has been increased to allow observation of the two populations, which are clearly distinguishable with some overlap region that would have to be removed for data analysis. Thus, flow cytometry can be used to sort or count multiple intensity populations.

4 Conclusions We have begun to investigate high-speed readout systems for a quantum dot-tagged DNA microarray based on polystyrene microspheres and narrow CdSe/ZnS quantum dot emission. This

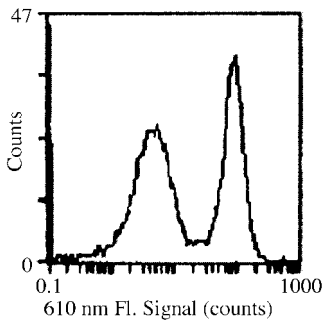

Fig. 4 Flow cytometer data for a mixed population of microspheres with different intersity levels.

type of system would be fluid-based and have distinct advantages over conventional biochip microarrays. The use of a flow cytometer for the required high-speed readout would permit the use of this technique with current hospital, clinical and research equipment. The results demonstrate the ability to perform DNA analysis with microspheres, the ability to infuse the microspheres with quantum dots for spectral tagging and the ability to differentiate muliple intensity populations. Unfortunately, the detectors on standard flow cytometers are not correlated. Therefore, multiple color work cannot be performed at this time. We are endeavouring to add this capability to the flow cytometer being used in this study. Additionally, we are gaining better control of the infusion process to narrow the signals and enable additional intensity differentiation. Thus far, the results indicate that flow cytometers provide an interesting option for performing the high speed readout of fluid-based microarrays.

Acknowledgement This work was supported by the American Cancer Society and the Carilion Biomedical Institute.

References

[1] L. H. Augenlicht, M. Z. Wahrman, H. Halsey, L. Anderson, J. Taylor, and M. Lipkin, Can. Res. **47**, 6017 (1987).
[2] R. Hauber and R. Geiger, Nucl. Acids Res. **16** (3), 1213 (1988).
[3] U. Maskos and E. M. Southern, Nucl. Acids Res. **21** (20), 4663 (1993).
[4] M. Schena, D. Shalon, R. W. Davis, and P. O. Brown, Science **270** (5235), 467 (1995).
[5] Z. A. Peng and X. Peng, J. Am. Chem. Soc. **123**, 183 (2001).
[6] Z. Peng, J. Wickman, and A. P. Alivisatos, J. Am. Chem. Soc. **120**, 5343 (1998).
[7] B. O. Dabbousi, J. Rodriguez-Viejo, F. V. Mikulec, J. R. Heine, H. Mattoussi, R. Ober, K. F. Jensen, and M. G. Bawendi, J. Phys. Chem. B **101**, 9463–9475 (1997).
[8] M. A. Hines and P. Guyot-Sionnest, J. Phys. Chem. **100**, 468 (1996).
[9] M. Han, X. Gao, J. Z. Su, and S. Nie, Nature Biotechnology **19**, 631 (2001).
[10] For protocols: Baylor College of Medicine Microarray Core Lab http://public.bcm.tmc.edu/mcfweb/index.htm.
[11] A. Spiro, M. Lowe, and D. Brown D, Appl. and Env. Microbiol. **10**(66), 4258 (2000).

Appendix B

CdSe/TOPO rods

For a typical rod producing reaction, cadmium oxide was heated under an argon blanket in 90% purity trioctylphosphine oxide (TOPO) and tetradecylphosphonic acid (TDPA) at 340°C until the color changed from dark red-brown to nearly colorless. Simultaneously, selenium shot was heated in trioctylphosphine (TOP) under argon until the selenium has gone into solution. The temperature was dropped to 270°C. Once these steps were finished, the selenium solution was injected into the cadmium solution and the reaction began immediately. Aliquots were removed periodically. The various aliquots produced different sized nanoparticles according to the growth time in solution and hence, different emission peaks were achieved. As Peng, *et al* mentioned, "the kinetics of crystal growth will also be influenced strongly by the variation of the surface energy with size, provided the crystallites are small enough that the Gibbs-Thomson effect is significant."[1] The product of the reaction must be washed with methanol and toluene and is then stored in a variety of nonpolar solvents such as heptane, dichloromethane, or toluene.

[1] Peng, Xiaogang, J. Wickham, and A.P. Alivisatos. "Kinetics of II-VI and III-V Colloidal Semiconductor Nanocrystal Growth: 'Focusing' of Size Distributions." *J. Am. Chem Soc.* Vol. 120. American Chemical Society, 1998.

Appendix C

Fluorimetry Procedure

Prepared by Molly Tinius for Erik Herz

FLUORIMETRY

Fluorimetry is the process of detecting the fluorescence or photoluminescence of a substance. A sample is excited at a certain wavelength of light and re-emits light at a different wavelength. The emission is detected and measured, allowing a quantitative analysis of the photoluminescence of the sample.

PREPARING THE FLUORIMETER

1. Turn on both cold-water taps so that they trickle into the sink. This will keep the excitation lamp from overheating.

2. Turn on the surge protector connected to the computer and fluorimeter. (If water is seen leaking near the machine, turn off both cold-water taps immediately and turn off the surge protector.)

3. On the lamp power supply, press the "power" button; then press and hold the "ignite" button until the number on the digital display reads between 130 and 140. The number will eventually stabilize at approximately 150. Turn on the high voltage power supply. The number readout should stabilize at -1168.

4. Turn on the computer. On the desktop, double-click the icon for the "Felix" program. From the "Acquire" menu, choose "Emission Scan."

5. After the monochromators have stopped spinning and clicking and haveset themselves, double-check the actual values on the monochromators with the on-screen values. If necessary, change the on-screen values to match the actual values.

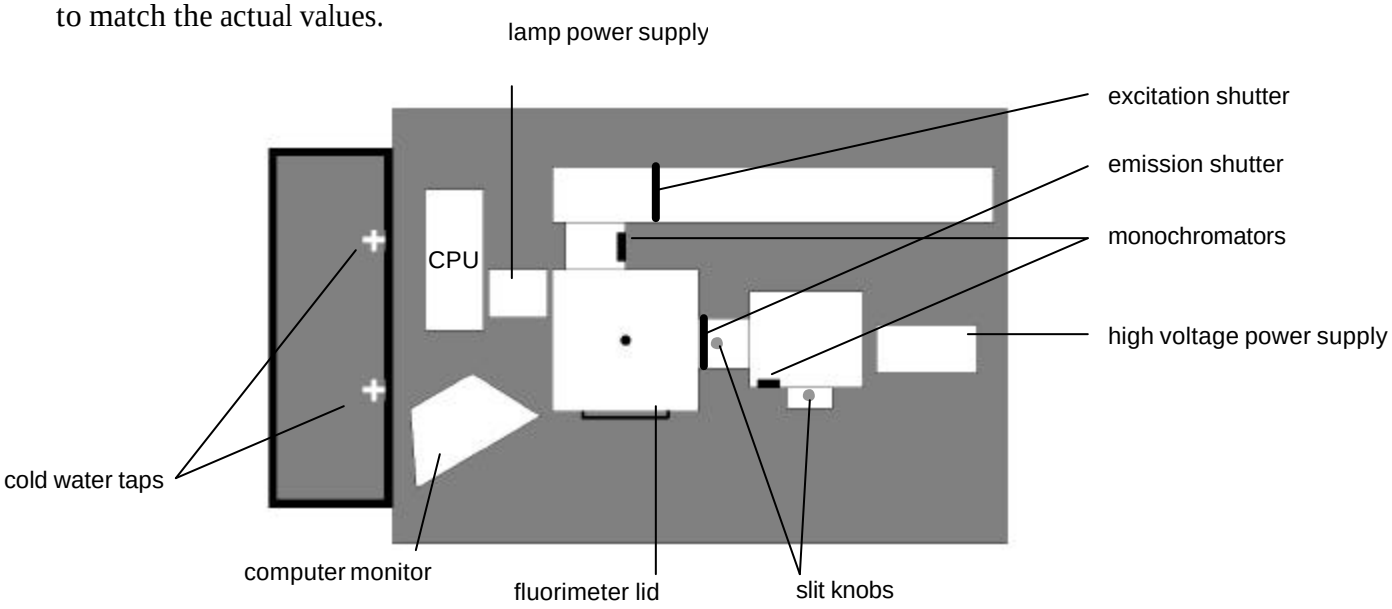

PREPARING THE SAMPLE

1. Using a Pasteur pipette, fill a sample cuvette with heptane to one millimeter (1 mm) below the line.

2. Transfer five (5) drops of concentrated sample solution from its vial to the heptane-filled cuvette using a Pasteur pipette. Mix the solution by sucking some of it up into the pipette and then squirting it gently back into the cuvette.

OBTAINING AN EMISSION SCAN

1. Open the lid to the fluorimeter and place the cuvette containing the sample solution inside. Make sure to close the lid. If you have propped it open, and it will not close, lift the latch on the right side of the lid to release it.

2. Ensure that the shutters to the excitation and emission monochromators are open. Using the silver knobs, adjust the slits to 10 microns.

3. On the computer screen in the "Emission Scan" window, set "Excitation" wavelength to between 300 and 450 nm. A good starting value is 350 nm. Set "Emission" range; the lowest value should be at least 70 nm greater than the excitation wavelength, and the highest value should be no greater than 50 nm less than twice the excitation wavelength. Change "Integration Time" to 0.1 s. Change "Number of Averages" to 4.

4. Click "Acquire" and allow the monochromators to adjust. Once the monochromators are set, click "Start." As the emission scan is acquired, keep a careful eye on the y-axis value. If the value approaches 1×10^6, immediately close the emission shutter to prevent overloading the detector. Cancel the emission scan, and dilute the sample solution with more heptane before re-running it.

RECORDING DATA AND CLEANING UP

1. After the emission scan is finished, record the following information in your lab notebook: Sample name, sample number, number of averages, excitation wavelength, emission peak wavelength, slit width, and emission scan number.

2. Remove the cuvette from the fluorimeter. Transfer the dilute solution into a clean vial. It should be labeled exactly like the concentrated solution, with the addition of the word "dilute." Rinse the cuvette well with heptane. The cuvette can be reused as long as it is rinsed well between samples. If, at any time, the cuvette appears stained or dirty, discontinue use until it can be cleaned properly.

3. After all samples have been run, save the file in the "My Documents" folder on the computer's hard drive. Write the file name in your lab notebook.

4. Shut down the computer; turn off the high voltage power supply and lamp power supply. Turn off the surge protector as well. Finally, make sure the cold water taps are turned off before you leave the room.

Appendix D

Full emission spectra plots of 50% ClPS/CdSe, 100% ClPS/CdSe, 50% CdSe/FPS, 100% CdSe/FPS, and 100% CdSe/SAM

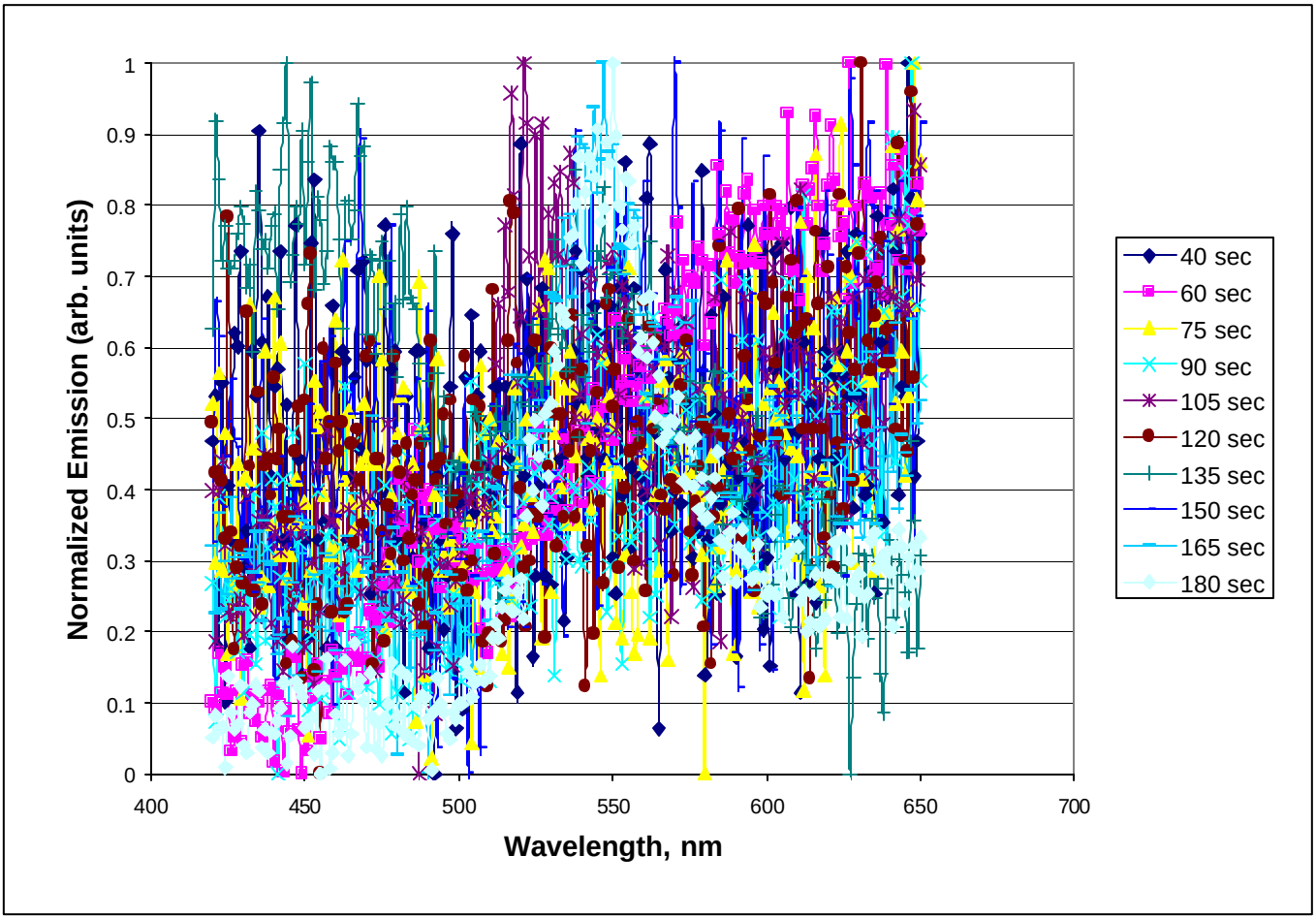

Figure D 1: Emission spectra of low yielding 50% ClPS/CdSe, sample at 180 sec is shown in the text for the representative peak around 550nm

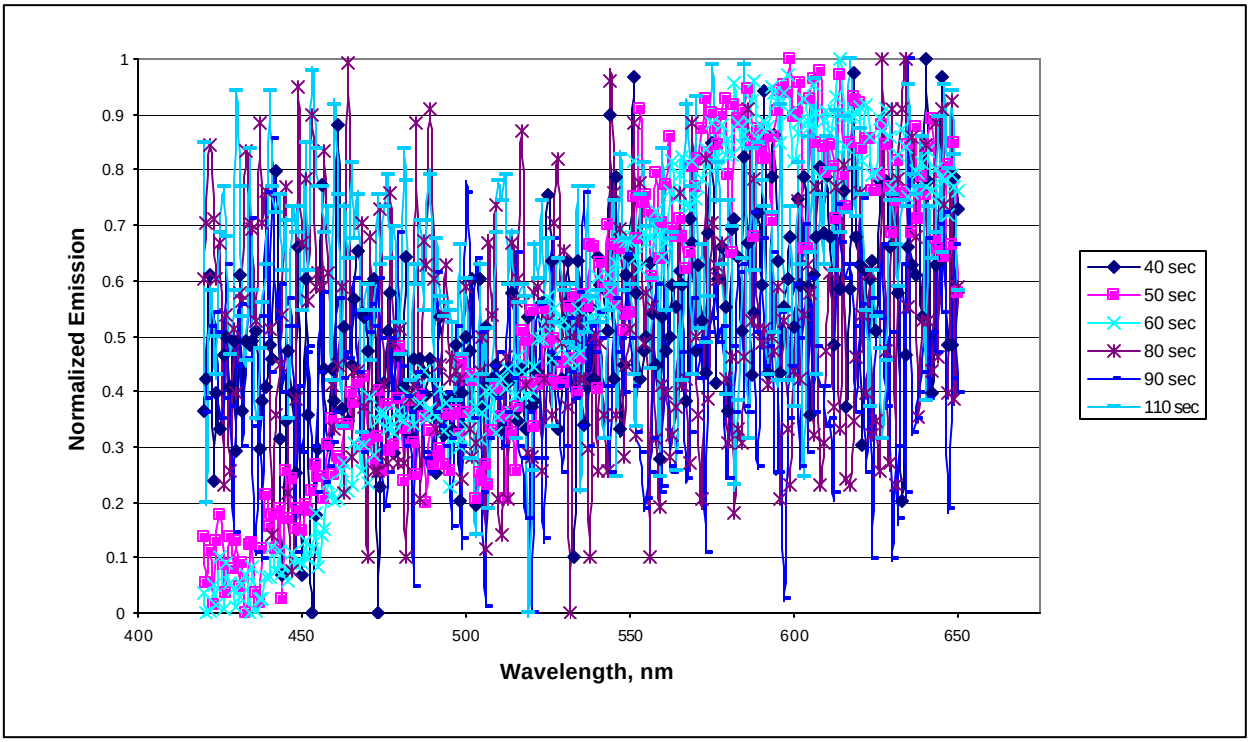

Figure D 2: The emission spectra of 100% ClPS/CdSe, indicating that no quantifiable material was produced

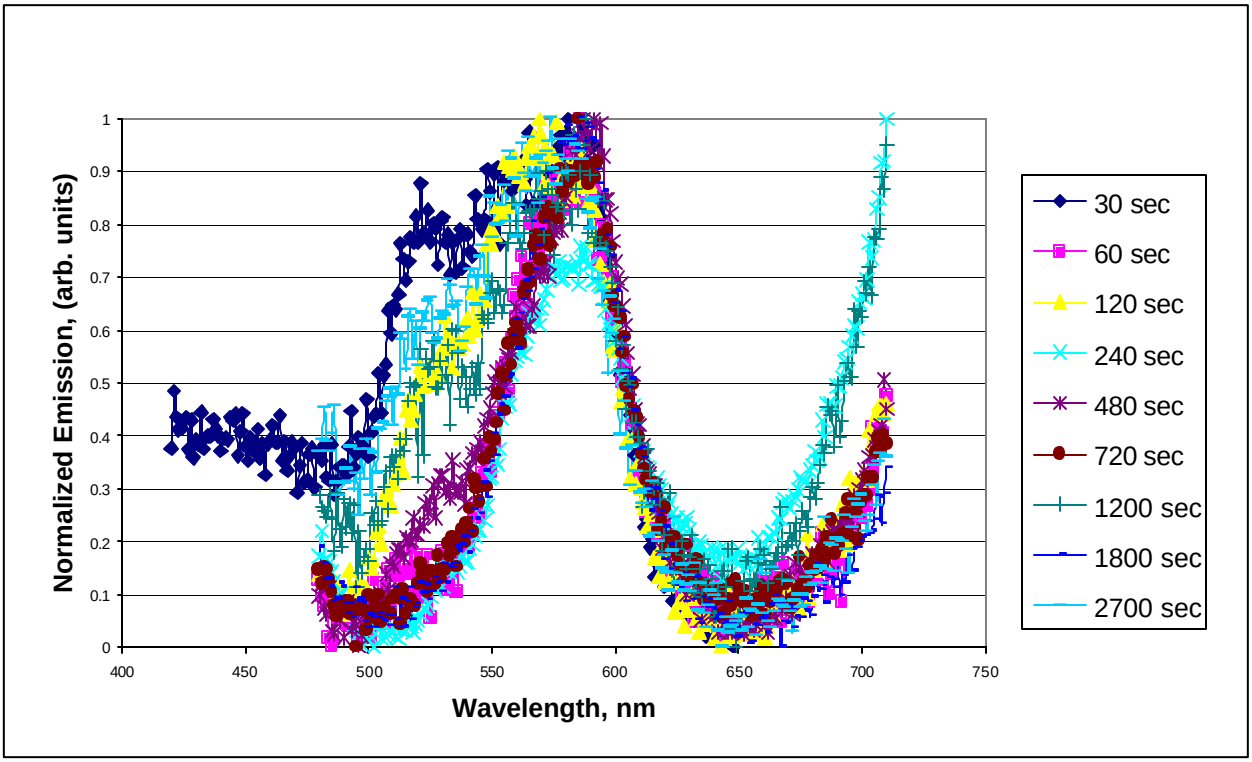

Figure D 3: Emission spectra for 50% CdSe/FPS, note the tendency toward a single wavelength

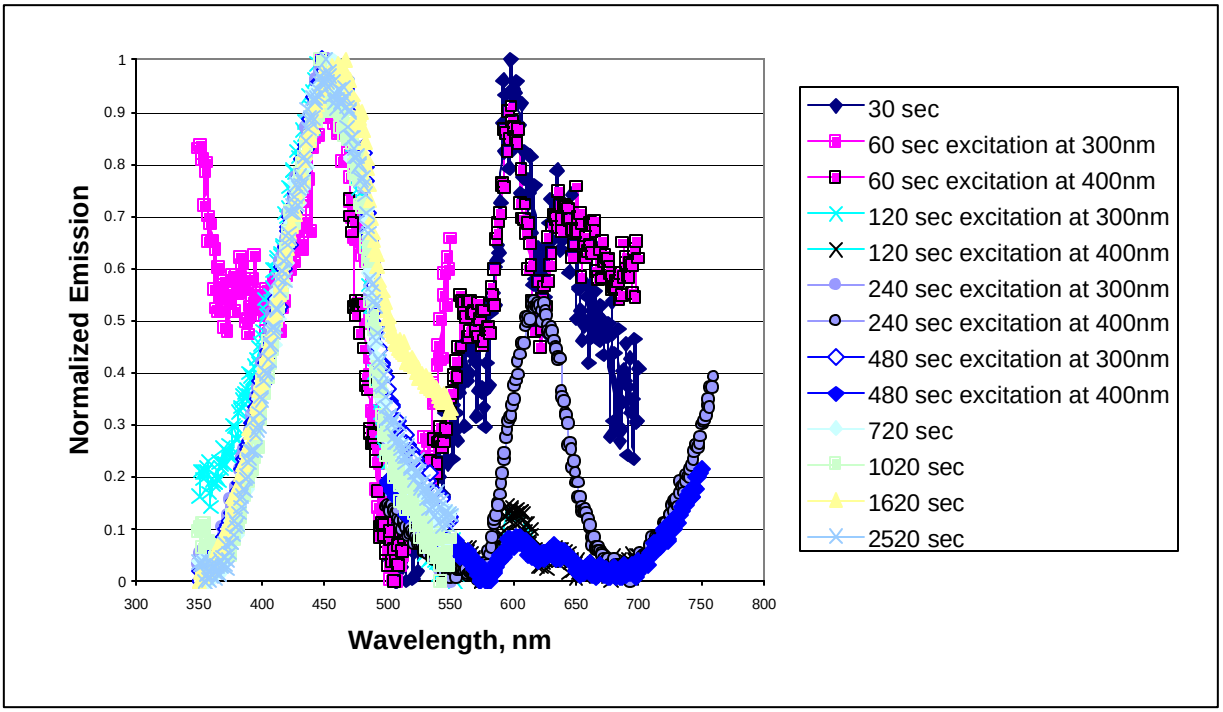

Figure D 4: Emission spectra of 100% CdSe/FPS, note how the data shows no distinct peaks except for the 240 second sample. This observation is under current investigation but overall the reaction showed little indication of having produced any viable CdSe QD product.

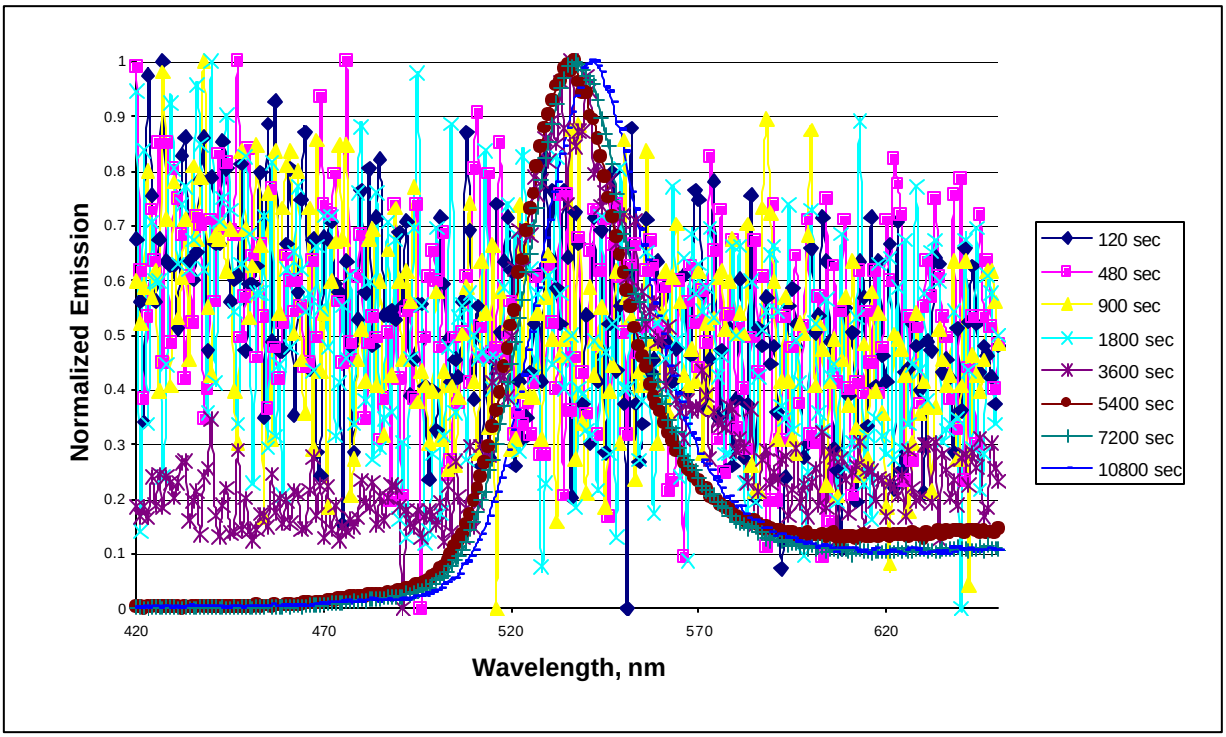

Figure D 5: 100% Sulfanilamide/CdSe reaction samples 120 sec – 1800 sec indicate interaction with toluene that destroys the samples and samples 3600 sec – 10800 sec indicate inhibited nucleation and growth

Vita

Erik Herz was born in Baltimore, Maryland on December 14, 1979. He attended Harford County Public Schools through twelfth grade and entered Virginia Tech in the Fall of 1998. Since then he has been awarded his Bachelors in materials science and engineering, Bachelors in economics, and Bachelors in international studies. His current studies focus on semiconductor nanoparticle synthesis and investigaiton, for which he will be traveling to Dortmund, Germany on a Fulbright grant in September of 2003 for nine months. Erik will be returning to the United States to attend Cornell University in pursuit of a PhD in materials science and engineering.